DOCTORAL THESIS

Oxidation of Aqueous Organic Molecules in Gas-Phase Pulsed Corona Discharge: Impact of Operation Parameters

Liina Onga

Oxidation of Aqueous Organic Molecules in Gas-Phase Pulsed Corona Discharge: Impact of Operation Parameters

LIINA ONGA

TAL TECH PRESS

TALLINN UNIVERSITY OF TECHNOLOGY
School of Engineering
Department of Materials and Environmental Technology
This dissertation was accepted for the defence of the degree 28/04/2022

Supervisor: Professor Sergei Preis
                            Dept. of Materials and Environmental Technology
                            Tallinn University of Technology
                            Tallinn, Estonia

Opponents: Prof. Dr. Miray Bekbolet
                            Institute of Environmental Sciences
                            Bogazici University
                            Istanbul, Turkey

                            Prof. Dr.-Ing. Sven-Uwe Geissen
                            Department of Environmental Technology
                            Technische Universität Berlin
                            Berlin, Germany

Defence of the thesis: 17/06/2022, Tallinn

Declaration:
Hereby I declare that this doctoral thesis, my original investigation and achievement, submitted for the doctoral degree at Tallinn University of Technology has not been submitted for doctoral or equivalent academic degree.

Liina Onga

_____
                                                signature

Orgaaniliste molekulide oksüdeerimine gaasifaasilise koroona-impulss elektrilahendusega: töörežiimi parameetrite mõju

LIINA ONGA

TAL TECH
KIRJASTUS

Contents

List of Publications

The list of author's publications, on the basis of which the thesis has been prepared:

I   Onga, L.; Kornev, I.; Preis, S. (2020). Oxidation of reactive azo-dyes with pulsed corona discharge: surface reaction enhancement. Journal of Electrostatics, 103, 103420. DOI: 10.1016/j.elstat.2020.103420.

II Onga, L.; Boroznjak, R.; Kornev, I.; Preis, S. (2021). Oxidation of aqueous organic molecules in gas-phase pulsed corona discharge affected by sodium dodecyl sulphate: Explanation of variability. Journal of Electrostatics, 111, #103581. DOI: 10.1016/j.elstat.2021.103581.

III Onga, L.; Kattel-Salusoo, E.; Trapido, M.; Preis, S. (2022). Oxidation of Aqueous Dexamethasone Solution by Gas-Phase Pulsed Corona Discharge. Water, 14 (3), #467. DOI: 10.3390/w14030467.

Author's Contribution to the Publications

Contribution to the papers in this thesis are:

I   The author carried out the experimental work and respective analyses, interpreted obtained data and wrote the paper with the help of co-authors.

II   The author carried out most of the experimental work, carried out the respective analyses, interpreted obtained data and wrote the paper with the help of co-authors.

III   The author carried out the experimental work and respective analyses, interpreted obtained data and wrote the paper with the help of co-authors.

Introduction

The increasing aquatic occurrence of contaminants originated from anthropogenic sources poses a threat to humans, animals and ecosystems. Emerging contaminants, such as pharmaceuticals enter the environment from manufacturing, disposal of unused products, excretion from human body, farming etc., which makes insufficiently treated wastewater effluents the main pathway of the pollutants to the environment.

Advanced oxidation processes (AOPs) based on generation and utilization of hydroxyl radicals (HO•) have shown a potential for degradation and mineralization of recalcitrant aqueous contaminants. Main obstacles for AOPs widespread application, however, are related to high operational and initial instalment costs. As an example, application of ozone synthesized in dielectric barrier discharge (DBD) *ex-situ* and thereafter transported to the treated aqueous medium suffers from substantial costs due to the discharge energy lost in 'oxygen-ozone' reversible reaction: the outlet gas contains ozone only as an equilibrium product, having active short-living intermediates, radicals and ions decayed long before the contact with treated water. Gas-phase pulsed corona discharge (PCD) studied in this research provides generation of the most powerful chemically active species, ozone and HO• *in-situ*, i.e., in the gas-liquid mixture with more efficient energy utilization. Previous works showed predominant generation of HO• radicals at the gas-liquid interface providing energy-efficient oxidation of aqueous species.

This thesis provides data disclosing the impact of operational parameters to PCD oxidation efficiency for selected hazardous water pollutants necessary for the method's scale-up. The pollutants under consideration include widely used textile dyes (acid orange 7, indigo tetrasulphonate, reactive blue 4 and 19), and anti-inflammatory pharmaceuticals paracetamol, indomethacin, and dexamethasone. The choice of the target pollutants was determined by the hazardous character of emerging contaminant species, and the structure of their molecules disclosing certain aspects of the PCD oxidation reaction mechanism. Textile dyes are toxic, carcinogenic, and mutagenic substances, causing also disturbances in aquatic life interfering with natural photosynthetic process. Pharmaceuticals in water disrupt aquatic life causing the biodiversity loss. Among those, dexamethasone used extensively for the past two years for COVID-19 treatment is increasing in its consumption and occurrence in the environment, thus requiring more attention in studies. The present thesis fills the gap in knowledge concerning dexamethasone oxidation with PCD and, for the lack of published data, conventional ozonation studied experimentally.

The impacts of pulse repetition frequency, treated solution conductivity, temperature and surfactant addition were studied for degradation of reactive textile dyes in PCD. The surfactant addition, besides its practical importance for the textile wastewaters treatment, disclosed the mechanism of surface oxidation reaction: dependent on the molecular structure of the target contaminant, the surfactant either obstructs oxidation or, on the contrary, substantially accelerates it. In respect to dexamethasone, in addition to the impact of operation parameters, the end products and their toxicity were also determined.

The knowledge gained in the thesis contributes to the further development of plasma technology promoting its scale-up as an energy-efficient method in water treatment.

Abbreviations

AO7	Acid orange 7
AOP	Advanced oxidation process
BOD	Biochemical oxygen demand
COD	Chemical oxygen demand
DBD	Dielectric barrier discharge
DPD	*N,N*-diethyl-*p*-phenylenediamine
DXM	Dexamethasone
E	Oxidation energy efficiency, g kW^{-1}h^{-1}
HO•	Hydroxyl radical
HPLC	High performance liquid chromatography
HPLC-MS	High performance liquid chromatography combined with mass spectrometry
I4S	Indigo tetrasulphonate
IC	Ion chromatography
IND	Indomethacin
PCD	Pulsed corona discharge
PCM	Paracetamol
pps	Pulses per second
RB19	Reactive blue 19
RB4	Reactive blue 4
SDS	Sodium dodecyl sulphate
TBA	*tert*-butyl alcohol
TOC	Total organic carbon
UV	Ultraviolet light

1 Literature Overview

1.1 Advanced Oxidation Processes

Advanced oxidation processes (AOPs) in water treatment usually operate at or near ambient temperature and pressure (Andreozzi et al., 1999; Oturan and Aaron, 2014) and are characterized by *in situ* production of extraordinarily reactive HO• radicals. One of the benefits of HO• radicals is little selectivity used in solving pollution problems. Application of AOPs is considered to have limits in economically justified applicability, allowing wastewaters with relatively small COD contents (>5.0 g O_2 L^{-1}) affordably treated with AOPs (Andreozzi et al., 1999). Among AOPs and their combinations, ozonation, UV/ozone, UV/hydrogen peroxide and UV/photocatalysis are the most studied and used for various applications. The common disadvantage shared by AOPs is their high operating costs limiting large-scale applications of otherwise powerful and human-friendly technologies.

1.1.1 Fenton Process

The Fenton reaction benefits from the production of HO• radicals by enhancement of oxidative potential of H_2O_2 when iron is used as a catalyst under acidic conditions. Studies show that Fenton process includes more than twenty chemical reactions summarized in the most accepted core reaction shown in equation (1) (Zhang et al., 2019):

$$Fe^{2+} + H_2O_2 \rightarrow Fe^{3+} + OH^- + HO\bullet \tag{1}$$

This reaction is attractive for wastewater treatment since iron is abundant and non-toxic element and hydrogen peroxide is easy to handle and environmentally safe (Andreozzi et al., 1999). The rate of degradation of organic pollutants with Fenton/Fenton-like reagents can be accelerated by irradiation with ultraviolet-visible (UV-VIS) light. This process takes advantage of UV-VIS irradiation at wavelengths above 300 nm. The light accelerates the HO• radicals' formation by photoreactions of H_2O_2 (Eq. 2) and allows the photolysis of Fe^{3+} complexes with Fe^{2+} regeneration (Eq. 3) (Andreozzi et al., 1999; Pignatello et al., 1999).

$$H_2O_2 \xrightarrow{hv} 2HO\bullet \tag{2}$$
$$Fe^{3+}(OH^-) \xrightarrow{hv} Fe^{2+} + HO\bullet \tag{3}$$

1.1.2 Ozonation

Ozone is one of the strongest disinfectants and oxidants widely used in drinking water treatment. Ozone removes effectively organic and inorganic matter, including micro-pollutants (pesticides, medications etc.), as well as odour and taste.

Ozone is effective over a wide pH, reacts rapidly with pathogens and pollutants, and does not add chemicals to water. Equipment and operational costs, however, are high, requiring operation by qualified professionals. It does not provide germicidal or disinfection residual to prevent regrowth in distribution networks.

Ozone oxidation at acidic and/or near-neutral conditions mainly occurs through the direct reaction of molecular ozone with organic substances (Dewil et al., 2017). Ozone

can react either directly to the contaminant or indirectly by generating hydroxyl radicals that react with contaminants less selectively (Eq. 4) (Deng and Zhao, 2015):

$$3O_3 + H_2O \rightarrow 2HO\bullet + 4O_2 \tag{4}$$

To accelerate the mineralization efficiency, alternative combinations like O_3/UV, O_3/H_2O_2, catalytic ozonation and photocatalytic ozonation can be used (Wei et al., 2016).

Peroxone (O_3/H_2O_2)
In the presence of H_2O_2, the yield of HO• radical is significantly improved. The ozone decomposition and HO• production are enhanced by hydroperoxide (HO_2^-) produced from H_2O_2 decomposition (Eq. 5 and 6) (Deng and Zhao, 2015):

$$H_2O_2 \rightarrow HO_2^- + H^+ \tag{5}$$
$$HO_2^- + O_3 \rightarrow HO\bullet + O_2^- + H_2O_2 \tag{6}$$

O_3/UV
In this process, H_2O_2 is generated as an additional oxidant primarily through O_3 photolysis (7) (Deng and Zhao, 2015):

$$O_3 + H_2O \xrightarrow{hv} H_2O_2 + O_2 \tag{7}$$

Catalytic ozonation
Adding a catalyst to the ozone-containing medium also accelerates HO• production and increase the efficiency of the process. Accelerating ozone decomposition, catalysts improve the absorption of ozone by the liquid phase and thus generation of hydroxyl radicals. Catalysts available for this process include transition metals Fe(II), Fe(III), Mn(II), Cu(II), Cr(III) as well as heterogeneous manganese oxide MnO_2, aluminum oxide Al_2O_3, titanium dioxide TiO_2 and zero-valent boron (Mansouri et al, 2019; Zhang et al., 2022). The mechanism of hydroxyl radical production with iron cations and ozone is shown in equations (8) and (9) (Boczkaj and Fernandes, 2017):

$$Fe^{2+} + O_3 \rightarrow FeO^{2+} + O_2 \tag{8}$$
$$FeO^{2+} + H_2O \rightarrow Fe^{3+} + OH^- + HO\bullet \tag{9}$$

1.1.3 UV based AOPs
As mentioned before, UV-light is combined with ozone, as well as with H_2O_2 to enhance the HO• production efficiency. In addition, wavelengths under 242 nm produce hydroxyl radicals through photolysis (Eq. 10). UV light may also be combined with catalysts (Boczkaj and Fernandes, 2017).
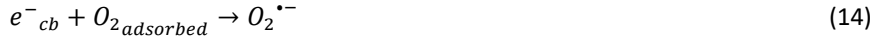
$$H_2O \xrightarrow{hv} HO\bullet + H\bullet \tag{10}$$

Photocatalysis
Most common catalyst used in photocatalysis is titanium dioxide TiO_2 in its anatase form doped with various metal and non-metal species (Birben et al., 2017). In this process, TiO_2 particles are excited with light to produce positively charged holes in the

valence band ($hv^+{}_{vb}$) with a strong oxidative capacity and negative electrons at the conduction band ($e^-{}_{cb}$) with a reductive capacity (Eq. 11) (Deng and Zhao, 2015):

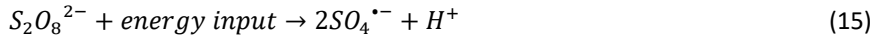$$TiO_2 \overset{hv}{\to} e^-{}_{cb} + hv^+{}_{vb} \tag{11}$$

With reactions of OH^-, H_2O and $O_2\bullet^-$ at the surface of the catalyst, the holes and electrons form hydroxyl radicals (Eq. 12 to 14) (Deng and Zhao, 2015):

$$hv^+{}_{vb} + OH^-{}_{surface} \to HO\bullet \tag{12}$$
$$hv^+{}_{vb} + H_2O_{absorbed} \to HO\bullet + H^+ \tag{13}$$
$$e^-{}_{cb} + O_{2\,adsorbed} \to O_2{}^{\bullet-} \tag{14}$$

1.1.4 Sulphate radical based technologies

Alternative to the above mentioned AOPs, sulphate-radical based technologies use persulphate and peroxymonosulphate as sources of radicals of high oxidation potential and longer than hydroxyl radical's lifetime (Boczkaj and Fernandes, 2017). Persulphate ($S_2O_8{}^{2-}$) and peroxymonosulphate ($HSO_5{}^-$) anions are strong oxidants, which need activation in order to produce sulphate radicals. UV irradiation, ultrasound and heat impart energy to the persulphate anion forming two sulphate radicals (Eq. 15). Alternately, persulphate can undergo an oxidation-reduction reaction with an electron donor from a transition metal or water radiolysis and produce only one sulphate radical (Eq. 16) (Matzek and Carter, 2016). Further generation of hydroxyl radical in aqueous solutions is shown in Eq. 17:

$$S_2O_8{}^{2-} + energy\ input \to 2SO_4{}^{\bullet-} + H^+ \tag{15}$$
$$S_2O_8{}^{2-} + e^- \to SO_4{}^{2-} + SO_4{}^{\bullet-} \tag{16}$$
$$SO_4{}^{\bullet-} + H_2O \to SO_4{}^{2-} + HO\bullet + H^+ \tag{17}$$

1.1.5 Electric discharges

Plasmas are ionized gases that consist of positive ions, electrons or negative ions and neutral particles (Bogaerts et al 2002; Chu and Lu, 2014). On the basis on relative temperature between these species, plasmas are classified as thermal equilibrium, local thermal equilibrium and non-thermal equilibrium plasmas. Cold non-equilibrium discharge is generated at atmospheric pressure, having the electron temperature much higher than the one of heavy particles, ions and molecules, making low energy consumption the main advantage of non-thermal plasmas. As no heat is produced, nearly all input energy is converted to energetic electrons (Parvulescu et al., 2012; Chu and Lu, 2014). Cold plasmas are produced with numerous methods, from which dielectric barrier discharge (DBD) and corona discharge (CD) are the most common ones (Nguyen et al., 2019). In this thesis, pulsed corona discharge (PCD) is discussed in the next chapter.

1.2 Pulsed Corona Discharge

Corona discharges appear near a pin or a thin wire electrode, where the electric field is significantly enhanced. Ionization and emission thus occur locally around the pin or the wire. Corona discharge is also known as partial discharge, since it does not normally extend to the counter electrode. Corona discharges are divided into continuous and pulsed ones: continuous discharges occur at DC or low-frequency AC

voltage, while pulsed corona is produced by applying a short voltage pulses to electrodes. The advantage of PCD consists of the short duration of pulse ensuring prevention of transition of corona to a spark terminal for the electrodes, allowing therefore higher applied voltages and currents, i.e. energy delivery into the plasma (Parvulescu et al., 2012; Chu and Lu, 2014).

Pulsed corona discharge reactor requires a pulse generator which is commonly based on the discharge of a capacitor on a low-inductance circuit. The reactor has metallic electrodes and fittings are made from insulating material (Malik et al., 2001). In a PCD reactor, high voltage pulses of sharp rise time and short duration are applied across the electrodes, which accelerate free electrons, energized electrons collide and ionize, dissociate, or excite the ambient molecules producing more free electrons and finally an electron avalanche called streamer. Dissociation of the ambient molecules produce O_3, H_2O_2, H•, HO• and O•. Neutral molecules in an exited state and ionic species produces by PCD are collectively called chemically active species (Kebriaei et al., 2015).

One of the main oxidative species formed in plasma is ozone, the formation of which is a two-step process, where free oxygen radicals are initially produced (Eq. 18-20) with subsequent formation of ozone molecule (Eq. 21). In air, NO_x production occurs from N_2 (eq 22-24) (Ono and Oda, 2003; Parvulescu et al., 2012).

$O_2 + e^- \rightarrow O^+ + O\bullet + 2e^-$ (18)
$O_2 + e^- \rightarrow 2O\bullet + e^-$ (19)
$O_2 + e^- \rightarrow O^- + O\bullet$ (20)
$O\bullet + O_2 + M \rightarrow O_3 + M$ (M = O_2 or N_2) (21)
$N_2 + e^- \rightarrow 2N\bullet + e^-$ (22)
$N\bullet + O_2 \rightarrow NO\bullet + O\bullet$ (23)
$N\bullet + NO\bullet \rightarrow N_2 + O\bullet$ (24)

Another important oxidant in non-thermal plasmas is hydroxyl radical produced via water splitting (Eq. 25). Hydrogen radicals most probably are scavenged by oxygen, or, in absence of the latter, form hydrogen molecules with another hydrogen or recombine with hydroxyl radicals. Recombination of OH-radicals may result in H_2O_2 formation (Eq. 26) (Ono and Oda, 2003, Parvulescu et al., 2012).

$H_2O + e^- \rightarrow HO\bullet + H\bullet + e^-$ (25)
$HO\bullet + HO\bullet \rightarrow H_2O_2$ (26)

In addition to hydroxyl radicals and ozone, certain UV emission is believed occurring in gas-phase plasma reactors. The amount and intensity of UV vary with the type of discharge and gas composition. UV causes H_2O_2, O_2 and H_2O dissociation (Eq. 27-29) as well as initiates reactions from NO_x to produce O or O_2 (Eq. 30-31) (Parvulescu et al., 2012).

$H_2O_2 + h\nu \rightarrow 2HO\bullet$ (27)
$O_2 + h\nu \rightarrow 2O\bullet$ (28)
$H_2O + h\nu \rightarrow H\bullet + HO\bullet$ (29)
$NO_2\bullet + h\nu \rightarrow NO\bullet + O\bullet$ (30)
$NO_3 + h\nu \rightarrow NO\bullet + O_2$ (31)

Advantages of plasma technologies include their chemical-free character and absent solid wastes formed during the treatment, as it is with conventional biological treatment and coagulation. Non-thermal plasma is operated in ambient conditions, which makes it more simple and safe method for application. Pulsed corona discharge has shown oxidation energy efficiencies that surpass ozonation by few times (Panorel et al., 2011, Ajo et al., 2016) which makes it potential cost-effective alternative to the existing AOPs. Pulsed corona discharge has been reported for its effective removal of chemical pollutants as well as microbial inactivation efficiency in water (Abou-Ghazala et al., 2002; Magureanu et al., 2015).

1.3 Water treatment using AOP's

Chemical pollution has become a major public concern in almost all parts of the world. Urban wastewater treatment plants are among the main sources of organic contaminants released to aquatic system and thus pollution of coastal waters. It is known that high structural diversity, variability of physico-chemical and chemical properties of the organic contaminants as well as different operational conditions in treatment plants cause substantially varying efficiencies of removal of these compounds (Huang et al., 2020). During wastewater treatment, solid matter is obtained from primary and secondary treatment producing sewage sludge. The possible use of sludge includes land application, composting, landfilling, and anaerobic digestion, which is another route where pollutants may find their way into the environment (Benedetti et al., 2020).

Emerging contaminants found in municipal sewage are mainly pharmaceuticals, personal care products, artificial sweeteners, flame retardants, hormones, pesticides, and plasticizers (Huang et al., 2020). Turner et al. (2019) studied whether micro-pollutants in irrigated greywater (water from household uses, except toilets) were transferred to shallow groundwater and adjacent surface waterway. They found presence of acesulfame, caffeine and N,N-diethyl-m-toluamide (DEET, personal care product used in insect repellents) in groundwater and salicylic acid in surface water. Caffeine and DEET in surface water were directly attributable to greywater irrigation.

1.3.1 Pharmaceuticals

Human pharmaceuticals enter the environment primarily after excretion from patients into wastewater. Alternative routes include disposal of unused medicine and release from the manufacturing process (Kostich and Lazorchak et al., 2008). Sources of antibiotics in the environment include their production, usage (both human and veterinary medicine), cattle breeding (promoting animal growth), crop production (avoiding certain bacterial diseases) as well as aquaculture (enhanced production and feeding) (Kümmerer et al., 2009).

Many studies have discussed the presence of pharmaceuticals in the environment. Benedetti et al. (2020) analysed sludge recovery material samples at ten different wastewater treatment plants and found them contaminated mainly by antibiotics and estrone, having ciprofloxacin and azithromycin as the most abundant compounds (up to 500-600 ng g^{-1}) (Benedetti et al., 2020). Tran et al. (2018) reported pharmaceuticals found in treated wastewater plant effluents in different concentrations. For example, in Europe ibuprofen has been found in effluents in concentrations up to 24.6 µg L^{-1}, while diclofenac and paracetamol have been found in concentrations up to 5.2 and 24.5 µg L^{-1} respectively (Tran et al., 2018). These reports show that many pharmaceuticals enter

the environment with wastewater effluents for their treatment technologies being insufficient in removal of the target compounds.

Table 1 gives a comparison of different methods used to remove paracetamol and ibuprofen. The table shows that ozone is more energy efficient than Fenton or photo-Fenton in degradation of given compounds, however PCD exceeds the efficiency of ozonation by few times. Dielectric barrier discharge tends to be much less efficient than any other method in this comparison.

Table 1. Examples of energy efficiencies of Paracetamol and Ibuprofen removal using AOPs.

Compound	C_0, mg L^{-1}	Process	Removal, %	Energy efficiency, g kW^{-1}h^{-1}	Reference
Paracetamol	25	DBD	50	0.56	Pan and Qiao, 2019
	50	Ozonation	80	5.13[1]	Bavasso et al., 2020
	100	Fenton	50	3.29[2]	Van et al., 2020
	1	Solar Photo-Fenton	90	2.07[2]	Guerra et al., 2019
	100	PCD (air, acidic)	25	14	Panorel et al., 2013 (A)
Ibuprofen	60	DBD	85	1.10	Markovic et al., 2015
	60	DBD/Fe^{2+}	99	1.59[2]	
	60	Fenton	78	3.07[2]	
	20	Ozonation	100	5.71[1]	Li et al., 2014
	100	PCD (O_2, acidic)	82	26.45	Panorel *et al.*, 2013 (B)

[1]*Energy efficiency was calculated for ozone synthesis energy expense of 15 kWh kg^{-1} O_3 when using oxygen.*

[2]*Costs of hydrogen peroxide (50% H_2O_2, 0.8217 EUR/kg) and iron (ferrous sulphate 0.7162 EUR/kg and ferric sulphate 1.13 EUR/kg) were considered in expense calculation by converting the cost into electric energy (0.0324 EUR/kWh) (*Krichevskaya *et al.,* 2011*). Energy of solar light was considered free.*

1.3.2 Textile dyes

Textile industry is one of the largest consumers of fresh water and emitters of wastewater containing hazardous contaminants. These wastewaters contain high organic contents resistant to biological degradation, e.g., reactive dyes can persist in the environment for more than forty years. In addition, these wastewaters exhibit biodegradability BOD/COD ratios below 0.1 due to the difficult biodegradability of the dyes (Hao *et al.*, 2000; Hsu *et al.*, 2004; Korenak *et al.*, 2019).

Characteristics of textile wastewaters vary significantly in colour, COD, suspended solids, turbidity and electrical conductivity due to large number of contained chemicals (Desa *et al.*, 2019). Chemicals include salts, surfactants, soaps, enzymes, dyes, oxidizing and reducing agents, starches, pesticides, and biocides (Korenak *et al.*, 2019; Hsu *et al.*, 2003). Fixation rates of dyes vary from 60 to 90%, which leaves 10% to 40% unfixed dyes in wastewaters (Low *et al.*, 2011) at concentrations up to 1.5 g L^{-1} and salinity of about 5-6% NaCl and Na_2SO_4 (Berkessa *et al.*, 2020). High pollutant concentrations make textile industry wastewater aesthetically undesirable, toxic, mutagenic and carcinogenic. Besides, the dyes breakdown products in effluents include benzidine, naphthalene and other toxic aromatic compounds (Desa *et al.*, 2019). Coloured wastewaters cause eutrophication and disturbances in aquatic life, interfering natural photosynthetic process by screening-off the light (Low *et al.*, 2011; De Campos Ventura-Camago and Marin-Morales, 2013).

Dependent on molecular moieties and application characteristics, dyes are categorized as reactive, acid, basic, anionic, direct, azo, anthraquinone, and vat ones. Reactive dyes are used extensively for their high stability, bright colours, and simple application techniques at low energy consumption (Sonal *et al.*, 2018). Remazol Brilliant Blue R (also called reactive blue 19, RB19) is one of the most frequently used dyes due to its high colour fastness and stability. This anthraquinone dye, however, is known to have low fixation rate of 50%, which results in high concentrations of RB19 in wastewaters (Berkessa *et al.*, 2020).

Conventional treatment methods of textile wastewaters are energy-consuming (UV/H_2O_2, electrochemical oxidation), forming substantial amounts of sludge (coagulation, Fenton's oxidation), or causing serious problems in handling concentrated residues (membrane filtration) and spent materials (adsorption). Colour removal using micro-organisms in aerobic and anaerobic processes is decisive in conventional treatment, although still remaining immature: combination of wastewater pre-treatment using advanced oxidation processes (AOPs) with subsequent biological treatment is considered as the most promising development (Parmar *et al.*, 2018, Paždzior et al., 2019).

Table 2 presents a comparison of energy efficiencies of degradation of RB19 and RB4 with different AOPs. The methods most competitive to PCD include ozonation reaching the energy efficiency of 30 g $kW^{-1}h^{-1}$ when degrading RB19, and photo-Fenton with 28 g $kW^{-1}h^{-1}$ degrading RB4. All the other methods did not reach energy efficiency over 5 g $kW^{-1}h^{-1}$. It is seen that PCD exceeds all other methods in regards of energy efficiency for a few times, exceeding the one of ozonation and photo-Fenton for over four times.

Table 2. Examples of AOPs' energy efficiencies in RB4 and RB19 removal.

Compound	C_0, mg L^{-1}	Process	Removal, %	E, g $kW^{-1}h^{-1}$	Reference
RB19	40.0	PCD	90	132.0	Onga *et al.*, 2020
	100.0	Ozonation	100	30.03[1]	Fanchiang and Tseng, 2009
	20.0	Sono-photocatalytic oxidation	100	0.008[2]	Khan *et al.*, 2015
	25.0	UV/H_2O_2	90	2.35[3]	Rezaee *et al.*, 2008
	100.0	Ozone-enhanced electrocoagulation	90	0.4[1]	Song *et al.*, 2008
RB4	40.0	PCD	90	132.8	Onga *et al.*, 2020
	63.6	Photo-Fenton	90	2,3[4]	Carneiro *et al.*, 2016
	231.0	Electrochemical oxidation	90	2.1-3.8[5]	Nakamura *et al.*, 2019
		Electro-Fenton	90	15.2-28.1[5]	
		Photoelectron-Fenton	90	2.4-3.4[5]	
	27.5	Fenton	22	1.01[6]	Duran *et al.*, 2008
	27.0	Solar photo-Fenton	92	4.14[6]	

[1]*Energy efficiency was calculated for ozone synthesis energy expense of 15 kWh kg^{-1} O_3 when using oxygen.*
[2]*Energy of ultrasound was considered, energy of light was not taken into consideration.*
[3]*Power of UV-lamp of 55W considered. At 15 W the efficiency comprised 1.88 g $kW^{-1}h^{-1}$ at 45% degradation of RB19.*
[4]*Energy of light source and hydrogen peroxide expense were considered. No catalyst expense included.*
[5]*Electrical energy per order (E_{EO}) was taken for decolourization in consistence with this research.*
[6]*Costs of hydrogen peroxide and ferrous sulphate were considered in expense calculation, solar energy was considered free.*

1.4 Objectives

Recently, electric discharges gained more attention in environmental technology as energy efficient method of water treatment. This work dedicates to identify and fill the knowledge gaps related to the application of PCD in treatment of water contaminated with textile dyes and pharmaceuticals.

Promising PCD method replacing ozonation in water and wastewater treatment needs determination of limitations and possible improvements resulted from additional studies assisting the technology scale-up. In practice, wastewater temperature, pH, and additive concentrations vary broadly, thus having the PCD feasibility limits and operational parameters to be established under experimental conditions.

The objectives of the study include:

- establishing the impact of operational conditions (pulse repetition frequency, temperature, pollutant initial concentration and electric conductivity) to the PCD treatment of aqueous textile dyes and selected pharmaceuticals, including emerging anti-COVID19 dexamethasone contaminant experimentally compared with ozonation;
- establishing the role of surfactant and non-surfactant OH-radical scavengers confirming the hypothesis of surface-borne character of PCD oxidation;
- derived from the results obtained on course of research, giving an explanation of varying impact of surfactant addition to PCD oxidation;
- establishing the potential of electrolytic phenomena in PCD;
- identifying the DXM oxidation intermediates and end products and evaluating their acute toxicity (*Vibrio ficheri* test).

2 Materials and Methods

2.1 Chemicals and Materials

Chemicals were of analytical grade used without further purification. Target compounds RB 4 and dexamethasone were obtained from Alfa Aesar, RB19, paracetamol and indomethacin were provided by Acros organics, and AO7 and indigo tetrasulphonate were obtained from Sigma Aldrich. Aqueous solutions were prepared with distilled water. Indomethacin was dissolved in alkaline 0.1 M Na_2CO_3 solution followed by pH adjustment to 7.6±0.2. pH was adjusted using sodium hydroxide or sulphuric acid. The structure and the main parameters of studied compounds are given in Table 3.

2.2 Software

The computational software Spartan '14 (version 1.1.4), providing energetic optimization, was adopted to simulate the preferable configuration for each target molecule and its complex with sodium dodecyl sulphte (SDS), visualizing the resulting structures. This software allows minimizing the energy of the complexes and determining the spatial localization for the moieties of the target molecules and their complexes.

2.3 Experimental Equipment and Procedure

2.3.1 Gas-Phase Pulsed Corona Discharge

The PCD experimental device (Flowrox Oy, Finland) consists of a reactor with 40-L storage tank, pulse generator and water circulation pump (Figure 1). The multiple string electrodes of 0.55 mm in diameter and 20 m of total length are positioned horizontally between two vertical parallel plates. The distance between wire electrodes and the grounded plates is 18 mm. The horizontal cross-section of the plasma zone is 36 mm in width and 500 mm in length.

The PCD is energized using a thyristor pulse generator with magnetic compression stages described by Kornev et al. (2017). Three compression stages shortened the pulse duration, making the output capacitor discharged to the electrode system for 100 ns. The output of the pulse generator was connected to the reactor using a high voltage coaxial cable of 50-Ω wave resistance. The voltage at the generator output capacitor resulted in 18 kV voltage peak value between reactor electrodes. The pulse repetition rate was variable from 50 to 880 pulses per second (pps) corresponding to the output power of 9 to 123.3 W with the current and voltage waveforms presented earlier at in Paper II. The voltage pulse duration was controlled by a saturable inductor connected to the generator's output parallel to the PCD reactor. The inductor changed the unipolar pulse shape to the bipolar one (Preis et al. 2013).

The 5- (Paper III), 10- (Paper I and II) and 20-L (Paper I) solution samples were circulated in the PCD reactor with a flow rate of 0.8 (Paper III) or 1.0 $m^3\,h^{-1}$ (Paper I and II) using circulation pump (Iwaki Co. Ltd., Japan) to feed the treated solution from the storage tank to the top of the reactor. Treated solutions were dispersed through the perforated plate having 51 perforations of 1 mm diameter in a line coplanar with the high voltage electrodes.

The energy efficiency of oxidation or energy yield E, g kW^{-1}h^{-1}, was calculated using Eq. 32:

$$E = \frac{\Delta C \cdot V}{W} \tag{32}$$

where ΔC is the decrease in pollutant concentration, g m^{-3}, V is the volume of treated solution, m^{-3}, and W is the energy consumption as a product of power delivered to the reactor and the time of treatment, kWh. The energy efficiency was calculated for 80% and 90% pollutant degradation (Paper III and Papers I-II, respectively).
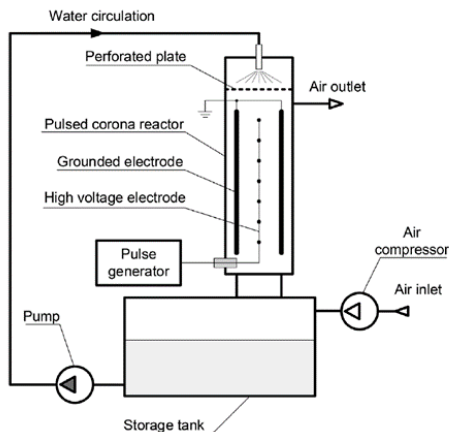

Figure 1. Schematic outline of pulsed corona discharge experimental device.

2.3.2 Ozonation

Paper III experimental equipment and procedure

Ozonation experiments were conducted in a 600-mL batch glass reactor (Figure 2). Ozonized air produced from dry air using A2ZS-10GLAB O$_3$ generator (A2Z Ozone Inc., USA) containing 3.0 mg L^{-1} of ozone was fed to the reactor at the flow rate of 0.4 L min^{-1}. Gaseous ozone concentration was monitored using O$_3$ analyser BMT 965 (BMT Messtechnik GMBH, USA). The ozonation experiments were conducted for 60 min with sampling at fixed time intervals. Residual ozone in samples was quenched with sodium sulphite added to stop the reaction.

The energy efficiency for DXM degradation in ozonation experiments was calculated using Eq. 33:

$$E = \frac{\Delta C \cdot V}{P \cdot t} \tag{33}$$

where ΔC is the decrease in DXM concentration, g m^{-3}, V is the volume of treated solution, m^{-3}, t is the treatment time, h, and P is the power consumed by ozone synthesis, kW. The power was calculated from gaseous O$_3$ initial concentration, g O$_3$ m^{-3}, the flow rate of ozone-containing air, m^3 h^{-1}, and the energy consumed by O$_3$ synthesis in air comprising 30 kWh kg O$_3$$^{-1}$.
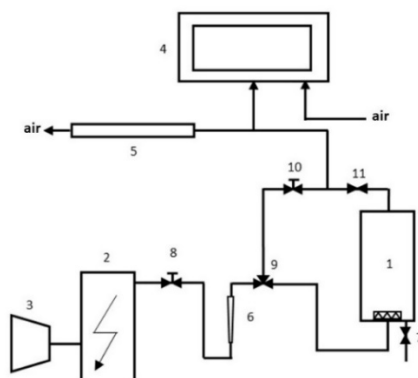
Figure 2. Ozonation gas distribution outline: 1 – reactor; 2 – O₃ generator; 3 – compressor; 4 – O3 analyser; 5 – residual O₃ thermo-catalytic destructor; 6 – rotameter; 7 – sampling port; 11 – non-return valve; 8, 10 – gate valves with manual actuators; 9 – 3-way valve

2.4 Analytical Methods

Dye concentrations were measured using Helios β spectrophotometer (Thermo Electron Corporation, USA) at maximum absorbance wavelengths of 485, 591, 592 and 595 nm for AO7, I4S, RB19 and RB4, respectively (Paper I and II). Concentrations of PCM, IND and DXM pharmaceuticals were quantified using high performance liquid chromatography combined with diode array detector (HPLC-PDA, Shimadzu, Japan) equipped with a Phenomenex Gemini column (150x2.0 mm, 1.7 mm) filled with stationary phase NX-C18 (110 Å, 5 µm) (Paper II and III). The analysis were performed using an isocratic method with mobile phase mixtures of 50:50, 60:40 and 92:8% of 0.3% aqueous formic acid and acetonitrile containing 0.3% formic acid for IND, DXM and PCM, respectively. The eluent flow rate was 0.2 mL min⁻¹. Samples injected in amount of 20 µL (PCM) and 75 µL (DXM and IND) were analysed at wavelengths 241, 243 and 320 nm for DXM, PXM and IND, respectively.

The transformation products formed during DXM oxidation were identified using high performance liquid chromatography combined with mass spectrometer (HPLC-MS, Shimadzu LC-MS, Japan) (Paper III). Mass spectra were acquired in full-scan mode in the range of 50-500 m/z. The instrument was operated in positive ESI mode and the results obtained were handled using Shimadzu Lab Solutions software. Ion chromatography with chemical suppression of the eluent conductivity was used to measure concentrations of formed anions (761 Compact IC, Metrohm Ltd., Switzerland) (Paper III).

Total organic carbon (TOC) was measured using Multi N/C 3100 analyser (Analytic Jena, Germany) (Paper III). pH was measured using S220 digital pH-meter (Mettler Toledo, Switzerland). Multi-parameter meter HQ430d (Hach Company, USA) was used for conductivity measurement (Paper I). Concentration of free chlorine was determined with standard N,N-diethyl-p-phenylenediamine (DPD) colorimetric method using spectrophotometer at 515 nm (Clesceri et al., 2012) (Paper I).

The acute toxicity of DXM solutions (Paper III) was determined using the Microtoc® method (Model 500 Analyzer SDI) according to ISO 11348-3:2007 (ISO, 2007).

Table 3. Properties of target compounds.

Compound	Formula	Classification	Graphical structure	IUPAC name	CAS nr	Molar mass, g·mol^{-1}
Reactive blue 4 (RB4)	$C_{23}H_{14}Cl_2N_6O_8S_2$	anthraquinone dye		1-amino-4-[3-[[(4,6-dichloro-1,3,5-triazin-2-yl)amino]-4-sulfoanilino]-9,10-dioxoanthracene-2-sulfonic acid	13324-20-4	637.43
Reactive blue 19 (RB19)	$C_{22}H_{16}N_2Na_2O_{11}S_3$	anthraquinone dye		disodium;1-amino-9,10-dioxo-4-[3-(2-sulfonatooxyethylsulfonyl)anilino]anthracene-2-sulfonate	2580-78-1	626.54
Acid orange 7 (AO7)	$C_{16}H_{11}N_2NaO_4S$	azo dye		sodium;4-[(2-hydroxynaphthalen-1-yl)diazenyl]benzenesulfonate	633-96-5	350.32
Indigo tetra-sulphonate (I4S)	$C_{16}H_6K_4N_2O_{14}S_4$	indigo dye		tetrapotassium;2-(3-hydroxy-5,7-disulfonato-1H-indol-2-yl)-3-oxoindole-5,7-disulfonate	67627-19-4	734.88
Paracetamol (PCM)	$C_8H_9NO_2$	anti-inflammatory drug		N-(4-hydroxyphenyl)acetamide	103-90-2	151.16
Indomethacin (IND)	$C_{19}H_{16}ClNO_4$	anti-inflammatory drug		2-[1-(4-chlorobenzoyl)-5-methoxy-2-methylindol-3-yl]acetic acid	53-86-1	357.79
Dexamethasone (DXM)	$C_{22}H_{29}FO_5$	anti-inflammatory drug		(8S,9R,10S,11S,13S,14S,16R,17R)-9-fluoro-11,17-dihydroxy-17-(2-hydroxyacetyl)-10,13,16-trimethyl-6,7,8,11,12,14,15,16-octahydrocyclopenta[a]phenanthren-3-one	50-02-2	392.46

3 Results and discussion

3.1 Oxidation energy efficiencies of aqueous pollutants in PCD treatment and ozonation

The energy efficiencies of aqueous RB4, RB19 and DXM oxidation in PCD and aqueous DXM ozonation at studied experimental conditions are shown in Table 4.

Table 4. Oxidation energy efficiencies for PCD treatment of RB4, RB19, and DXM, and ozonation of DXM.

PCD treatment conditions for RB4	Energy efficiency at 90% removal
C_0= 40 mg L^{-1}, 200 pps, pH_0 6.9, T_0 20°C	132.8
C_0= 40 mg L^{-1}, 880 pps, pH_0 6.9, T_0 20°C	94.4
C_0= 40 mg L^{-1}, 200 pps, pH_0 6.9, T_0 35°C	79.1
C_0= 40 mg L^{-1}, 200 pps, pH_0 6.9, T_0 45°C	55.8
PCD treatment conditions for RB19	**Energy efficiency at 90% removal**
C_0= 40 mg L^{-1}, 200 pps, pH_0 6.9, T_0 20°C	132.0
C_0= 40 mg L^{-1}, 880 pps, pH_0 6.9, T_0 20°C	119.1
C_0= 40 mg L^{-1}, 200 pps, pH_0 6.9, T_0 35°C	29.7
C_0= 40 mg L^{-1}, 200 pps, pH_0 6.9, T_0 45°C	24.7
PCD treatment conditions for DXM	**Energy efficiency at 80% removal**
C_0= 10 mg L^{-1}, 50 pps, pH_0 6.8	8.9
C_0= 10 mg L^{-1}, 200 pps, pH_0 6.8	8.5
C_0= 10 mg L^{-1}, 880 pps, pH_0 6.8	6.0
C_0= 10 mg L^{-1}, 50 pps, pH_0 3.0	18.3
C_0= 10 mg L^{-1}, 50 pps, pH_0 10.8	13.8
C_0= 20 mg L^{-1}, 50 pps, pH_0 6.8	18.5
C_0= 40 mg L^{-1}, 50 pps, pH_0 6.8	22.9
Ozonation treatment conditions for DXM	**Energy efficiency at 80% removal**
C_0= 40 mg L^{-1}, inlet gaseous ozone concentration 3.0 mg L^{-1}, gas flow rate 0.4 L min^{-1}, pH_0 6.8	9.7

The effect of pulse repetition frequency exhibits the role of ozone in PCD treatment (Preis et al., 2013). The frequency of 200 pps resulted in energy efficiencies 8.5, 132.0 and 132.8 g $kW^{-1}h^{-1}$ for DXM, RB19 and RB4, respectively. Increasing the frequency to 880 pps resulted in the oxidation energy efficiency decreased for 29% for RB4 and DXM, and for 10% for RB19. Relatively small effect of pulse repetition frequency on the RB19 oxidation indicates its more rapid reaction with ozone compared to RB4 and DXM. For DXM, the effect of the frequency as low as 50 pps was also tested showing the difference between 50 and 200 pps not exceeding 5%, which may be explained by equal consumption of ozone synthesized at these frequencies by the substrate at the time of treatment. However, the DXM oxidation energy efficiency at 880 pps was about 33% lower than the one at 50 pps. The rate of energy delivery is proportional to the

pulse repetition frequency making the treatment longer at lower frequencies (Figure 3). This indicates moderate contribution of ozone to the DXM degradation, with lower pulse repetition frequency giving ozone more time to react between pulses.
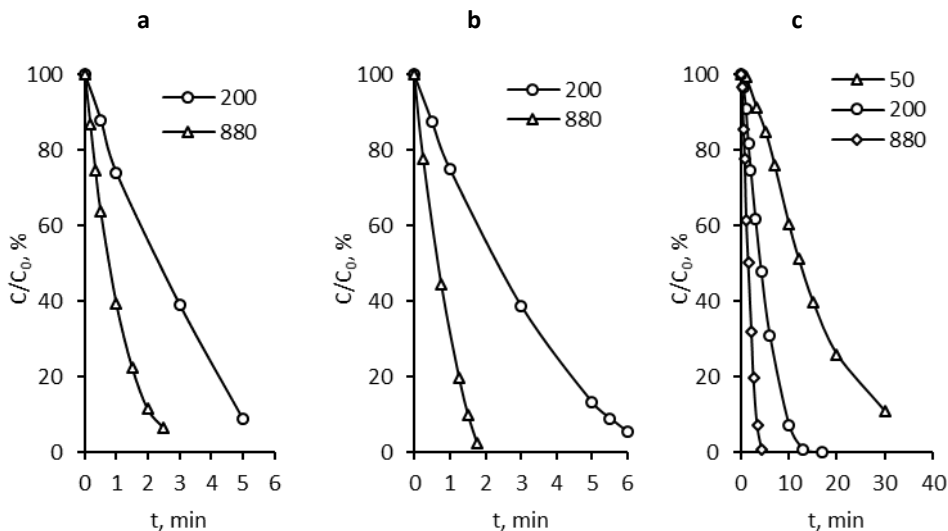

Figure 3. RB4 (a), RB19 (b) and DXM (c) residual relative concentrations dependent on time at pulse repetition frequencies of 200 and 880 pps for RB4 and RB19, and 50, 200, and 880 pps for DXM: starting concentrations of RB - C_0=40 mg L^{-1}, and DXM - C_0=10 mg L^{-1}.

Raising the temperature of the treated solutions had a notable effect on the oxidation efficiency: the temperature of the RB4 solution raised from 20 to 35 and 45 °C resulted in the efficiency decreased for 41 and 58%, respectively. The corresponding efficiency decrease for RB19 comprised 78 and 81% under similar temperature conditions (Paper I, Figure 3). Increased temperature accelerates OH-radical termination reaction, noticed previously for oxalate (Ajo et al., 2017), as well as promotes ozone decomposition reaction (Ono and Oda, 2003). Noticeably stronger effect of temperature in RB19 oxidation is consistent with behaviour of the dyes at pulse repetition frequency variation: smaller effect of frequency at overall rapid oxidation indicates the RB19 reaction with ozone being faster than that of RB4; analogously, lower solubility and productivity of ozone in the discharge at higher temperature exhibit stronger negative effect with rapidly reacting RB19.

The initial concentration of the target pollutant determines the energy efficiency of oxidation as expected from the second-order reactions observed in PCD treatment of aqueous media (Preis et al., 2013). The impact of variable DXM concentration was studied at initial ones of 10, 20 and 40 mg L^{-1}. At the constant pulsed power released in the PCD reactor, the growing initial concentration exhibits a growing trend in oxidation efficiency, requiring, however, higher energy dose and longer treatment time (Figure 4a). Similarly, increased DXM concentration resulted in better performance of, e.g., photocatalytic oxidation (Markic et al., 2018).

Experiments with initial pH of 3.0, 6.8 and 10.8 were conducted to evaluate pH impact to DXM oxidation. During experiments, pH of acidic media remained practically constant, whereas in neutral and alkaline media the pH decreased from 6.8 and 10.8 to 4.1 and 10.0, respectively. The observed decrease in pH values during PCD oxidation is

mainly associated with formation of nitric acid as well as formation of acidic DMX transformation products (Preis et al., 2014).

Oxidation of DXM was accelerated in acidic and alkaline media for 2.1 and 1.6 times, respectively, as compared to the neutral one (Figure 4b). The higher efficiency in acidic media may be attributed to the higher HO• oxidation potential of 2.8 eV (Wardman, 1989) as well as synergistic effect of directly reacting dissolved ozone. The lower efficiency at the increased pH may be attributed to the HO• oxidation potential decreasing from 2.8 eV in acidic medium to 1.9 eV at neutral pH. The energy efficiency increasing with pH growing from neutral to alkaline media may be attributed to faster decomposed ozone molecules producing hydroxyl radicals in the solution, although decreased efficiency in alkaline media compared to acidic one may also be associated with generation of hydroperoxyl radicals (E_0=1.65 V). Dissociation of DXM (pKa 12.42) moieties in alkaline solutions might also accelerate oxidation (Cuerda-Correa et al., 2020).
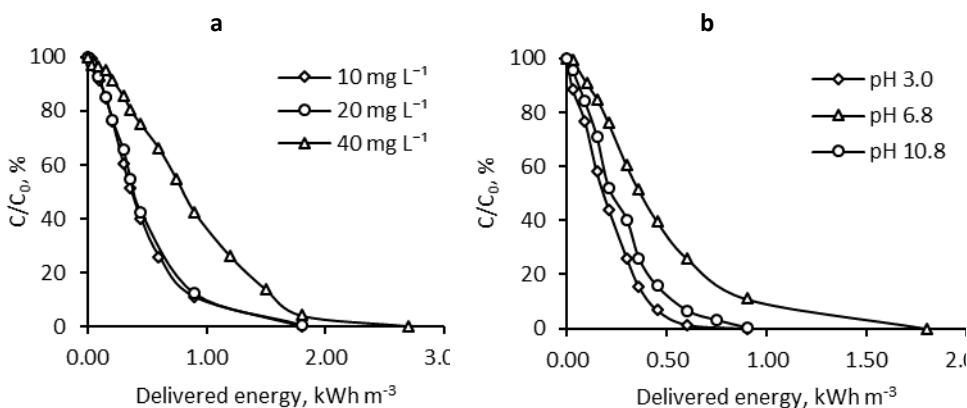
Figure 4. Dexamethasone residual relative concentration dependent on the delivered pulsed energy at varying DXM initial concentrations (a) and initial pH (b): pulse repetition frequency 50 pps, DXM starting concentration 10 mg L^{-1} (b).

In order to compare DXM degradation in PCD treatment to other conventional treatment methods, experiments with ozonation were undertaken. For higher reliability of establishing the oxidation products (see chapter 3.2), DXM was degraded at higher initial concentration of 40 mg L^{-1}. Both oxidation processes exhibited similarity in pH decreasing from 6.8 to 3.6 and 3.2 as a result of treatment with PCD and ozonation, respectively, associated with nitrate formation in the treated solutions: NO_3^- formed in amounts of approximately 36 mg L^{-1} at 3.6 kWh m^{-3} energy doses in both processes. The treatment with PCD showed higher energy efficiency in DXM degradation reaching 99% at the energy dose of 2.9 kWh m^{-3}. The reaction yield in PCD at 80% of DXM removal equals to 22.9 g $kW^{-1}h^{-1}$. At the end of ozonation experiment applying the same energy dose of 3.6 kWh m^{-3}, the treated solution still contained 7.7 mg L^{-1}, i.e. 19.2% of residual DXM. The oxidation energy efficiency at 80% of DXM degradation thus comprised in ozonation experiment about 9.7 g $kW^{-1}h^{-1}$, which is 2.4 times smaller than the PCD efficiency (Figure 5).

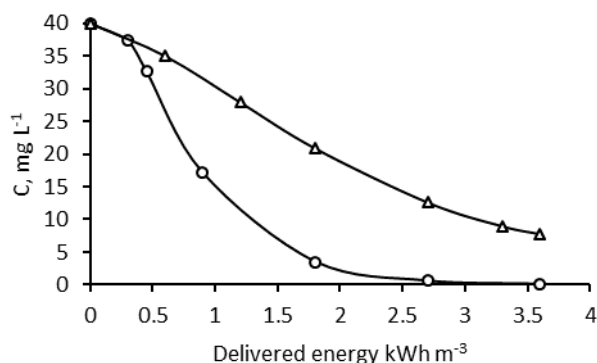*Figure 5. Degradation of Dexamethasone with ozonation (Δ) and PCD (○) treatment: C_0=40 mg L^{-1}, pH_0 6.8, PCD: pulsed repetition frequency 50 pps, O_3: inlet gaseous ozone concentration 3.0 mg L^{-1}, gas flow rate 0.4 L min^{-1}.*

3.2 Acute toxicity and degradation products of DXM oxidation

Measurement of TOC showed no decrease in comparison with original DXM solution remaining at 26.1 mg C L^{-1} in all samples treated with either PCD or ozonation. Having DXM degraded without mineralization, DXM oxidation end- and by-products were experimentally studied using ion chromatography and mass-spectrometry. Ion chromatography analysis of the samples treated with PCD and ozone revealed fluoride and acetate being the main identified end-products of DXM oxidation. Being refractory towards oxidation, acetate accumulated along with DXM removal. It is worth noting that formation of fluoride in PCD was in stoichiometric ratio with DXM removal: 40 mg L^{-1} or 0.1 mM of DXM provides about 1.9 mg L^{-1} of fluoride, which approximately equals to the 0.1 mM content. However, acetate was formed in quantity of 26.6 mg L^{-1} or 0.45 mM which is about 40% of initial carbon content (Paper III, Figure 8). Ozonation experiments showed about three times smaller amounts of end products than in PCD-treated samples at the same energy delivery level. Moreover, no stoichiometric ratio was observed between the removed DXM and formed fluoride quantities: the content of fluoride comprised 0.03 mM, i.e. about three times smaller than would be expected. Acetate was also observed in smaller yield of 0.16 mM (about 15% of initial carbon content) (Paper III, Figure 9). In PCD experiments, traces of oxalate and formate were also detected, although no accumulation of these products was observed. Traces of formate were also present in samples treated with ozonation, but no oxalate was observed. Smaller amounts of identified oxidation end-products in ozonated samples indicate smaller degree of DXM destruction.

LC-MS analysis revealed six most common DXM transformation products numbered as TPs presented in Figure 6. The proposed m/z fragments of DXM obtained in MS analysis were 393 and 373, the latter being associated with breaking C-F bond and release of HF during analysis (Calza et al., 2001). No qualitative difference in products composition was observed between two treatment processes. The most frequently detected products were TP2, TP3 and TP6 with m/z values 409, 407 and 413, respectively. TP1 with m/z 391 could be associated with the alcohol moiety oxidation to the aldehyde one. TP2 can be associated with OH-radical attack with addition of the OH-group. Further OH-radical attack results with TP3 by oxidation of alcoholic group to aldehyde one, followed by carboxylic derivative formation and generation of TP5.

26

The binary initial OH-radical attack to DXM may explain the TP4 formation (Figure 6a). The products TP1-TP5 have been previously reported in photocatalysis studies (Calza et al., 2001), and TP4 in gamma irradiation studies (Rahmani et al., 2015). Cycloaddition (Criegee mechanism) with further hydroxylation and loss of HCOOH (He et al., 2019) is suggested to lead to TP6 as a product of ozonation (Figure 6b). These results further suggest that OH-radicals have the main role in oxidation of DXM.

Supplementary to transformation products identification, the acute toxicity of intermediates was assessed using the *Vibrio fischeri* bioluminescence inhibition assay on DXM solutions treated with PCD and ozone at the energy dose of 3.6 kWh m^{-3}. The effective concentration for 30% bacterial bioluminescence inhibition (EC30) of the solution containing 40 mg L^{-1} of DXM was 37.5%. Treatment with ozone did not noticeably affect toxicity of the solution, showing negligble EC30 growth to 39.3%, i.e. small toxicity reduction. The treatment with PCD, however, showed increased inhibition of *Vibrio fischeri* bioluminescence resulting in EC30 of 23.3%, i.e. the toxicity somewhat increased as a result of PCD treatment. The toxicity test showed no difference carried out immediately after treatment and 24 h later, thus excluding the impact of active compounds temporarily supressing bacterial activity. The results may show formation of DXM by-products with higher toxicity on course of its destruction in PCD treatment, thus possibly making smaller DXM removal by ozone the reason of smaller toxicity of treated samples.
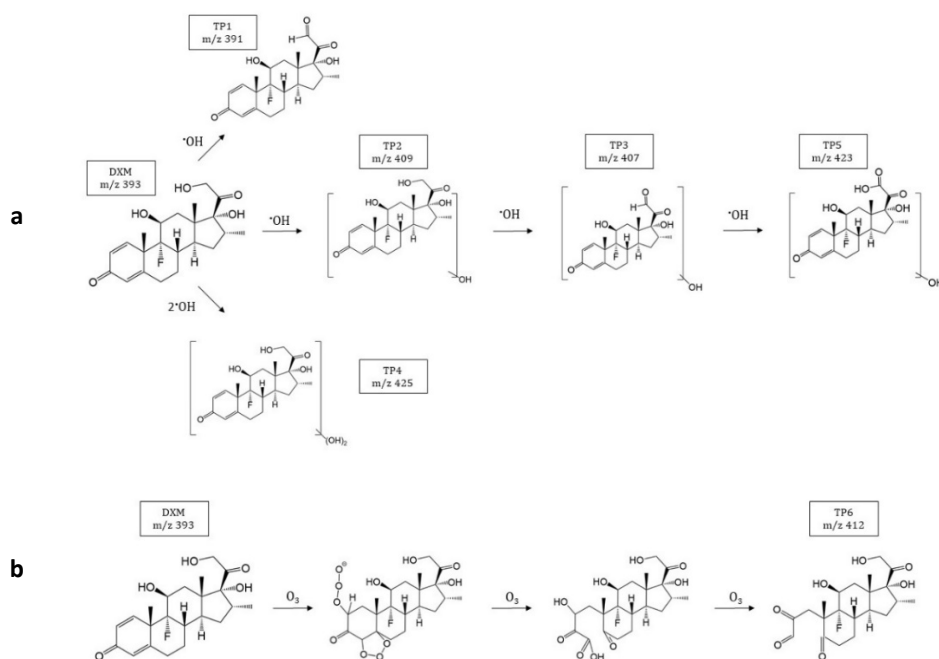
Figure 6. Proposed degradation pathways and transformation products of DXM in oxidation with (a) hydroxyl radicals and (b) ozone

3.3 Effect of solution conductivity on PCD oxidation

Effect of increased conductivity was studied using two salts, sodium sulphate and chloride: it was found previously that conductivity causes certain losses in the discharge energy (Kornev et al., 2017). Besides the effect of conductivity, sodium chloride was used to study possible effect of electrolysis with free chlorine liberation: hypothetical free chlorine presents an interest concerning well-known textile dyes discoloration. For example, Nakamura et al. (2019) treated RB4 solutions in electro-Fenton process using Na_2SO_4 and $NaCl$ as supporting electrolytes and found the colour removal being twofold faster with NaCl on account of free chlorine. Possible formation of chlorinated organic compounds is also of interest due to their resistance towards biodegradability with limitations thus placed to PCD application.

Sodium chloride was dissolved in distilled water in amounts of 5.6 and 11.2 g L^{-1} resulting in electric conductivity of solutions 10 and 20 mS cm^{-1} at 20 °C, respectively. The experiments were conducted at 20 °C and treated for 1 to 60 minutes at 880 pps thus supplying up to 12.3 kWh m^{-3} energy dose. Analysis of samples taken on the course of treatment conducted using DPD colorimetric method showed no trace of free chlorine within the method's detection limit of 18 μg L^{-1}.

The experiments with PCD-oxidation of RB4 and RB19 in conductive solutions showed noticeable yet moderate reduction in oxidation efficiency (Figure 7). Salts exhibited only a small difference in experimentally observed oxidation efficiency reduction regardless the character of salt, sulphate or chloride. Conductivities of sodium sulphate at 10 and 20 mS cm^{-1} at 20 °C were provided with dissolution of 8.4 and 16.8 g L^{-1} of Na_2SO_4, respectively. At 10 mS cm^{-1}, the decrease in oxidation efficiency was practically identical for both chloride and sulphate salts, whereas at 20 mS cm^{-1} the decrease of oxidation efficiency was slightly stronger with sulphate.

The negligible difference of the impact from sulphate and chloride to the oxidation efficiency of textile dyes together with the absence of free chlorine observed in direct measurements implies the absence of electrolytic phenomena in PCD. The explanation can be given by the shape of the pulse designed for reliability and safety: the starting positive pulse changes in about 100 ns to the negative one of almost equal amplitude and duration thus giving no progressive movement to massive chloride ions, and thus no direct current to evoke electrolysis.
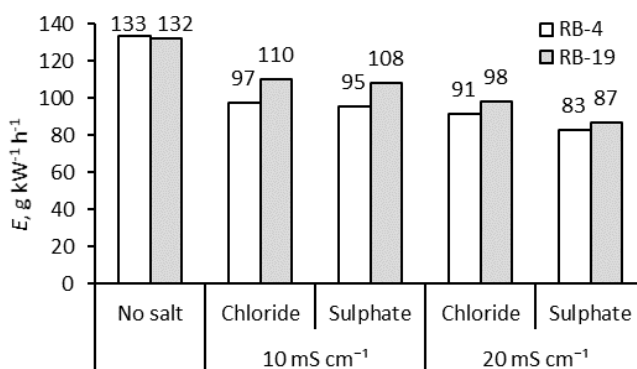

Figure 7. Effect of conductivity of 10 and 20 mS cm^{-1} on oxidation efficiencies of RB4 and RB19 dyes: starting dyes concentration 40 mg L^{-1}, pulse repetition frequency 200 pps (32 W), oxidation efficiency given for 90-% colour removal

3.4 The effect of SDS to the PCD treatment

Surface character of reactions initiated with PCD-treatment attracts attention to the role of surfactant radical scavengers. Besides, surfactants are widely used in textile industry for dying as well as for the removal of excess dyes, making surfactants present in textile industry wastewaters. Widely used low cost surfactant SDS was chosen to study its impact to the dye degradation in PCD. It was previously determined that SDS slowed down the reactions in PCD when humic substances, as well as phenol and oxalate were oxidized, i.e., SDS scavenged surface-borne hydroxyl radicals (Wang *et al.*, 2019). Experimental study was undertaken to establish the effect of SDS to the target pollutants oxidation.

Contrary to previous results, SDS addition dramatically improved the oxidation of reactive dyes: addition of 100 mg L^{-1} of SDS resulted in the increase in oxidation energy efficiency from 132.8 to 318.4, and from 132.0 to 359.0 g $kW^{-1}h^{-1}$ for RB4 and RB19, respectively. At 50 mg L^{-1} of SDS content, RB19 dye discoloration rate was somewhat smaller comprising about 274 g $kW^{-1}h^{-1}$, however increasing the SDS concentration to 200 mg L^{-1} did not result with further changes in oxidation efficiency (Figure 8.).
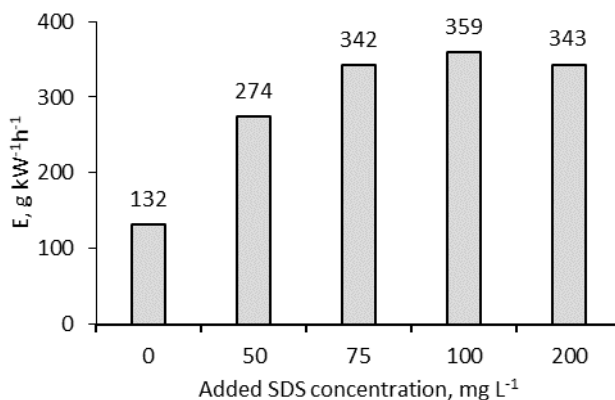
Figure 8. Effect of SDS concentration on oxidation energy efficiency of RB19 at 90% removal: starting RB19 concentration 40 mg L^{-1}, 200 pps (32 W)

Accelerated textile dyes oxidation may be explained by molecular interaction between SDS surfactant and a dye molecule resulting in transportation of the latter to the gas-liquid interface, where RB molecules appear exposed to oxidation with surface-borne reactive oxygen species. A model using Spartan '14 software was adopted to simulate the preferable configurations for each molecule and its complex with SDS. The model presumes the OH-radical attack on the hydrophobic tail of SDS, removing a hydrogen atom from the –CH_3 group forming a slow reacting –CH_2•-radical at the end of the tail. RB4 and RB19 contain aromatic rings with high electron densities in their chromophore groups. Due to the possibility of radical dissociation of SDS hydrophobic tail and in the chromophore groups of dye, the slow-reacting hydrophobic SDS-radical attaches itself to the chromophore parts of RB4 and RB19 (Paper II, Figure 3), subsequently bringing the target molecule to the plasma-liquid interface, where steric access for further OH-radical attacks is provided and the dye molecules are oxidized with higher efficiency.

The software was used further to model interactions between SDS and other target compounds. Another textile dye AO7 contains two high electron density groups – benzene ring and 2-naphthol group thus having sites with high electron density attracting SDS-radical. The 2-naphtol moiety has no attached groups thus no steric effects obstruct SDS-radical attaching itself to the molecule. Probable attachment of SDS to the aromatic ring of AO7 implies the surfactant bringing the molecule to the plasma-liquid interface and exposing it to plasma active species (Paper II, Figure 4a). Verification of the modelled interactions revealed the AO7 oxidation efficiency rising from 66 to 108 g $kW^{-1}h^{-1}$ in 150 mg L^{-1} SDS solution providing noticeable positive effect. However, further SDS concentration increasing to 200 mg L^{-1} resulted in energy efficiency decreased to 98 g $kW^{-1}h^{-1}$ indicating the excess amount of SDS partially screening off the surface-borne radicals.

Large I4S molecule contains two aromatic rings with four sulphonate groups attached in meta-positions practically surrounding the rings with steric obstacles preventing, at least partially, affiliation with the SDS-radical. The non-covalent interaction between dissociative and hydrophilic sulphonate groups of the I4S and SDS could possibly result with SDS covering the chromophore groups of dye against OH-radical attack and thus hindering the oxidation (Paper II, Figure 4b). The oxidation experiments showed oxidation efficiency gradually decreased from 676 to 610 g $kW^{-1}h^{-1}$ with SDS concentration increasing from 0 to 200 mg L^{-1}. Moderate deceleration of oxidation may be explained by limited steric effect of sulphonate groups of the large I4S molecule. Similar results were obtained with humic substances, where SDS only moderately affected the oxidation (Wang et al., 2019).

Previous work with oxidation of oxalic acid (Wang et al., 2019) in presence of SDS resulted in the decreased for 3 to 8 times oxidation rate compared to SDS-free treatment. This can be explained by the surfactant forming a non-covalent complex around polar groups of the compound thus constructing the shields composed of alkyl tails. Due to relatively small size of the molecules, SDS forms steric hindrances against OH-attacks.

Paracetamol was chosen as another relatively small molecule with possibly similar mechanism of interaction with SDS as oxalic acid. The PCM molecule contains one aromatic ring with attached hydrophilic moieties at its two opposite sides. The electron-rich aromatic ring attracts the SDS-radical, while –OH and –NH- groups leave no space for SDS-radical to attach to a radicalized benzene ring. Experiments revealed weakly negative, close to neutral effect of SDS to the PCD oxidation of PCM, when SDS concentration from 0 to 100 mg L^{-1} resulted in oxidation energy efficiency decreased from 39 to 34 g $kW^{-1}h^{-1}$. Further SDS addition restored the efficiency back to 39 g $kW^{-1}h^{-1}$, which may be explained by two phenomena competing in PCM interaction with SDS – attachment of SDS-radical to the aromatic ring of PCM, and hydrophilic character of the PCM molecule shielded with complexing SDS molecules. These phenomena, as well as relatively small size of PCM molecule make it difficult for SDS to find a spot to covalently attach itself to. Weak affinity of the SDS-radical to the small PCM molecule is thus responsible for the effect of SDS addition close to neutral.

The indomethacin molecule containing two benzene rings, one of which is connected to pyridine ring, is larger than PCM. Two benzene rings provide more sites with high electron density potentially attracting SDS-radicals stronger than a single-ring PCM. However, the hydrophilic carboxylic moiety as well as –Cl and –OCH$_3$ moieties around the benzene rings thin out the electron densities of aromatic groups and potentially complicate the SDS-radical attachment. Experiments showed the oxidation efficiency

moderately rising in presence of SDS from 129 to 150 g kW^{-1}h^{-1} at SDS concentration of 100 mg L^{-1}. However, further rise in SDS concentration to 150 mg L^{-1} resulted in decreased oxidation efficiency indicating strengthened screening effects of the excess surfactant molecules as was previously noticed with AO7.

Preliminary consideration of the DXM molecule allows the assumption of complex SDS impact: (a) the part of the molecule rich in polar hydroxyl groups provides good affinity with hydrolysed sulphate moieties of SDS, thus sinking DXM under the gas–liquid interface reducing the rate of oxidation at the gas–liquid interface, whereas (b) the fluoride moiety, being easily displaced from the molecule with the HO• radical, provides a convenient attachment site for the SDS-radical delivering the DXM molecule to the surface. Addition of 50 to 100 mg L^{-1} SDS showed oxidation efficiency decreased 2.3-2.7 times, while addition of the same amount of common HO• radical scavenger *tert*-butyl alcohol (TBA) reduced the efficiency 1.8-2.1 times (Paper III, Figure 7), confirming the predominantly surface character of oxidation. The HO• radical scavenging action of SDS is explained by the dominant bonding of dissociated sulphate groups of SDS with DXM hydrophilic hydroxyls (mechanism (a)) overpowering DXM-radical lifting to the surface with SDS-radical (mechanism (b)). The scavenging effect of TBA is explained by the role of in-depth HO• radicals in DXM oxidation. The small difference between SDS and TBA effects points to opposing tendencies of mechanisms (a) and (b) in the DXM interaction with SDS: in the absence of mechanism (b) of SDS interaction with the target pollutant, the former shows remarkably stronger radical-scavenging properties than TBA (Preis et al., 2013).

The SDS addition to gas-phase plasma oxidation of waterborne organic molecules can have both positive and negative effect on oxidation rate dependent on the target molecule structure. This is explained by SDS-radical formation after primary OH-radical attack. The SDS radical attaches itself to the target pollutant molecule and transports it to the surface for more effective oxidation. However, moieties around the target molecule can hinder this interaction, and SDS can shield smaller molecules from OH-radical attack thus decreasing the efficiency.

Conclusions

Pulsed corona discharge (PCD) was studied for the energy efficient oxidation of hazardous pollutants in aqueous solutions. Reactive textile dyes and emerging anti-inflammatory corticosteroid dexamethasone were oxidized for the first time using PCD. Impacts of operational conditions to PCD oxidation were studied in variation of pulse repetition frequency, pH, initial pollutant concentration, temperature and electric conductivity. The effect of surfactant sodium dodecyl sulphate addition to the treated solutions was determined and explained.

Operation parameters

Oxidation efficiency shown by PCD in respect of studied pollutants surpasses the one shown by any of known AOPs. Reactive blue-19 reacts faster with ozone than RB4 showing higher oxidation efficiency at higher pulse repetition frequency. Application of PCD to sodium chloride- and sulphate-containing RBs solutions with conductivity up to 20 mS cm^{-1} showed noticeable, although moderate reduction of oxidation efficiency. The difference in the character of salts is negligible indicating, together with failed detection of free chlorine in PCD-treated sodium chloride solutions, the absence of electrolytic phenomena. This is explained with short duration of pulses of bipolar profile with the secondary negative pulse current being close to the primary positive one thus avoiding progressive movement of heavy aqueous ions. Reduced oxidation rate at elevated temperature indicates limiting character of this factor for PCD application. Both conductivity and elevated temperature showed negative effects on the oxidation rate. Accelerated oxidation of RBs in solutions containing SDS surfactant is described for the first time confirming the surface character of reactions.

Explanation of surfactant impact

The variety in surfactant effect on gas-phase plasma oxidation of waterborne organic molecules was demonstrated with extensively used pharmaceuticals and textile dyes: additions of SDS may have both positive and negative effect on oxidation rate dependent on the target molecule structure. Explanation for such variety is proposed in SDS-radical formed as a result of primary OH-radical attack. This radical actively affiliates with the target pollutant molecule also radicalized with the OH-radical attack in a covalent bond and transports it to the plasma-liquid interface for effective oxidation with surface-borne OH-radicals, i.e. provides an accelerating impact of SDS addition. The transportation is more effective if the SDS-radical is attached strongly enough to the target molecule at sites of high electron density, e.g. aromatic rings. Side moieties at aromatic rings of the target molecules, however, may provide steric obstacles for the affinity of SDS-radical thus weakening transportation to the interface overpowered by OH-radical off-screening, which results in decelerating impact of SDS. Small hydrophilic molecules, such as oxalic acid, are complexed with the SDS sulfonate groups thus shielding those against OH-radical attacks and dramatically reducing the oxidation efficiency.

Dexamethasone oxidation

The study showed the promising character of PCD as a method of oxidation of aqueous corticosteroid with reliable performance in a variety of initial concentrations and pH values. Comparative ozonation demonstrated 2.4 times lower efficiency than PCD oxidation under analogous environmental conditions. The addition of TBA and SDS resulted in decreased oxidation energy efficiency, indicating the major role of HO• radicals in the oxidation process. Suggested transformation by-products confirm the

prevalence of HO• radicals in oxidation. The identification of oxidation end-products revealed fluoride and acetate as the products of DXM oxidation accumulating in the course of treatment; fluoride was produced in stoichiometric amounts in DXM PCD oxidation, i.e., was fully mineralized. Toxicity of DXM PCD-oxidation intermediate products measured by using the *Vibrio fischeri* test increased to some extent, indicating toxic transformation products, which were observed at a rather high DXM starting concentration of 40 mg L^{-1}. The oxidation of toxic by-products in further toxicity abatement presents a subject for supplementary studies.

The knowledge gained in this thesis contributes to the further development of plasma technology and possibly to the application of PCD in larger-scale as an energy efficient method for water treatment. The PCD is an utmost energy efficient alternative to the known advanced oxidation methods.

References

Abou-Ghazala, A., Katsuki, S., Schoenbach, K. H., Dobbs, F. C., Moreira, K. R. (2002). Bacterial decontamination of water by means of pulsed-corona discharges. *IEEE Transactions on Plasma Science*, 30(4), 1449–1453, DOI: 10.1109/TPS.2002.804193.

Ajo, P., Kornev, I., Preis, S. (2017). Pulsed corona discharge induced hydroxyl radical transfer through the gas-liquid interface, *Sci. Rep.*, 7, 16152, DOI: doi.org/10.1038/s41598-017-16333-1.

Ajo, P., Krzymyk, E., Preis, S., Kornev, I., Kronber, L., Louhi-Kultanen, M. (2016). Pulsed corona discharge oxidation of aqueous carbamazepine micropollutant. *Environ. Technol.*, 37 (16), 2072-2081, DOI: 10.1080/09593330.2016.1141236.

Andreozzi, R., Caprio, V., Insola, A., Marotta, R. (1999). Advanced oxidation processes (AOP) for water purification and recovery, *Catal. Today*, 53 (1), 51–59, DOI: 10.1016/S0920-5861(99)00102-9.

Bavasso, I., Poggi, C., Petrucci, E. (2020). Enhanced degradation of paracetamol by combining UV with electrogenerated hydrogen peroxide and ozone. *J. Water Process Eng.*, 34, 101102, DOI: 10.1016/j.jwpe.2019.101102.

Benedetti, B., Majone, M., Cavaliere, C., Montone, C. M., Fatone, F., Frison, N., Lagana, A., Capriotti, A. L. (2020). Determination of multi-class emerging contaminants in sludge and recovery materials from waste water treatment plants: Development of a modified QuEChERS method coupled to LC-MS/MS. *Microchem. J.*, 155, 104732, DOI: 10.1016/j.microc.2020.104732.

Berkessa, Y. W., Yan, B., Li, T., Jegatheesan, V., Zhang, Y. (2020). Treatment of anthraquinone dye textile wastewater using anaerobic dynamic membrane bioreactor: Performance and microbial dynamics, *Chemosphere*, 238, 124539, DOI: 10.1016/j.chemosphere.2019.124539.

Birben, N. C., Tomruk, A., Bekbolet, M. (2017). The role of visible light active TiO_2 specimens on the solar photocatalytic disinfection of E. coli, Environ. Sci. Pollut. Res., 24, 12618–12627, DOI: 10.1007/s11356-016-7769-8.

Boczkaj, G., Fernandes, A. (2017). Wastewater treatment by means of advanced oxidation processes at basic pH conditions: A review. *Chem. Eng. J.*, 320, 608–633, DOI: doi.org/10.1016/j.cej.2017.03.084.

Bogaerts, A., Neyts, E., Gijbels, R., van der Mullen, J. (2002). Gas discharge plasmas and their applications, *Spectrochim. Acta B: At. Spectrosc.*, 57(4), 609–658, DOI: 10.1016/S0584-8547(01)00406-2.

Calza, P., Pelizzetti, E., Brussino, M., Baiocchi, C. (2001). Ion Trap Tandem Mass Spectrometry Study of Dexamethasone Transformation Products on Light Activated TiO2 Surface. *J. Am. Soc. Mass Spectrom.*, 12 (12), 1286–1295, DOI: 10.1016/S1044-0305(01)00319-1.

Carneiro, P. A., Osugi, M. E., Fugivara, C. S., Boralle, N., Furlan, M., B Zanoni, M. V. (2005). Evaluation of different electrochemical methods on the oxidation and degradation of Reactive Blue 4 in aqueous solution. *Chemosphere*, 59 (3), 431–439, DOI: 10.1016/j.chemosphere.2004.10.043.

Chu, P. K., Lu, X. P., (2014) Low Temperature Plasma Technology: Methods and Applications, CRC Press, 1–488.

Cuerda-Correa, E. M., Alexandre-Franco, M. F., Fernandez-Gonzales, C. (2020). Advanced Oxidation Processes for the Removal of Antibiotics from Water. An Overview. *Water*, 12(1), 102, DOI: doi.org/10.3390/w12010102.

De Campos Ventura-Camago, B., Marin-Morales, M. A. (2013). Azo Dyes: Characterization and Toxicity – A Review. *Textile and Light Industrial Science and Technology*, 2 (2), 85–103.

Deng, Y., Zhao, R. (2015). Advanced Oxidation Processes (AOPs) in Wastewater Treatment. *Curr. Pollut. Rep.*, 1, 167–176, DOI: doi.org/10.1007/s40726-015-0015-z.

Desa, A. L., Hairom, N. H. H., Ng, L. Y., Ng, C. Y., Ahmad, M. K., Mohammad, A. W. (2019). Industrial textile wastewater treatment via membrane photocatalytic reactor (MPR) in the presence of ZeO-PEG nanoparticles and tight ultrafiltration. *J. Water Process Eng.*, 31, 100872, DOI: doi.org/10.1016/j.jwpe.2019.100872.

Dewil, R., Mantzavinos, D., Poulios, I., Rodrigo, M.A. (2017). New perspectives for advanced oxidation processes. *J. Environ. Manage.*, 195 (2), 93–99, DOI: 10.1016/j.jenvman.2017.04.010.

Durán, A., Monteagudo, J. M., Amores, V. (2008). Solar photo-Fenton degradation of Reactive Blue 4 in a CPC reactor, Appl. Catal. B Environ., 80 (1-2), 42–50, DOI: 10.1016/j.apcatb.2007.11.016.

Fanchiang, J. M., Tseng, D. H. (2009). Degradation of anthraquinone dye C.I. Reactive Blue 19 in aqueous solution by ozonation. *Chemosphere*, 77 (2), 214–221, DOI: 10.1016/j.chemosphere.2009.07.038.

Hao, O. J., Kim, H., Chiang, P. C. (2000). Decolorization of Wastewater. *Crit. Rev. Environ. Sci. Technol.*, 30 (4), 449–505, DOI: 10.1080/10643380091184237.

He, X.; Huang, H.; Tang, Y.; Guo, L. (2019). Kinetics and mechanistic study on degradation of prednisone acetate by ozone. *J. Environ. Sci. Health A*, 55 (3), 292–304, DOI: 10.1080/10934529.2019.1688020.

Hinojosa Guerra, M. M., Oller Alberola, I., Malato Rodriguez, S., Agüera López, A., Acevedo Merino, A., Quiroga Alonso, J. M. (2019). Oxidation mechanisms of amoxicillin and paracetamol in the photo-Fenton solar process, *Water Res.*, 156, 232–240, DOI: 10.1016/j.watres.2019.02.055.

Hsu, Y. C., Chen, Y. F., Chen, J. H. (2004). Decolorization of Dye RB-19 Solution in a Continuous Ozone Process. *J. Environ. Sci. Health*, 39 (1), 127–144, DOI: 10.1081/ese-120027373.

Hunag, Y., Dsikowitzky, L., Yang, F., Schwarzbauer, J. (2020). Emerging contaminants in municipal wastewaters and their relevance for the surface water contamination in the tropical coastal City Haikou, China. *Estruar. Coast. Shelf Sci.*, 235, 106611, DOI: 10.1016/j.ecss.2020.106611.

Kebriaei, M., Ketabi, A., Niasar, A. H. (2015). Pulsed Corona Discharge, a New and Effective Technique for Water and Air Treatment. *Biol. Forum*, 7 (1), 1686–1692.

Khan M. A. N., Siddique M., Wahid F., Khan R. (2015). Removal of reactive blue 19 dye by sono, photo and sonophotocatalytic oxidation using visible light. *Ultrason. Sonochem.*, 26, 370–377, DOI: 10.1016/j.ultsonch.2015.04.012.

Korenak, J., Helix-Nielsen, C., Bukšek, H., Petrinić, I. (2019). Efficiency and economic feasibility of forward osmosis in textile wastewater treatment. *J. Clean. Prod.*, 210, 1483–1495, DOI: 10.1016/j.jclepro.2018.11.130.

Kornev, I., Saprykin, F., Preis, S. (2017) Stability and energy efficiency of pulsed corona discharge in treatment of dispersed high-conductivity aqueous solutions, *J. Electrostat.*, 89, 42–50, DOI: 10.1016/j.elstat.2017.07.001.

Kornev, I., Saprykin, F., Preis, S. (2017). Stability and energy efficiency of pulsed corona discharge in treatment of dispersed high-conductivity aqueous solutions, *J. Electrostat.*, 89, 42–50, DOI: 10.1016/j.elstat.2017.07.001.

Kostich, M. S., Lazorchak, J. M. (2008). Risks to aquatic organisms posed by human pharmaceutical use. *Sci. Total Environ.*, 389 (2–3), 329–339, DOI: 10.1016/j.scitotenv.2007.09.008.

Krichevskaja, M., Klauson, D., Portjanskaja, E., Preis, S. (2011). The Cost Evaluation of Advanced Oxidation Processes in Laboratory and Pilot-Scale Experiments. *Ozone Sci. Eng.,* 33 (3), 211–223, DOI: 10.1080/01919512.2011.554141.

Kümmerer, K. (2009). Antibiotics in the aquatic environment – A review – Part I. *Chemosphere*, 75 (4), 417–434, DOI: 10.1016/j.chemosphere.2008.11.086.

Li, X., Wang, Y., Yuan, S., Li, Z., Wang, B., Huang, J., Deng, S., Yu, G. (2014). Degradation of the anti-inflammatory drug ibuprofen by electro-peroxone process. *Water Res.*, 63, 81–93, DOI: doi.org/10.1016/j.watres.2014.06.009.

Low, F. C. F., Wu, T. Y., The, C. Y., Juan, J. C., Balasubramanian, N. (2011). Investigation into photocatalytic decolorisation of CI Reactive Black 5 using titanium dioxide nanopowder. *Color. Technol.*, 128 (1), 44–50, DOI: 10.1111/j.1478-4408.2011.00326.x.

Magureanu, M., Mandache, N. B., Parvulescu, V. I. (2015). Degradation of pharmaceutical compounds in water by non-thermal plasma treatment, *Water Res.*, 81, 124–136, DOI: 10.1016/j.watres.2015.05.037.

Mansouri, L., Tizaoui, C., Geissen, S.-U., Bousselmi, L. (2019). A comparative study on ozone, hydrogen peroxide and UV based advanced oxidation processes for efficient removal of diethyl phthalate in water, *J. Hazard. Mater.*, 363, 401–411, DOI: 10.1016/j.jhazmat.2018.10.003.

Markic, M.; Cvetnic, M.; Ukic, S.; Kusic, H.; Bolanca, T.; Bozic, A.L. (2018). Influence of process parameters on the effectiveness of photooxidative treatment of pharmaceuticals. *J. Environ. Sci. Health A*, 53 (4), 338–351, DOI: 10.1080/10934529.2017.1401394.

Marković, M., Jović, M., Stanković, D., Kovačević, V, Roglić, G., Gojgić-Cvijović, G., Manojlović, D. (2015). Application of non-thermal plasma reactor and Fenton reaction for degradation of ibuprofen. *Sci. Total Environ.*, 505, 1148–1155, DOI: 10.1016/j.scitotenv.2014.11.017.

Matzek, L. W., Carter, K. E. (2016) Activated persulfate for organic chemical degradation: a review. *Chemosphere*, 151, 178–188, DOI: 10.1016/j.chemosphere.2016.02.055.

Nakamura, K. C., Guimarães, L. S., Magdalena, A. G., Angelo, A. C. D., De Andrade, A. R., Garcia-Segura, S., Pipi, A. R. F. (2019) Electrochemically-driven mineralization of Reactive Blue 4 cotton dye: On the role of in situ generated oxidants. *J. Electroanal. Chem*., 840, 415–422, DOI: doi.org/10.1016/j.jelechem.2019.04.016.

Nguyen, D. V., Ho, P. Q., Pham, T. V., Nguyen, T. V., Kim, L. (2019). Treatment of surface water using cold plasma for domestic water supply. *Environ. Eng. Res*., 24 (3), 412–417, DOI: 10.4491/eer.2018.215.

Onga, L., Kornev, I., Preis, S. (2020). Oxidation of reactive azo-dyes with pulsed corona discharge: surface reaction enhancement. *J. Electrostat*., 103, 103420. DOI: 10.1016/j.elstat.2020.103420.

Ono, R.; Oda, T. (2003). Dynamics of ozone and OH radicals generated by pulsed corona discharge in humid-air flow reactor measured by laser spectroscopy, *J. Appl. Phys*., 93, 5876–5882, DOI: doi.org/10.1063/1.1567796.

Oturan, M. A., Aaron, J.-J. (2014) Advanced Oxidation Processes in Water/Wastewater Treatment: Principles and Applications. A Review. *Crit. Rev. Environ. Sci. Technol.*, 44 (23), 2577–2641, DOI: 10.1080/10643389.2013.829765.

Pan, X. Y., Qiao, X. Ch. (2019). Influences of nitrite on paracetamol degradation in dielectric barrier discharge reactor. *Ecotoxicol. Environ. Saf*., 180, 610–615, DOI: 10.1016/j.ecoenv.2019.04.037.

Panorel, I., Preis, S., Kornev, I., Hatakka, H., Louhi-Kultanen, M. (2013). Oxidation of Aqueous Paracetamol by Pulsed Corona Discharge. *Ozone Sci. Eng*., 35 (2), 116–124, DOI: 10.1080/01919512.2013.760415. (A)

Panorel, I., Preis, S., Kornev, I., Hatakka, H., Louhi-Kultanen, M. (2013). Oxidation of aqueous pharmaceuticals by pulsed corona discharge. *Environ. Technol.*, 34 (7), 923–930, DOI: 10.1080/09593330.2012.722691. (B)

Parmar, N. D., Shukla, S. R. (2018). Decolourization of dye wastewater by microbial methods – A review. *Indian J. Chem. Technol*., 25 (4), 315–323.

Parvulescu, V. I., Magureanu, M., Lukes, P. (2012). Plasma Chemistry and Catalysis in Gases and Liquids, Wiley-VCH Verlag & Co. KGaA, 1–401, DOI: 10.1002/9783527649525.

Paždzior, K., Bilińska, L., Ledakowicz, S. (2019). A review of the existing and emerging technologies in the combination of AOPs and biological processes in industrial textile wastewater treatment. *Chem. Eng. J.*, 376, 120597, DOI: 10.1016/j.cej.2018.12.057.

Pignatello, J. J., Liu, D., Huston, P. (1999). Evidence for an Additional Oxidant in the Photoassisted Fenton Reaction. *Environ. Sci. Technol*., 33 (11), 1832–1839, DOI: 10.1021/es980969b.

Preis, S., Kornev, I., Hatakka, H., Kallas, J., Yavorovskiy, N. (2016). *Method and device for a liquid purifying and use of device*. (Patent of Finland No. 125772), Finnish Patent and Registration Office.

Preis, S.; Panorel, I.C.; Kornev, I.; Hatakka, H.; Kallas, J. (2013). Pulsed corona discharge: The role of ozone and hydroxyl radical in aqueous pollutants oxidation. *Wat. Sci. Technol.,* 68 (7), 1536–1542, DOI: 10.2166/wst.2013.399.

Preis, S.; Panorel, I.C.; Llauger Coll, S.; Kornev, I. (2014). Formation of nitrates in aqueous solutions treated with pulsed corona discharge: The impact of organic pollutants. *Ozone Sci. Eng*., 36 (1), 94–99, DOI: 10.1080/01919512.2013.836955.

Rahmani, H.; Rahmani, K.; Rahmani, A.; Zare, M.-R. (2015). Removal of dexamethasone from aqueous solutions using sono-nanocatalysis process. *Res. J. Environ. Sci*., 9 (7), 320–331, DOI: 10.3923/rjes.2015.320.331.

Rezaee A., Ghaneian M.T., Hashemian S.J., Moussavi G., Khavanin A., Ghanizadeh G. (2008). Decolorization of Reactive Blue 19 Dye from Textile Wastewater by the UV/H2O2 Process. *J. Appl. Sci*., 8 (6), 1108–1112, DOI: 10.3923/jas.2008.1108.1112.

Sonal, S., Singh, A., Mishra, B. K. (2018). Decolourization of reactive dye Remazol Brilliant Blue R by zirconium oxychloride as a novel coagulant: optimization through response surface methodology. *Water Science and Technology*, 78 (2), 379–389, DOI: 10.2166/wst.2018.307.

Song, S., Yao, J., He, Z., Qiu, J., Chen, J. (2008). Effect of operational parameters on the decolorization of C.I. Reactive Blue 19 in aqueous solution by ozone-enhanced electrocoagulation, *J. Hazard. Mater*., 152 (1), 204–210, DOI: 10.1016/j.jhazmat.2007.06.104.

Tran, N. H., Reinhard, M., Gin, K. Y. H. (2018). Occurrence and fate of emerging contaminants in municipal wastewater treatment plants from different geographical regions – a review. *Water Res*., 133, 182–207, DOI: 10.1016/j.watres.2017.12.029.

Turner, R. D. R., Warne, M. St. J., Dawes, L. A., Thompson, K., Will, G. D. (2019). Greywater irrigation as a source of organic micro-pollutants to shallow groundwater and nearby surface water. *Sci. Total Environ*., 669, 570–578, DOI: 10.1016/j.scitotenv.2019.03.073.

Van, H. T., Nguyen, L. H., Hoang, T. K., Nguyen, T. T., Tran, T. N. H., Nguyen, T. B. H., Vu, X. H., Pham, M. T., Tran, T. P., Pham, T. T., Nguyen, H. D., Chao, H. P., Lin, C. C., Nguyen, X. C. (2020). Heterogeneous Fenton oxidation of paracetamol in aqueous solution using iron slag as a catalyst: Degradation mechanisms and kinetics. *Environ. Technol. Innov.*, 18, 100670, DOI: 10.1016/j.eti.2020.100670.

Wang, Y.-X., Kornev, I., Wei, C.-H., Preis, S. (2019). Surfactant and non-surfactant radical scavengers in aqueous reactions induced by pulsed corona discharge treatment, *J. Electrostat*., 98, 82–86, DOI: 10.1016/j.elstat.2019.03.001.

Wardman, P. (1989). Reduction potentials of one electron couples involving free radicals in aqueous solution. *J. Phys. Chem. Ref. Data*, 18, 1637–1755, DOI: 10.1063/1.555843.

Wei, C., Zhang, F., Hu, Y., Feng, C., Wu, H. (2016). Ozonation in water treatment: the generation, basic properties of ozone and its practical application. R*ev. Chem. Eng*., 33 (1), 49–89, DOI: 10.1515/revce-2016-0008.

Zhang, F.-Z., Kong, Q.-P., Chen, H.-H., Zhao, X., Yang, B., Preis, S. (2022) Zero valent boron activated ozonation for ultra-fast degradation of organic pollutants: Atomic orbital matching, oxygen spillover and intra-electron transfer. *Chem. Eng. J.*, 436, 134674, DOI: 10.1016/j.cej.2022.134674.

Zhang, M., Dong, H., Zhao, L., Wang, D., Meng, D. (2019). A review on Fenton process for organic wastewater treatment based on optimization perspective*. Sci. Total Environ*., 670, 110–121, DOI: 10.1016/j.scitotenv.2019.03.180.

Acknowledgements

I would like to express my gratitude to my supervisor Prof. Sergei Preis for his guidance and valuable ideas throughout the years of my PhD study. I am sincerely thankful to Prof. Marina Trapido for giving me the opportunity to carry out this PhD research. I am thankful to all the colleagues in the Laboratory of Environmental Technology. I would especially like to thank Dr. Niina Dulova for her continuous encouragement and support throughout my PhD studies. My deepest gratitude goes to my friends and loving family: my husband, sister, mother and father.

Abstract

Oxidation of aqueous organic molecules in gas-phase pulsed corona discharge: impact of operation parameters

The urbanization and industrialization of society results in increasing aquatic occurrence of recalcitrant compounds such as personal care products, pharmaceuticals and other harmful compounds from industries and households that pose threat to human health as well as animals and the environment. Textile industry generates large amounts of wastewater containing textile dyes, fixatives, sizing and dying agents. Often toxic, mutagenic and carcinogenic textile dyes cause disturbances in aquatic life as well as interfere with photosynthesis. Human pharmaceuticals enter the environment primarily when excreted by patients, being disposed as unused medicine and released from manufacturing.

Application of advanced oxidation processes (AOPs) based on generation and utilization of hydroxyl radicals (HO•) have shown great potential for degradation and mineralization of recalcitrant compounds. However, the problems related to the application of AOPs are high operational and initial instalment costs. Ozone application is commercially available powerful and human-friendly advanced oxidation method, however, the approach is energy consuming, narrowing the AOPs application field and leaving water treatment problems unsolved. Thus, more reliable and cost-effective alternatives to ozonation are needed. Gas-phase pulsed corona discharge (PCD) has proven its advanced character surpassing conventional ozonation for a few times in respect of various pollutants. The target pollutants taken in consideration in this study include textile dyes reactive blue 4, reactive blue 19, indigo tetrasulphonate, acid orange 7, and pharmaceuticals paracetamol, indomethacin, and dexamethasone (DXM).

The objectives of the study include stablishing the impacts of pulse repetition frequency, temperature, and electric conductivity to the PCD treatment of selected aqueous textile dyes and pharmaceuticals confirming the hypothesis of surface-borne character of PCD oxidation; clarifying the potential of electrolytic phenomena in PCD; giving an explanation to varying impact of surfactant addition to PCD oxidation; establishing the effect of pulse repetition frequency, pH, and pollutant initial concentration to PCD oxidation of emerging anti-COVID-19 drug DXM in experimental comparison with ozonation; establishing the role of surfactant and non-surfactant OH-radical scavengers to DXM oxidation together with identifying oxidation products in PCD and ozone treatment together with their toxicity.

The PCD oxidation of reactive dyes showed negative effect of elevated conductivity and temperature to energy efficiency. Sodium sulphate and chloride reduced the RBs' oxidation efficiencies equally in respect to conductivity with no electrolysis and free chlorine effect observed. To study the surface character of PCD-initiated reactions, surfactant radical scavenger sodium dodecyl sulphate (SDS) was added to the reactive dye solution. Contrary to previous observations, SDS addition improved the oxidation efficiency of the reactive dyes for 2.2 times. Further study of the surfactant effect to the dyes and pharmaceuticals brought to the conclusion that additions of SDS may have both positive and negative effect on oxidation rate dependent on the target molecule structure.

Oxidation of DXM with PCD and conventional ozonation studied under similar conditions for the first time showed PCD surpassing ozonation in energy efficiency. The highest efficiency observed in respect of DXM oxidation was observed in acidic solutions. Under neutral medium conditions, the energy efficiency at 50 pps reached 8.9 g $kW^{-1}h^{-1}$, while at 880 pps the efficiency comprised only 6.0 g $kW^{-1}h^{-1}$ indicating substantial role of ozone. The PCD oxidation demonstrated oxidation energy efficiency 2.4 times higher than ozonation. Identification of DXM oxidation products revealed acetate and fluoride as the main end products. Toxicity determined by using the *Vibrio fischeri* test of PCD-treated DXM solutions somewhat increased on course of treatment, which was observed at rather high DXM starting concentration of 40 mg L^{-1}.

The knowledge gained in this thesis contributes to the further development of plasma technology and possibly to the application of PCD in larger scale as energy efficient method for water treatment, potentially replacing conventional ozonation.

Lühikokkuvõte

Orgaaniliste molekulide oksüdeerimine gaasifaasilise koroona-impulss elektrilahendusega: töörežiimi parameetrite mõju

Tööstuse arengu ning linnastumise tagajärjel leidub vesikeskkonnas üha sagedamini raskesti lagundatavaid saasteaineid nagu hügieenitooteid, ravimeid ning teisi ohtlikke ühendeid, mis kujutavad ohtu nii inimtervisele kui ka loomadele ja keskkonnale. Tekstiilitööstuse reoveed sisaldavad palju erinevaid saasteaineid nagu tekstiilvärvid, fiksaatorid ning muud lisaained. Tekstiilvärvid on tihti toksilised, mutageensed ja kantserogeensed, põhjustades probleeme vee-elustikule ning takistades fotosünteesi. Ravimid satuvad keskkonda peamiselt inimorganismist eritudes, kasutamata ravimite vale käitlemise tõttu ning tööstusest.

Raskesti lagundatavate ainete eemaldamiseks ja mineraliseerumiseks on suurt võimekust näidanud süvaoksüdatsiooniprotsessid (SOP), mis põhinevad suure oksüdatsioonipotentsiaaliga hüdroksüülradikaalide (HO•) genereerimisel. SOPide rakendamisega seotud probleemide hulka kuuluvad aga kõrged tegevuskulud ning esmased väljaminekud. Osoonimine on laialdaselt kasutuses olev veetöötlusmeetod, mille puuduseks on suur energiakulu ning seetõttu ka kõrge hind, mistõttu jäävad paljud veepuhastusega seotud probleemid lahendamata. Sellest tulenevalt on veepuhastuses nõudlus usaldusväärsete ning energiatõhusamate alternatiivide järele. Gaasifaasiline koroona-impulss elektrilahendus (KIEL) on näidanud mitmekordselt paremat energiaefektiivsust võrreldes osoonimisega. Käesolevas töös vaatluse all olevad saasteained on tekstiilvärvid reaktiivsinine 4, reaktiivsinine 19, indigotetrasulfonaat ja happeoranž 7 ning ravimid paratsetamool, indometatsiin ja deksametasoon (DXM).

Doktoritöö eesmärkideks oli uurida töötingimuste nagu imupulsisagedus, temperatuur ja elektrijuhtivus mõju tekstiilvärvide eemaldamisele veest. Samuti oli eesmärgiks kinnitada pinnapealse reaktsiooni toimumist tekstiilvärvide näitel ning uurida elektrolüüsi tekke võimalikkust KIEL reaktoris. Töö hõlmas ka pindaktiivse aine varieeruva mõju selgitamist erinevate tekstiilvärvide ning ravimite näitel. Uudse ravimi deksametasooni lagundamisel oli eesmärgiks leida töötlemisparameetrite, nagu impulsisagedus, pH, saasteaine algkontsentratsioon, mõju ning võrrelda KIEL töötluse energiaefektiivsust osoonimisega. Samuti oli DXM puhul eesmärgiks hüdroksüülradikaalide mõju uurimine erinevate radikaalipüüdurite lisamisel ning laguproduktide uurimine ja toksilisuse hindamine kasutades bioluminestsents analüüsi bakteritel *Vibrio ficheri*.

Temperatuuri ning elektrijuhtivuse tõstmine mõjutasid reaktiivsiniste tekstiilvärvide oksüdeerimist KIEL reaktoris negatiivselt. Naatriumsulfaadi ning –kloriidi lisamine langetasid oksüdeerimise efektiivsust võrdselt ning vaba kloori sisaldust ning elektrolüüsi olemasolu KIEL reaktoris ei tuvastatud. Pinnareaktsioonide toimumise uurimiseks lisati KIEL reaktorisse tekstiilvärvide lagundamisel pindaktiivset radikaalide püüdjat naatriumdodetsüülsulfaati (SDS). Eelnevatele uuringutele vastupidiselt tõstis SDS reaktiivsete siniste tekstiilvärvide oksüdeerimisefektiivsust 2.2 korda. Edasine uuring pindaktiivse aine mõju kohta tõi järelduse, et pindaktiivse aine lisamine KIEL reaktorisse võib saasteainete eemaldamise efektiivsusele mõjuda nii positiivselt kui ka negatiivselt, sõltuvalt saasteaine molekuli struktuurist.

DXM lagundamist uuriti esmakordselt võrreldes KIEL-i ning traditsioonilist osoonimist. Tulemused näitasid, et KIEL oli osoonimisest 2.4 korda kõrgema energiaefektiivsusega. DXM lagundamine oli kõige efektiivsem happelises keskkonnas. Neutraalses keskkonnas andis impulsi sagedus 50 pps energiaefektiivsuseks 8.9 g kW^{-1}h^{-1}, kui 880 pps juures oli see vaid 6.0 g kW^{-1}h^{-1}, millest võib järeldada, et osoonil on DXM lagundamisel suur roll. DXM laguproduktide uurimisel leiti peamisteks lõpp-produktideks atsetaat ning fluoriid. Töödeldud DXM lahuste toksilisuse uurimisel *Vibrio fischeri* abil leiti, et toksilisus kasvab töötluse järel, mis näitab, et DXM laguproduktid on toksilisemad kui lähteühend. Antud toksilisuse testi tehti üsna kõrgel saasteaine algkontsentratsioonil 40 mg L^{-1}.

Doktoritöö tulemused aitavad kaasa plasmatehnoloogia edasisele arengule ning suuremas mahus KIEL rakendamisele veepuhastuses. KIEL pakub energiaefektiivset asendust või alternatiivi olemasolevatele traditsioonilistele veepuhastusmeetoditele.

Appendix 1

Paper I

Onga, L.; Kornev, I.; Preis, S. (2020). Oxidation of reactive azo-dyes with pulsed corona discharge: surface reaction enhancement. Journal of Electrostatics, 103, 103420.

Oxidation of reactive azo-dyes with pulsed corona discharge: Surface reaction enhancement

Liina Onga [a], Iakov Kornev [b], Sergei Preis [a, *]

[a] *Laboratory of Environmental Technology, Department of Materials and Environmental Technology, Tallinn University of Technology, 5 Ehitajate Tee, Tallinn, 19086, Estonia*
[b] *School of Advanced Manufacturing Technologies, National Research Tomsk Polytechnic University, 2A Lenin Ave, 634028, Tomsk, Russian Federation*

ABSTRACT

Emissions of textile dyes result in biological hazard. The technology response to the problem of textile dyes suffers unaffordable costs. Application of pulsed corona discharge (PCD) to azo-dyes oxidation requires establishing operation conditions. Experimental studies in oxidation of reactive blue RB4 and RB19 were undertaken with variation of pulse, temperature, electrolyte and surfactant parameters. Application of PCD demonstrated dyes removed at high energy efficiency, up to 340–360 g kW^{-1} h^{-1} in presence of a surfactant. Sodium sulphate and chloride reduced RBs' oxidation efficiencies equally in respect to conductivity with no electrolysis observed. The negative effect of elevated temperature was quantified.

1. Introduction

Wet processes in textile industry generate large amounts of wastewater containing textile dyes, fixatives, sizing and dying agents [1]. The main environmental hazard related to the textile industry consists of the use of azo dyes resistant to natural degradation with toxic, mutagenic and carcinogenic effects on aquatic organisms, together with screening-off the light interfering with the natural photosynthetic processes [2]. Reactive azo dyes are used extensively for their high stability, bright colour and simple application techniques with low energy consumption [3]. The reactive dying procedure demands substantial amounts of sodium chloride and sulphate in alkaline solutions, making dye concentrations in wastewaters reaching 1.5 g L^{-1} at salinity about 5–6% of NaCl and Na$_2$SO$_4$ [4].

Wastewaters containing azo-dyes are difficult and expensive in conventional treatment methods being energy-consuming (UV/H$_2$O$_2$, electrochemical oxidation), forming substantial amounts of sludge (coagulation, Fenton's oxidation) and causing serious problems in handling concentrated residues (membrane filtration) and spent materials (adsorption). Colour removal using micro-organisms in aerobic and anaerobic processes is decisive in conventional treatment, although still remaining immature: combination of wastewater pre-treatment using advanced oxidation processes (AOPs) with subsequent biological treatment is considered as the most promising direction of development [5,

6]. Advanced oxidation is making its way to the market mostly in the form of ozone application, which remains a powerful, human-friendly, but energy-consuming approach. Comparative cost analysis of AOPs applied to the target azo dyes oxidation was conducted using available literature with results shown in Table 1. The target compounds were chosen for their wide use with the research data accumulated in their degradation with AOPs. Comparison was made in respect to reactive blue RB4 (1-Amino-4-[3-(4,6-dichlorotriazin-2-ylamino)-4-sulfophenylamino] anthraquinone-2-sulfonic acid, C$_{23}$H$_{14}$Cl$_2$N$_6$O$_8$S$_2$) and RB19 (remazol brilliant blue R, 2-(3-(4-amino-9,10-dihydro-3-sulpho-9,90-dioxoanthracen-4-yl)aminobenzenesulphonyl)vinyl)disodiumsulphate, C$_{22}$H$_{16}$O$_{11}$N$_2$S$_3$Na$_2$). The energy efficiencies for AOPs were calculated considering costs used by Krichevskaya et al. [7] for electric energy (0.0343 EUR kW^{-1}h^{-1}), 50-% solution of H$_2$O$_2$ (0.8217 EUR kg^{-1}) and ferrous sulphate (0.7163 EUR kg^{-1}). Costs of chemicals were recalculated to energy expense. Energy expense for ozone synthesis was considered comprising no less than 15 kWh kg^{-1} O$_3$ when using oxygen, which is doubled when using air [8].

Previous research in application of gas-phase pulsed corona discharge (PCD) to the treatment of aqueous solutions and polluted waters showered through the discharge zone showed its highest energy efficiency among AOPs in removal of various aqueous pollutants surpassing conventional ozonation for a few times [9,10]. Potential application of PCD towards elimination of textile azo dyes requires, however,

experimental establishing regularities in oxidation for beneficial operation conditions. Impacts of temperature, salts and a surfactant constitute also subjects for studies for being attributable for the textile treatment processes.

2. Materials and methods

2.1. Chemicals

The dye RB4 with the pigment content ≥35% was purchased from Alfa Aesar, and RB19, marked as 'pure', and N,N-diethyl-p-phenylenediamine (DPD) sulphate (≥99%) - from Acros Organics. Dye solutions containing about 40 mg L^{-1} of target compound were prepared using distilled water. Sodium dodecyl sulphate (SDS, $NaC_{12}H_{25}SO_4$) and mineral salts of analytical grade, Na_2SO_4, NaCl, Na_2HPO_4 and KH_2PO_4 (≥98%) were purchased from Lach-Ner, Ltd. (Czech Republic).

2.2. Methods of analysis

Dye concentrations were measured using Helios β spectrophotometer (Thermo Electron Corporation, USA) at maximum absorbance wavelengths of 595 and 592 nm for RB4 and RB19, respectively. pH was measured using S220 digital pH-meter (Mettler Toledo, Switzerland) and oscillated in experiments between 6.5 and 6.9. Multi-parameter meter HQ430d (Hach Company, USA) was used for conductivity measurement. Concentration of free chlorine was determined with standard DPD colorimetric method using spectrophotometer at 515 nm [18].

2.3. Experimental equipment

The experimental equipment manufactured by Flowrox Oy (Finland) consists of PCD reactor with the storage tank of 40 L capacity, pulse generator and circulation pump providing the treated solutions flow rate of 1.0 $m^3 h^{-1}$. The multiple string electrodes 0.55 mm in diameter and 20 m of total length are positioned horizontally between vertical parallel plates as described earlier [19]. The electrode system configuration was chosen to provide smaller conductivity losses using construction described by Kornev et al. [20]. The distance between wire electrodes and the grounded plate is 18 mm. Treated solutions were dispersed through the perforated plate with 49 perforations of 1.5 mm diameter positioned in a vertical plane with the high voltage string electrodes. Pulses of voltage amplitude of 18 kV, current of 380 A, and 100 ns duration with power delivered to the reactor of 32 W and 123 W at 200 and 880 pulses per second (pps), respectively, were provided by the generator. The pulse characteristics were quantified with a Rigol

DS1102E Mixed Signal Oscilloscope, a Tektronix P6015 high voltage probe (Tektronix Inc., USA) and a current monitor PT-7802 (PinTek, China). The energy of a pulse delivered to the reactor was 0.19 and 0.15 J at 200 and 880 pps, respectively, calculated by integration of voltage and current time profiles [20]. The reactor was filled with air ventilated at 2.0 L min^{-1} with a compressor.

The energy efficiency of oxidation was calculated using Eq. (1):

$$E = \frac{\Delta C \cdot V}{W} \tag{1}$$

where ΔC is the decrease in dye concentration, mg L^{-1}, V is the volume of treated solution, L, and W is the energy consumption as a product of power delivered to the reactor and the time of treatment, kWh. The output-input ratio of pulse generator equals 65%.

3. Results and discussion

3.1. Oxidation efficiency

The impact of pulse repetition frequency exhibits to a certain extent the balance between short- and long-living oxidants involved in oxidation of pollutants [21]. Experimental results shown in Fig. 1 indicate high efficiencies (Table 1) of both RB4 and RB19 dyes oxidation reaching at 200 pps about 132–133 g $kW^{-1} h^{-1}$ at 90% dye removal. Higher oxidation efficiency of RB19 at 880 pps indicates its higher reactivity with both short- and long-living oxidation species, than RB4. One can see relatively small with RB19 but more noticeable with RB4 effect of pulse repetition frequency on oxidation efficiency indicating certain role of ozone played in their oxidation: more rapid reaction of RB19 with ozone makes the difference between pulse repetition frequencies smaller. The difference in reaction kinetics of two target compounds is explained by the difference in reactive groups influencing oxidation of identical chromophore moieties of the molecules. The moderate effect of pulse repetition frequency is characteristic for fast-reacting substances as was observed earlier for phenol [19].

3.2. Effect of conductivity

Effect of increased conductivity was studied using two salts, sodium sulphate and chloride: conductivity was found to determine losses in the discharge energy [20]. Besides the effect of conductivity, chloride was used to study possible effect of electrolysis with free chlorine evolution: hypothetical free chlorine presents an interest concerning well-known textile dyes discoloration. For example, Nakamura et al. [16] treated RB4 solutions in electro-Fenton process using Na_2SO_4 and NaCl as

Table 1
Examples of energy efficiencies of RB4 and RB19 removal using AOPs.

Compound	Initial concentration, mg L^{-1}	Process	Colour removal, %	Energy efficiency, g $kW^{-1}h^{-1}$	Reference
RB19	100.0	Ozonation	100	30.03[a]	[11]
	20.0	Sonophotocatalytic oxidation	100	0.008[b]	[12]
	25.0	UV/H_2O_2	90	2.35[c]	[13]
	100.0	Ozone-enhanced electrocoagulation	90	0.4[a]	[14]
RB4	63.6	Photo-Fenton	90	2,3[d]	[15]
	231.0	Electrochemical oxidation	90	2.1–3.8[e]	[16]
		Electro-Fenton	90	15.2–28.1[e]	
		Photoelectron-Fenton	90	2.4–3.4[e]	
	27.5	Fenton	22	1.01[f]	[17]
	27.0	Solar photo-Fenton	92	4.14[f]	

[a] Energy efficiency was calculated for ozone synthesis energy expense of 15 kWh kg^{-1} O_3 when using oxygen. Published data were insufficient to calculate the energy efficiency relative to consumed ozone, i.e. no outlet gaseous ozone concentration was reported, making the authors operating with delivered ozone doses. In ozone-enhanced electrocoagulation, only the energy expense for ozone synthesis was taken in calculation.
[b] Energy of ultrasound was considered; energy of light was not taken into consideration.
[c] Power of UV-lamp of 55W considered. At 15 W the efficiency comprised 1.88 g $kW^{-1}h^{-1}$ at 45% degradation of RB19.
[d] Energy of light source and hydrogen peroxide expense were considered. No catalyst expense included.
[e] Electrical energy per order (E_{EO}) was taken for decolourization in consistence with the present research.
[f] Costs of hydrogen peroxide and ferrous sulphate were considered in expense calculation; solar energy was considered free.
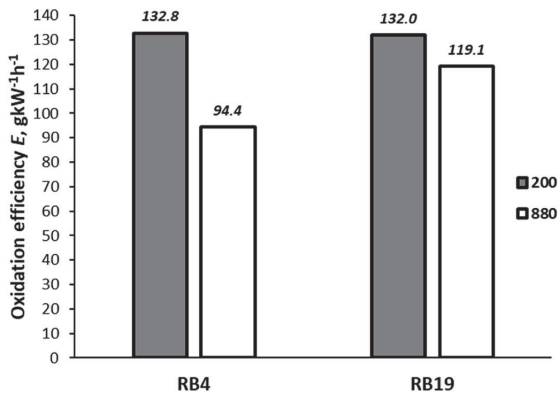
Fig. 1. Effect of pulse repetition frequency on oxidation efficiencies of RB4 and RB19 textile dyes: starting concentration 40 mg L^{-1}, frequencies of 200 and 880 pps correspond to 32 and 123 W of power delivered to the reactor, oxidation efficiency given for 90-% colour removal.

supporting electrolytes and found the colour removal being twofold faster with NaCl on account of free chlorine. Possible formation of chlorinated organic compounds is also of vivid interest due to their resistance towards biodegradability with limitations thus placed to PCD application.

Sodium chloride dissolved in distilled water in amounts of 5.6 and 11.2 g L^{-1} resulting in electric conductivity of solutions 10 and 20 mS cm^{-1} at 20 °C, respectively, was PCD-treated for times from 1 to 60 min at 880 pps thus supplying up to 12.3 kWh m^{-3} energy dose. Analysis of samples taken on the course of treatment conducted with DPD colorimetric method showed no trace of free chlorine within the method's detection limit of 18 μg L^{-1}.

The experiments with PCD-oxidation of RB4 and RB19 dyes in conductive solutions showed noticeable reduction in oxidation efficiency due to ohmic losses in conductive solutions described earlier [20]. Salts exhibited only a small difference in experimentally observed oxidation efficiency reduction regardless the character of salt, sulphate or chloride (Fig. 2).

Conductivities with sodium sulphate at 10 and 20 mS cm^{-1} at 20 °C were provided with dissolution of 8.4 and 16.8 g L^{-1} of Na$_2$SO$_4$, respectively. One can see that the oxidation efficiency at 10 mS cm^{-1} decreased for practically identical numbers for both chloride and sulphate salts. The effect of 20 mS cm^{-1} was only slightly stronger with sulphate.
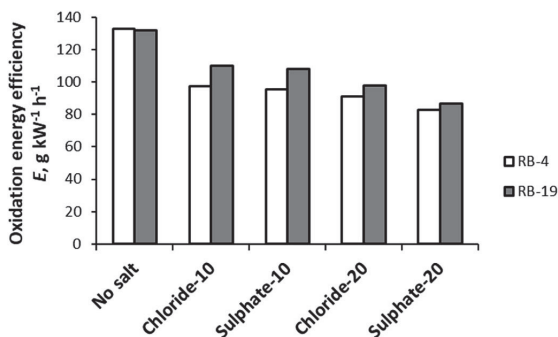
The absence of free chlorine observed in direct measurements and the absence of difference between sulphate and chloride reducing the dyes' oxidation efficiency indicate negligible electrolysis in treated solutions. Bipolar shape of the voltage pulse was implemented to minimize the pulse duration thus reducing the probability of spark formation. The starting positive pulse changes in about 100 ns to the negative one of similar amplitude and duration [20] giving no progressive movement to massive chloride ions and minimizing the direct current to evoke electrolysis.

3.3. Effect of temperature

Raising the temperature of the treated solution had a notable effect on the oxidation efficiency: the temperature of the RB4 solution raised from 20 to 35 and 45 °C resulted in the efficiency decreased for 41 and 58%, respectively. The corresponding efficiency decrease for RB19 comprised 78 and 81% under similar temperature conditions (Fig. 3). Deterioration of oxidation efficiency with increased temperature in respect to oxalate was noticed earlier and explained with accelerated OH-radical termination reaction [22] and thus confirmed in present study. Noticeably stronger effect of temperature in RB19 oxidation is consistent with behaviour of the dyes at pulse repetition frequency variation: smaller effect of frequency at overall rapid oxidation indicates the RB19 reaction with ozone being faster than that of RB4; analogously, lower solubility and productivity of ozone in the discharge at higher temperature exhibit stronger negative effect with rapidly reacting RB19.

The additive effect of temperature and conductivity was tested at maximum temperature applied in the study of 45 °C and conductivity of 10 mS cm^{-1} provided by addition of both salts. The results are shown in Fig. 4, from which one can see the effect of conductivity at elevated temperature deteriorating oxidation efficiency consistently with the one observed at ambient conditions. At 45 °C, the effect of chloride is consistently close to the one of sulphate indicating no free chlorine involved in the dyes discoloration at elevated temperature.

3.4. Effect of surfactant

Surface character of reactions initiated with PCD-treatment attracts attention to the role of surfactant radical scavengers in those [19]. Surfactants are also present in textile production wastewaters being used in fabrics dyeing and for removal of excess dyes. The role of detergents thus appears important in textile dye PCD oxidation being studied in the research. To study the impact of surfactants to the dye degradation, SDS was chosen for its wide usage at low cost.

Contrary to the deceleration effect in PCD oxidation of phenol, oxalate and humic substances reported earlier [19], addition of SDS dramatically improved oxidation of RB4 and RB19 (Fig. 5): oxidation
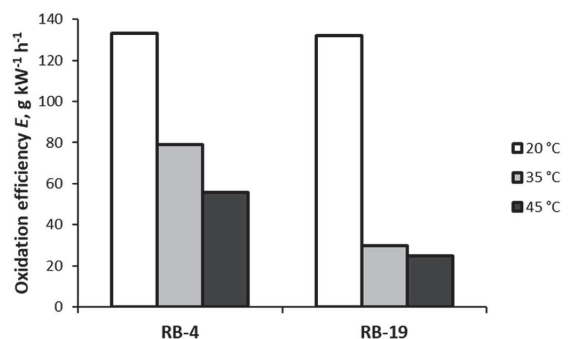

Fig. 2. Effect of conductivity of 10 and 20 mS cm^{-1} on oxidation efficiencies of RB4 and RB19 dyes: starting dyes concentration 40 mg L^{-1}, pulse repetition frequency 200 pps (32 W), oxidation efficiency given for 90-% colour removal.
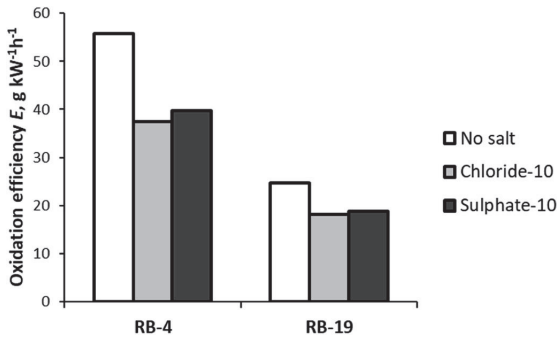

Fig. 3. Effect of temperature on oxidation efficiencies of RB4 and RB19 dyes: starting dyes concentration 40 mg L^{-1}, pulse repetition frequency 200 pps (32 W), oxidation efficiency given for 90-% colour removal.

Fig. 4. Effect of conductivity of 10 mS cm^{-1} on oxidation efficiencies of RB4 and RB19 dyes at 45 °C: starting dyes concentration 40 mg L^{-1}, pulse repetition frequency 200 pps (32 W), oxidation efficiency given for 90-% colour removal.

efficiency increased with the SDS concentration at about 75–100 mg L^{-1}, which is close to the equimolar ratio with RBs at their 40 mg L^{-1} content, for 2.4 and 2.2 times for RB4 and RB19, respectively, reaching 340–360 g kW^{-1} h^{-1} at 90-% discoloration. At 50 mg L^{-1} of SDS content, the RB19 dye discoloration rate was somewhat smaller comprising about 274 g kW^{-1} h^{-1}; increased SDS concentration to 200 mg L^{-1} did not result in further changes in oxidation efficiency. Concentration of SDS of 75 mg L^{-1} was further applied in experiments clarifying the additive effect of elevated temperature and conductivity.

Due to surface character of reaction in PCD treatment of aqueous media [19,22], accelerated textile dyes oxidation may be explained by molecular interaction between SDS and a dye resulting in transportation of the latter to the gas-liquid interface, where RB molecules appear exposed to oxidation with surface-borne reactive oxygen species. Anionic surfactant SDS and anionic reactive blue dye molecules are of organosulphate class with identical hydrophilic sulphate functional groups and disparate organic residues. Interaction between surfactant and textile dye molecules is well-known as applied in so-called cloud point extraction (CPE) used for textile dye removal from wastewaters, which includes RB19 [23]. Textile dyes molecules are removed by flotation being entrapped at surfactant micelles formed in the bulk of solution due to steric restrictions of hydrophobic alkyl chains not involving interaction between charged groups [24]. Concentrations of surfactants in CPE, however, must exceed critical micelle concentration

comprising 8.2 mM at 25 °C, which for SDS is 2362 mg L^{-1} substantially exceeding concentrations applied in the study. Nevertheless, mixed aggregates of the dye and surfactant below the critical micellar concentration of the latter were observed by Petcu et al. [25] supporting the explanation given in this study.

To verify the additive effect of conductivity and temperature to the oxidation of RB19 dissolved together with SDS, PCD experiments with variety of these parameters were conducted with aqueous solutions containing 40 mg L^{-1} of RB19 and 75 mg L^{-1} of SDS. Conductivity was adjusted with sodium chloride solution. The resultant oxidation efficiencies are shown in Fig. 6.

The dramatic effect of SDS addition is seen in the two first columns, oxidation of RB19 with SDS is 2.6 times faster than without admixtures. One can see that effects of temperature and conductivity in SDS-containing solutions are consistent with those observed without SDS additions: increased temperature resulted in decreased oxidation rate (Figs. 2 and 3); conductivity negative effect was additive with the temperature one (Fig. 4). It is worth to notice, that higher conductivity of 20 mS cm^{-1} provided with higher salt content resulted in foaming intense enough to interfere with experiments at 20 °C filling the reactor thus short-circuiting the discharge. Foaming was, however, almost entirely supressed at higher temperature applied in experiments.
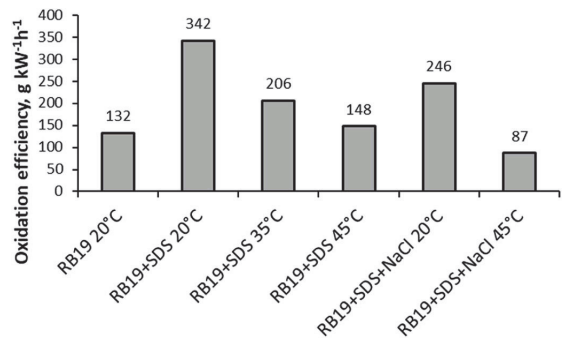

Fig. 6. Additive effects of temperature and conductivity (10 mS cm^{-1}) on oxidation efficiency of RB19 in solutions containing SDS (75 mg L^{-1}): starting RB19 concentration 40 mg L^{-1}, pulse repetition frequency 200 pps (32 W).
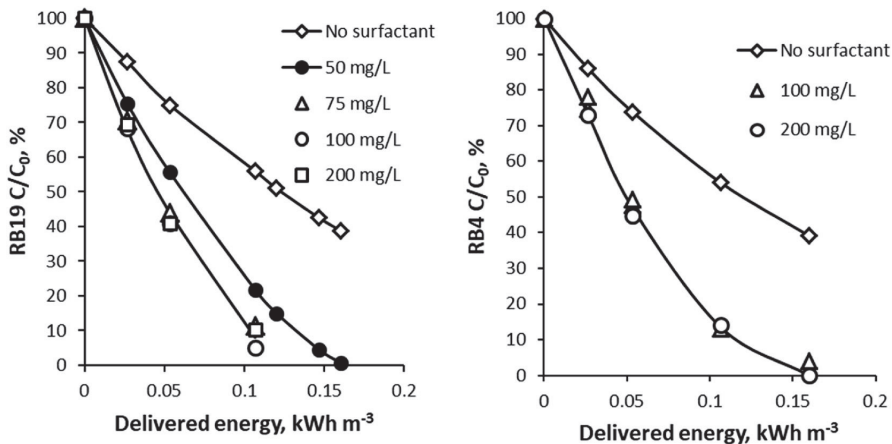

Fig. 5. Dependence of RB19 (left) and RB4 (right) discoloration on pulsed energy delivery at SDS concentration variations: conductivity 100–150 μS cm-1 (distilled water), 20 °C, starting dyes concentration 40 mg L^{-1}, pulse repetition frequency 200 pps (32 W).

4. Conclusions

The study showed promising character of pulsed corona discharge as a method of oxidation of aqueous reactive blue textile dyes with the role of impact factors clarified. Oxidation efficiency shown by PCD in respect of RB4 and RB19 surpasses the one shown by any of known AOPs. Reactive blue-19 reacts faster with ozone than RB4 showing higher oxidation efficiency at higher pulse repetition frequency. Application of PCD to sodium chloride- and sulphate-containing solutions in concentrations up to 11.2 and 16.8 g L^{-1}, respectively, with conductivity reaching 20 mS cm^{-1} showed noticeable, although moderate reduction of oxidation efficiency. The difference in the effect of salts is negligible indicating, together with failed detection of free chlorine in PCD-treated sodium chloride solutions, the absence of electrolytic phenomena. This is explained with short duration of pulses of binary profile with the secondary negative pulse current being close to the primary positive one thus avoiding progressive movement of heavy aqueous ions. Reduced oxidation rate at elevated temperature indicates limiting character of this factor for PCD application. Conductivity and elevated temperature showed additive negative effect on the oxidation rate. Accelerated oxidation of RBs in solutions containing SDS surfactant is described for the first time confirming the surface character of reactions. In applications of PCD to textile production wastewater treatment, the observation may have practical importance.

Declaration of competing interest

The authors declare that they have no known competing financial interests or personal relationships that could have appeared to influence the work reported in this paper.

Acknowledgements

References

[1] Y.-C. Hsu, Y.-F. Chen, J.-H. Chen, Decolorization of dye RB-19 solution in a continuous ozone process, J. Environ. Sci. Health Part A 39 (2004) 127–144, https://doi.org/10.1081/ESE-120027373.

[2] B. de Campos Ventura-Camargo, M. Aparecida Marin-Morales, Azo dyes: characterization and toxicity – a review, Text. Light Ind. Sci. Technol. 2 (2013) 85–103.

[3] S. Sonal, A. Singh, B.K. Mishra, Decolorization of reactive dye remazol brilliant blue R by zirconium oxychloride as a novel coagulant: optimization through response surface methodology, Water Sci. Technol. 78 (2018) 379–389, https://doi.org/10.2166/wst.2018.307.

[4] Y.W. Berkessa, B. Yan, T. Li, V. Jegatheesan, Y. Zhang, Treatment of anthraquinone dye textile wastewater using anaerobic dynamic membrane bioreactor: performance and microbial dynamics, Chemosphere 238 (2020), 124539, https://doi.org/10.1016/j.chemosphere.2019.124539.

[5] N.D. Parmar, S.R. Shukla, Decolourization of dye wastewater by microbial methods - a review, Indian J. Chem. Technol. 25 (2018) 315–323.

[6] K. Paździor, L. Bilińska, S. Ledakowicz, A review of the existing and emerging technologies in the combination of AOPs and biological processes in industrial textile wastewater treatment, Chem. Eng. J. 376 (2019), 120597, https://doi.org/10.1016/j.cej.2018.12.057.

[7] M. Krichevskaya, D. Klauson, E. Portjanskaja, S. Preis, The cost evaluation of advanced oxidation processes in laboratory and pilot-scale experiments, Ozone: Sci. Eng. 33 (2011) 211–223, https://doi.org/10.1080/01919512.2011.554141.

[8] I.A. Katsoyiannis, S. Canonica, U. von Gunten, Efficiency and energy requirements for the transformation of organic micropollutants by ozone, O_3/H_2O_2 and UV/H_2O_2, Water Res. 45 (2011) 3811–3822, https://doi.org/10.1016/j.watres.2011.04.038, 2011.

[9] I. Panorel, I. Kornev, H. Hatakka, S. Preis, Pulsed corona discharge for degradation of aqueous humic substances, Water Supply 11 (2011) 238–245, https://doi.org/10.2166/ws.2011.045.

[10] S. Preis, I.C. Panorel, I. Kornev, H. Hatakka, J. Kallas, Pulsed corona discharge: the role of ozone and hydroxyl radical in aqueous pollutants oxidation, Water Sci. Technol. 68 (2013) 1536–1542, https://doi.org/10.2166/wst.2013.399.

[11] J.-M. Fanchiang, D.-H. Tseng, Degradation of anthraquinone dye C.I. Reactive Blue 19 in aqueous solution by ozonation, Chemosphere 77 (2009) 214–221, https://doi.org/10.1016/j.chemosphere.2009.07.038.

[12] M.A.N. Khan, M. Siddique, F. Wahid, R. Khan, Removal of reactive blue 19 dye by sono, photo and sonophotocatalytic oxidation using visible light, Ultrason. Sonochem. 26 (2015) 370–377, https://doi.org/10.1016/j.ultsonch.2015.04.012.

[13] A. Rezaee, M.T. Ghaneian, S.J. Hashemian, G. Moussavi, A. Khavanin, G. Ghanizadeh, Decolorization of reactive blue 19 dye from textile wastewater by the UV/H_2O_2 process, J. Appl. Sci. 8 (2008) 1108–1112, https://doi.org/10.3923/jas.2008.1108.1112.

[14] S. Song, J. Yao, Z. He, J. Qiu, J. Chen, Effect of operational parameters on the decolorization of C.I. Reactive Blue 19 in aqueous solution by ozone-enhanced electrocoagulation, J. Hazard Mater. 152 (2008) 204–210, https://doi.org/10.1016/j.jhazmat.2007.06.104.

[15] P.A. Carneiro, M.E. Osugi, C.S. Fugivara, N. Boralle, M. Furlan, M.V.B. Zanoni, Evaluation of different electrochemical methods on the oxidation and degradation of Reactive Blue 4 in aqueous solution, Chemosphere 59 (2005) 431–439, https://doi.org/10.1016/j.chemosphere.2004.10.043.

[16] K.C. Nakamura, L.S. Guimarães, A.G. Magdalena, A.C.D. Angelo, A.R. De Andrade, S. Garcia-Segura, A.R.F. Pipi, Electrochemically-driven mineralization of Reactive Blue 4 cotton dye: on the role of in situ generated oxidants, J. Electroanal. Chem. 840 (2019) 415–422, https://doi.org/10.1016/j.jelechem.2019.04.016.

[17] A. Durán, J.M. Monteagudo, E. Amores, Solar photo-Fenton degradation of Reactive Blue 4 in a CPC reactor, Appl. Catal. B Environ. 80 (2008) 42–50, https://doi.org/10.1016/j.apcatb.2007.11.016.

[18] L.S. Clesceri, A.E. Greenberg, R.R. Trussel, Standard Methods for the Examination of Water and Wastewater, twenty-first ed., APHA, AWWA, WPCF, Washington (DC), 2012.

[19] Y.-X. Wang, I. Kornev, C.-H. Wei, S. Preis, Surfactant and non-surfactant radical scavengers in aqueous reactions induced by pulsed corona discharge treatment, J. Electrost. 98 (2019) 82–86, https://doi.org/10.1016/j.elstat.2019.03.001.

[20] I. Kornev, F. Saprykin, S. Preis, Stability and energy efficiency of pulsed corona discharge in treatment of dispersed high-conductivity aqueous solutions, J. Electrost. 89 (2017) 42–50, https://doi.org/10.1016/j.elstat.2017.07.001.

[21] S. Preis, I.C. Panorel, I. Kornev, H. Hatakka, J. Kallas, Pulsed corona discharge: the role of ozone and hydroxyl radical in aqueous pollutants oxidation, Water Sci. Technol. 68 (2013) 1536–1542, https://doi.org/10.2166/wst.2013.399.

[22] P. Ajo, I. Kornev, S. Preis, Pulsed corona discharge induced hydroxyl radical transfer through the gas-liquid interface, Sci. Rep. 7 (2017), 16152, https://doi.org/10.1038/s41598-017-16333-1.

[23] R.P.F. Melo, E.L. Barros Neto, M.C.P.A. Moura, T.N. Castro Dantas, A.A. Dantas Neto, H.N.M. Oliveira, Removal of reactive blue 19 using nonionic surfactant in cloud point extraction, Separ. Purif. Technol. 138 (2014) 71–76, https://doi.org/10.1016/j.seppur.2014.10.009.

[24] Ç. Kartal, H. Akbaş, Study on the interaction of anionic dye–nonionic surfactants in a mixture of anionic and nonionic surfactants by absorption spectroscopy, Dyes Pigments 65 (2005) 191–195, https://doi.org/10.1016/j.dyepig.2004.07.003.

[25] A.R. Petcu, E.A. Rogozea, C.A. Lazar, N.L. Olteanu, A. Meghea, M. Mihaly, Specific interactions within micelle microenvironment in different charged dye/surfactant systems, Arab. J. Chem. 9 (2016) 9–17, https://doi.org/10.1016/j.arabjc.2015.09.009.

Appendix 2

Paper II

Onga, L.; Boroznjak, R.; Kornev, I.; Preis, S. (2021). Oxidation of aqueous organic molecules in gas-phase pulsed corona discharge affected by sodium dodecyl sulphate: Explanation of variability. Journal of Electrostatics, 111, #103581.

Oxidation of aqueous organic molecules in gas-phase pulsed corona discharge affected by sodium dodecyl sulphate: Explanation of variability

Liina Onga [a], Roman Boroznjak [b], Iakov Kornev [c], Sergei Preis [a],*

[a] *Laboratory of Environmental Technology, Department of Materials and Environmental Technology, Tallinn University of Technology, Ehitajate Tee 5, 19086, Tallinn, Estonia*
[b] *Laboratory of Biofunctional Materials, Department of Materials and Environmental Technology, Tallinn University of Technology, Ehitajate Tee 5, 19086, Tallinn, Estonia*
[c] *R&D Laboratory for Clean Water, School of Advanced Manufacturing Technologies, National Research Tomsk Polytechnic University, 30 Lenin Ave., Tomsk, 634050, Russian Federation*

A B S T R A C T

Oxidation of waterborne organic compounds by gas-phase pulsed corona discharge (PCD) provides substantial energy efficiency benefits. Surfactant sodium dodecyl sulphate (SDS) alters the energy efficiency of oxidation providing decelerating, neutral or accelerating effect. Determining the causal connection between the pollutant's molecular structure and the effect of SDS addition presents the research objective. Computational chemistry Spartan 14 1.1.4 software was used for modelling of SDS molecule interaction with selected textile dyes and pharmaceuticals with subsequent verification in PCD treatment experiments. Effects of SDS addition were predicted for acid orange 7, indigotetrasulfonate, paracetamol and indomethacin and confirmed experimentally.

1. Introduction

Gas-phase pulsed electric discharges are known to initiate surface reactions involving a set of oxidants [1]. Surfactants such as sodium dodecyl sulphate (SDS) were used for radical scavenging studies for surface reactions in PCD process [2]. Oxidation of short chained phenol and oxalate in the presence of surfactant showed its scavenging effect reducing the oxidation rate of target compounds [3]. However, addition of SDS to aqueous solutions of reactive blue 4 (RB4) and reactive blue 19 (RB19) textile dyes exhibited remarkable, 2.2 to 2.5 times improvement in the dyes oxidation rates [4]. Explanation of the variety of SDS effect on oxidation of aqueous organic molecules presents the objective of the research. Pollutant molecules of various structure and size from the row of textile dyes and pharmaceuticals were chosen for verification of working hypothesis in both calculations and experiments.

Often toxic, mutagenic and carcinogenic textile dyes, causing disturbances in aquatic life as well as interfering with photosynthesis, mainly enter the environment from industry [5–8]. They are characterised by a wide variety in molecular structure potentially interacting with surfactants present in wastewaters, thus converting the question under the scope into the practical one: the removal of undesirable dyes

may find a more efficient answer at the PCD oxidation stage with subsequent effective biological abatement of the surfactant. Human pharmaceuticals enter the environment primarily when excreted by patients, being disposed with unused medicine, and released from manufacturing [9]. Pharmaceuticals in the environment pose threats to both human health, as well as aquatic biota. For example, paracetamol, one of the most used analgesic pharmaceuticals, is found in European wastewater treatment plant (WWTP) effluents in concentrations up to 32 μg L^{-1} and surface waters 3.6 μg L^{-1} [10–12]. Nonsteroidal anti-inflammatory drug indomethacin has also been frequently reported in WWTP effluents as well as surface waters with concentrations up to 100 ng L^{-1} [13–15]. Domestic wastewaters also often contain surfactants, which makes the combination of realistic value. The abovementioned drugs were chosen as subjects of the study together with two popular textile dyes, acid orange 7 (AO7) and indigotetrasulfonate (I4S). All the mentioned chemicals are extensively used and were chosen for their diverse molecular structure.

The variety of SDS effect on PCD-oxidation of aqueous organic molecules raises a question about key factors determining the role of surfactant. An explanation given by using computational chemistry in modelling of possible interactions between the surfactant and pollutant

---

* Corresponding author.
  E-mail address: sergei.preis@taltech.ee (S. Preis).

molecules was verified in PCD experiments with molecules under the study.

Computational simulation using Spartan'14 (version 1.1.4) package for energetically minimized complexes between target compounds and SDS allowed presuming the mechanism of formation of those. Their role in interaction with OH-radicals is thus described and visualized. The visualized energetically minimized structures demonstrated spatial hindrances or accessibilities of molecular moieties in oxidative degradation. The spatial localization of the moieties is critical in the context for the dramatic difference observed in oxidation rates: promoting the reaction of molecules exposed to the radical attack in one case changes to spatial hindering, i.e. protection with aggregated dodecyl tails of SDS.

2. Materials and methods

2.1. Software

The computational software Spartan '14 (version 1.1.4), providing energetic optimization, was adopted to simulate the preferable configuration for each target molecule and its complex with SDS, visualizing the resulting structures. This software allows minimizing the energy of the complexes and determining the spatial localization for the moieties of the target molecules and their complexes.
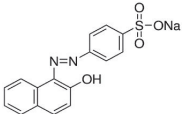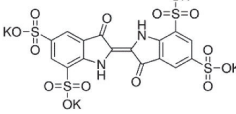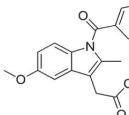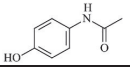
2.2. Chemicals

Sodium dodecyl sulphate (SDS, $NaC_{12}H_{25}SO_4$) was purchased from Lach-Ner (Czech Republic). Target compounds with their structures are given in Table 1. Acid orange 7 ($C_{16}H_{11}N_2NaO_4S$, dye content $\geq$ 85%) and indigotetrasulfonate ($C_{16}H_6K_4N_2O_{14}S_4$, dye content $\geq$ 85%) were provided by Sigma Aldrich. Paracetamol ($C_8H_9NO_2$, purity $\geq$98%) and indomethacin ($C_{19}H_{16}ClNO_4$, purity $\geq$97.5%) were obtained from Acros Organics. All chemicals were used without further purification having solutions prepared in distilled water. Indomethacin was first dissolved in alkaline 0.1 M Na_2CO_3 solution followed by pH adjustment to 7.6 $\pm$ 0.2 with 5-M H_2SO_4. pH was measured using S220 digital pH-meter (Mettler Toledo, Switzerland).

3. Methods of analysis

Dye concentrations were measured using Helios β spectrophotometer (Thermo Electron Corporation, USA) at maximum absorbance wavelengths of 485 and 591 nm for AO7 and I4S, respectively. Concentrations of PCM and IND were quantified using high performance liquid chromatography combined with diode array detector (HPLC-PDA, Shimadzu, Japan) equipped with a Phenomenex Gemini column (150 × 2.0 mm, 1.7 mm) filled with stationary phase NX-C18 (110 Å, 5 μm). The analysis of PCM was performed using an isocratic method with a mobile phase mixture of 92% aqueous formic acid solution containing 0.3% of HCOOH, and 8% acetonitrile containing 0.3% of formic acid; IND analysis was performed with the 50:50% mixture of the abovementioned solutions. The eluent flow rate was 0.2 mL min^{-1} at the analysed sample injection volume of 20 and 75 μL for PCM and IND, respectively.

3.1. Experimental equipment

The experimental device (Flowrox Oy, Finland) consists of PCD reactor with a 40-L storage tank, pulse generator and water circulation pump (Fig. 1). The PCD reactor contains multiple string electrodes of 0.55 mm in diameter and 20 m of total length positioned horizontally between two grounded vertical parallel plate electrodes. The distance between wire electrodes and the grounded plate is 18 mm. The horizontal cross-section of the plasma zone is 36 mm in width and 500 mm in length. Treated solutions are dispersed through the perforated plate with 51 perforations of 1 mm diameter positioned in a vertical plane with the high voltage string electrodes. Frequencies of 50–880 pulses per second (pps) are used to generate high voltage pulses corresponding to the output power of 9–123.2 W with the details of pulse described earlier [4]. The voltage and current waveforms of the pulse are shown in Fig. 2 registered by means of RTB2004-300 MHz oscilloscope (Rohde and Schwarz, Germany). The circulation pump (Iwaki Co. Ltd., Japan) was used to circulate the treated solution from the storage tank to the top of the reactor. All experiments were tripled with result deviations not exceeding 5%.

The energy efficiency of oxidation was calculated using Eq. (1):

$$E = \frac{\Delta C \cdot V}{W} \tag{1}$$

where ΔC is the decrease in substrate concentration, mg L^{-1}, V is the volume of treated solution, L, and W is the energy consumption as a product of power delivered to the reactor and the time of treatment, kWh. The output-input ratio of pulse generator equals 65%.
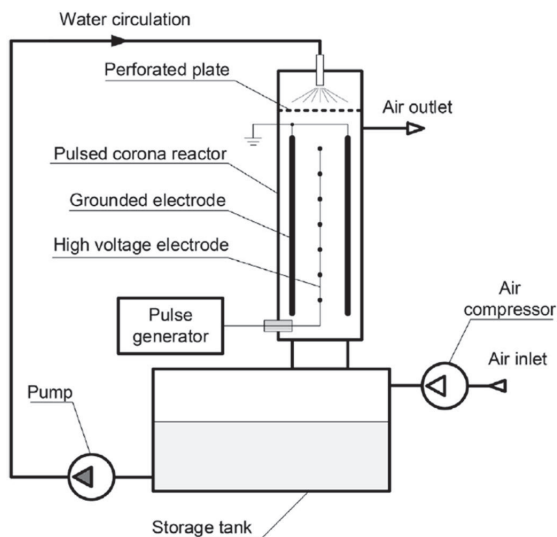
Table 1
Target compounds: formulae, graphical structures and molar masses.

Compound/IUPAC name	Formula	Graphical structure	Molar mass, g mol^{-1}
Acid orange 7 /sodium 4-[(2-hydroxynaphthalen-1-yl) diazenyl]benzenesulfonate	$C_{16}H_{11}N_2NaO_4S$		350.3
Indigotetrasulfonate/tetrapotassium 2-(3-hydroxy-5,7-disulfonato-1H-indol-2-yl)-3-oxoindole-5,7-disulfonate	$C_{16}H_6K_4N_2O_{14}S_4$		734.9
Indomethacin /2-[1-(4-chlorobenzoyl)-5-methoxy-2-methylindol-3-yl]acetic acid	$C_{19}H_{16}ClNO_4$		357.8
Paracetamol /N-(4-hydroxyphenyl)acetamide	$C_8H_9NO_2$		151.16

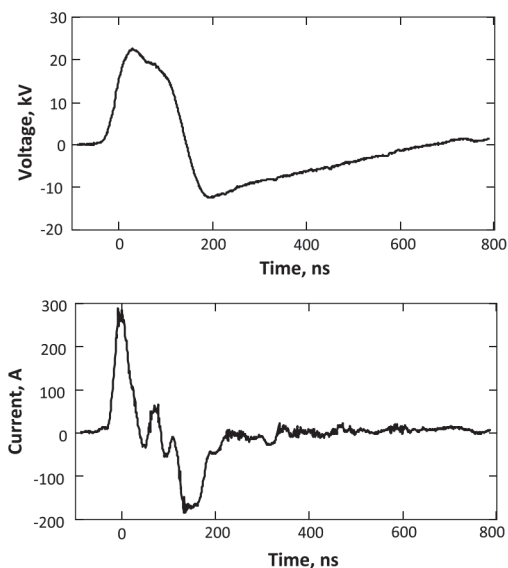Fig. 1. Scheme of pulsed corona discharge experimental device.

Fig. 2. Voltage and current waveforms of the discharge pulse.

4. Results and discussion

4.1. Modelling

The model explaining the behaviour of oxidized target compound presumes the OH-radical attack on the hydrophobic tail of SDS, removing a hydrogen atom from the –CH$_3$ group forming a slow –CH$_{2\bullet}$- radical at the end of the tail. Previously studied reactive blue dyes RB4 and RB19 contain aromatic rings with high electron densities in their chromophore groups [4]. Due to the possibility of radical dissociation of SDS hydrophobic tail and in the chromophore groups of dye, the slow-reacting hydrophobic SDS-radical attaches itself to the chromophore parts of RB4 and RB19, subsequently bringing the target molecule to the plasma-liquid interface, where further radical attacks oxidize the dye molecules with higher oxidation efficiency. Fig. 3 demonstrates the product of covalent bond formation via radical species formed by action of OH-radical characterized by radical dissociation of C–H bonds on the first atom of SDS tail and aromatic rings of RB4 and RB19 molecules. The resulting compounds provide steric access for intensive OH-radical attacks by holding the target molecule on the end of the hydrophobic alkyl tail. Because the rate of SDS oxidation is relatively low, the chromophore moiety is degraded more actively with SDS than without it, providing the highest oxidation rates for RB4 and RB19.

Another textile dye, AO7 has a chromophore group consisting of two aromatic rings, which makes this molecule attractive for the SDS-radical. Fig. 4 shows the probable attachment of SDS to the aromatic ring of AO7 thus bringing the target molecule to the plasma-liquid interface exposing them to plasma active species. Large SDS molecule, however, suffers steric restrictions in interaction with, for example, I4S molecule, the aromatic moieties of which are surrounded by four hydrophilic sulfonate groups. In this case, SDS is difficult to attach itself to the I4S molecule, most likely hindering the I4S from active oxidant species (Fig. 4).

Oxidation of AO7 follows a principle similar to RB4 and RB19 with the SDS-induced energy efficiency improvement for about two times.

Fig. 4 demonstrates non-covalent interaction between dissociative and hydrophilic sulfonate groups of the indigotetrasulfonate and SDS. As a result of these interactions, hydrophobic moieties of SDS cover and thus protect the chromophore groups of dye against OH-radical attacks thus inhibiting dye oxidation. Inhibition of PCD-oxidation with SDS addition was observed for e.g. paracetamol (see below) and oxalic acid [3]. The surfactant forms a non-covalent complex around polar groups of the compounds thus constructing the shields composed of alkyl tails: due to relatively small size of these molecules, SDS molecules form steric hindrances against OH-radical attacks (Fig. 5). Moderate, about 10% obstruction of oxidation was observed with paracetamol, although oxidation of oxalic acid was dramatically hindered with SDS addition, the oxidation rate decreased 3–8 times compared with SDS-free treatment. Slight, for about 15% improvement of indomethacin oxidation seems to be attributed to little concentration of polar moieties in the target molecule to form both a shield of complexed non-covalently bound SDS molecules and certain covalent binding via radicalized sites as described for RB4 and RB19 enhancing oxidation.

4.2. Model verification

Paracetamol molecule is a small one with the aromatic ring with attached hydrophilic moieties at its two opposite sides. Fig. 6 presents the PCM oxidation efficiencies with SDS addition ranging from 0 to 200 mg L^{-1}. One can see the effect of SDS, weakly negative, ranging within small deviation in oxidation efficiency manifesting negative, close to neutral impact. This may be explained by two phenomena competing in PCM interaction with SDS, attachment of SDS-radical to the aromatic ring of PCM and hydrophilic character of the PCM molecule shielded with complexing SDS molecules (Fig. 5). These phenomena together with the small size of PCM molecule make it difficult for SDS to find a spot to covalently attach itself to. Another obstacle for the covalent bond consists of –OH and –NH- groups leaving no space for SDS-radical to attach to a radicalized benzene ring. In this case SDS acts as an OH-radical scavenger by screening the radical attack from PCM molecules brought, nevertheless, to the interface. Weak affinity of the SDS-radical to the small PCM molecule is thus responsible for the effect of SDS addition close to neutral.

Indomethacin is much bigger molecule compared to paracetamol: two benzene rings provide more sites with high electron density potentially attracting SDS-radical stronger than a single-ring PCM. The benzene rings, however, are neighboured by a hydrophilic carboxylic
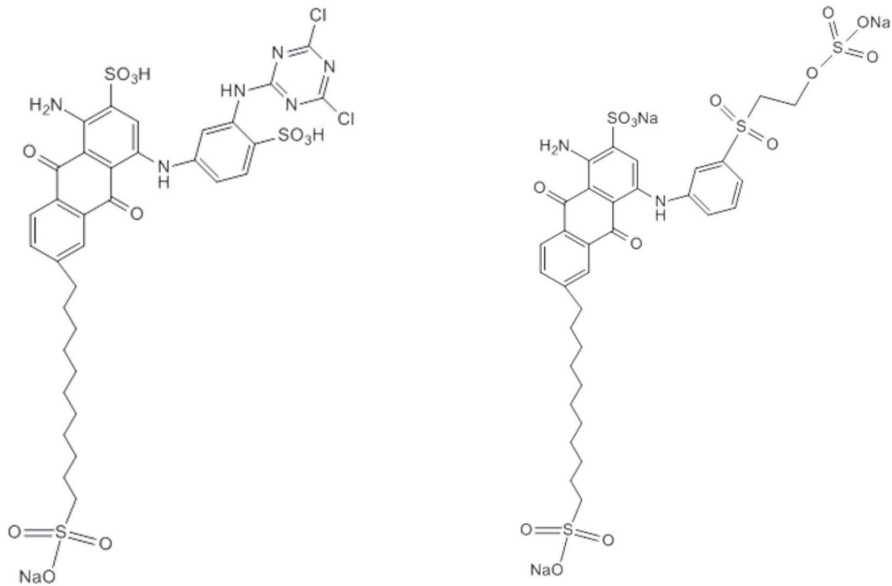
Fig. 3. Modelled products of covalent interactions between sodium dodecyl sulphate (SDS) and reactive blue 4 (left) and 19 (right) textile dyes.
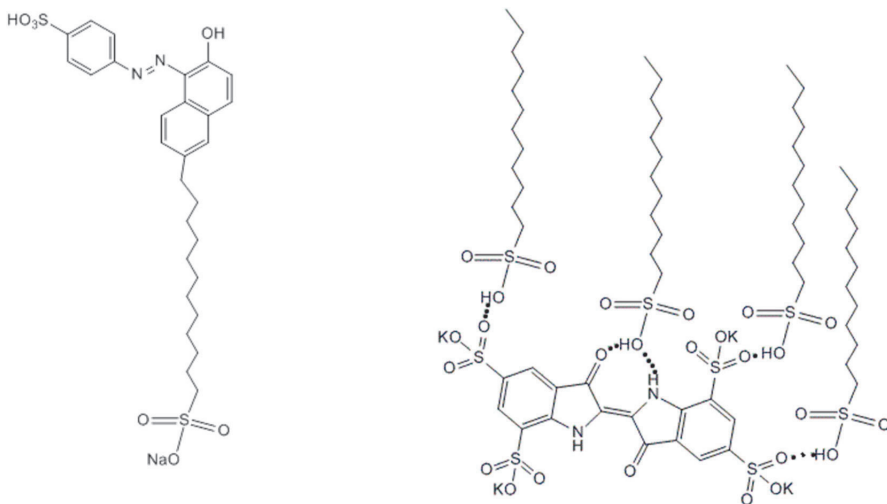

Fig. 4. Modelled products of covalent binding between SDS and acid orange 7 via radical mechanism started with radical C–H bond dissociation in the both molecules (left) and non-covalent interaction between SDS and potassium indigotetrasulfonate (right) showing spatial orientation of SDS molecules around the dye. Black points are hydrogen bonds between hydrolysed SDS and potassium indigotetrasulfonate.

moiety together with –Cl and –OCH$_3$ moieties thinning the electron densities at aromatic groups complicating the SDS-radical attachment. This makes the oxidation efficiency moderately rising in presence of SDS from 129 to 150 g kW^{-1}h^{-1} at SDS concentration of 100 mg L^{-1}, when SDS:IND molar ratio comprised about 3:1 (Fig. 7). The rise in concentration of SDS to 150 mg L^{-1}, i.e. at SDS:IND molar ratio of about 4:1 results in decreased oxidation efficiency indicating strengthened screening effect of the excess surfactant molecules.

Acid orange 7 contains a benzene ring and 2-naphthol group thus having sites with high electron density attracting SDS-radical. The 2-

naphthol moiety has no attached groups and, thus, steric effects obstructing affiliation with SDS-radical. As a result, the AO7 oxidation efficiency rose from 66 to 108 g kW^{-1}h^{-1} in 150 mg L^{-1} SDS solution providing noticeable positive effect (Fig. 8). This supports the concept of SDS-radical transporting the affiliated molecule to the plasma-liquid interface increasing the oxidation efficiency. The excess SDS concentration of 200 mg L^{-1} resulted in hindered oxidation as was observed with IND.

Potassium indigotetrasulfonate molecule contains two aromatic rings with four sulfonate groups attached in meta-positions practically
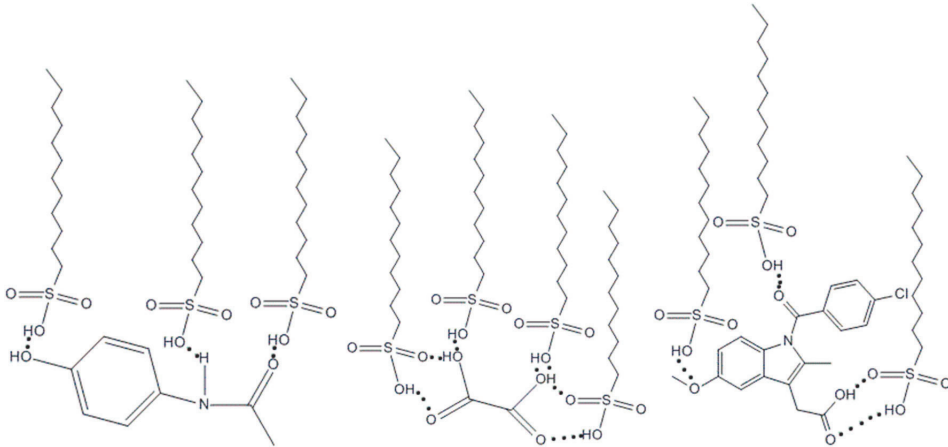
Fig. 5. Visualized non-covalent complexes of paracetamol (left), oxalic acid (centre), and indomethacin (right) with SDS producing protective shields around target molecules.
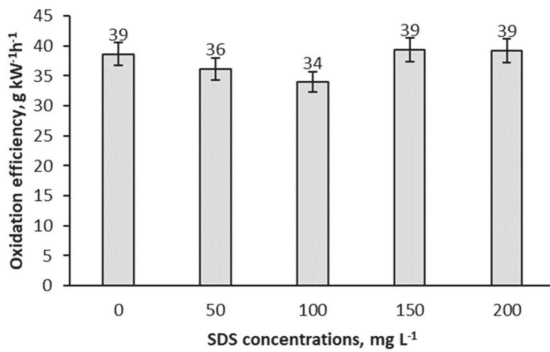

Fig. 6. Oxidation efficiency of paracetamol dependent on SDS concentration: PCM starting concentration 48 mg L^{-1}, pulse repetition frequency 200 pps (32 W), maximum energy dose 1.6 kWh m^{-3} at treatment time 30 min with 5-min sampling interval, pH = 6.8 ± 0.2, efficiency determined for PCM 90% removal.
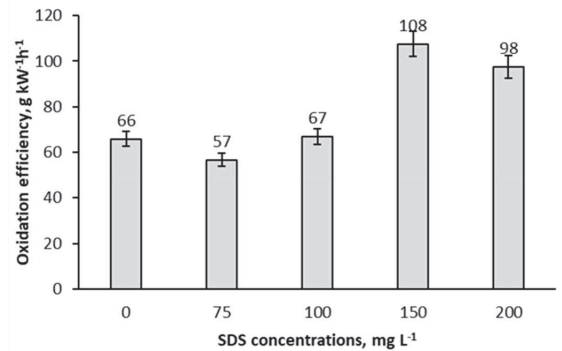

Fig. 8. Oxidation efficiency of acid orange 7 dependent on SDS concentration: AO7 starting concentration 10 mg L^{-1}, pulse repetition frequency 200 pps (32 W), maximum energy dose 0.21 kWh m^{-3} at treatment time 4 min with 0.5-min sampling interval, pH = 6.5 ± 0.3, efficiency determined for AO7 90% removal.
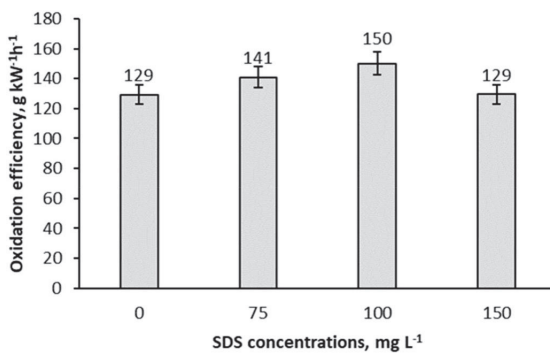

Fig. 7. Oxidation efficiency of indomethacin dependent on SDS concentration: IND starting concentration 42 mg L^{-1}, pulse repetition frequency 200 pps (32 W), maximum energy dose 0.37 kWh m^{-3} at treatment time 7 min with 1-min sampling interval, pH = 7.7 ± 0.1, efficiency determined for IND 90% removal.

surrounding the rings with steric obstacles preventing, at least partially, affiliation with the SDS-radical. Having weakened affinity between SDS-radical and I4S molecule, one may expect negative impact of SDS addition for its OH-radical screening effect. As shown in Fig. 9, oxidation efficiency gradually decreased from 676 to 610 g $kW^{-1}h^{-1}$ with SDS concentration increasing from 0 to 200 mg L^{-1}. Moderate deceleration of oxidation for 11% only may be explained by limited steric effect of sulfonate groups, i.e. I4S molecules are transported by SDS to the interface to a certain extent. Similarly, PCD oxidation of large molecules of hydrophilic humic substances was moderately negatively affected by SDS additions [3].

5. Conclusions

The variety in surfactant effect on gas-phase plasma oxidation of waterborne organic molecules was demonstrated with extensively used pharmaceuticals and textile dyes: additions of SDS may have both positive and negative effect on oxidation rate dependent on the target molecule structure. Explanation for such variety is proposed in SDS-radical formed as a result of primary OH-radical attack. This radical
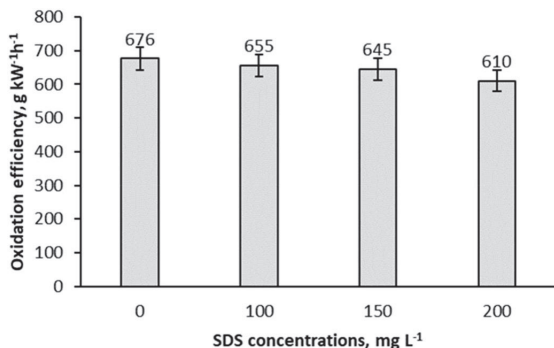
Fig. 9. Oxidation efficiency of indigotetrasulfonate dependent on SDS concentration: I4S starting concentration 35 mg L^{-1}, pulse repetition frequency 50 pps (9 W), maximum energy dose 0.06 kWh m^{-3} at treatment time 4 min with 0.5-min sampling interval, pH = 7.1 $\pm$ 0.3, efficiency determined for I4S 90% removal.

actively affiliates with the target pollutant molecule also radicalized with the OH-radical attack in a covalent bond and transports it to the plasma-liquid interface for effective oxidation with surface-borne OH-radicals, i.e. provides an accelerating impact of SDS addition. The transportation is more effective if the SDS-radical is attached strongly enough to the target molecule at sites of high electron density, e.g. aromatic rings. Side moieties at aromatic rings of the target molecules, however, may provide steric obstacles for the affinity of SDS-radical thus weakening transportation to the interface overpowered by OH-radical off-screening, which results in decelerating impact of SDS. Small hydrophilic molecules, such as oxalic acid, are complexed with the SDS sulfonate groups thus shielding those against OH-radical attacks and dramatically reducing the oxidation efficiency.

Spartan 14 1.1.4 software proved to be a tool for predicting the SDS impact on plasma oxidation efficiency in aqueous solutions, although further experiments with various compounds are necessary to confirm and specify the proposed approach. The study may be of practical importance in plasma treatment of surfactant-containing industrial and municipal wastewaters.

Declaration of competing interest

The authors declare that they have no known competing financial interests or personal relationships that could have appeared to influence the work reported in this paper.

Acknowledgements

This work was supported by the Institutional Development Program

References

[1] K. Shang, N. Wang, W. Li, N. Jiang, N. Lu, J. Li, Y. Wu, Generation characteristics of long-lived active species in a water falling film DBD reactor, Plasma Chem. Plasma Process. 41 (2021) 477–491, https://doi.org/10.1007/s11090-020-10124-9.

[2] S. Preis, I.C. Panorel, I. Kornev, H. Hatakka, J. Kallas, Pulsed corona discharge: the role of ozone and hydroxyl radical in aqueous pollutants oxidation, Water Sci. Technol. 68 (2013) 1536–1542, https://doi.org/10.2166/wst.2013.399.

[3] Y.-X. Wang, I. Kornev, C.-H. Wei, S. Preis, Surfactant and non-surfactant radical scavengers in aqueous reactions induced by pulsed corona discharge treatment, J. Electrost. 98 (2019) 82–86, https://doi.org/10.1016/j.elstat.2019.03.001.

[4] L. Onga, I. Kornev, S. Preis, Oxidation of reactive azo-dyes with pulsed corona discharge: surface reaction enhancement, J. Electrost. 103 (2020) 103420, https://doi.org/10.1016/j.elstat.2020.103420.

[5] F.C.F. Low, T.Y. Wu, C.Y. Teh, J.C. Juan, N. Balasubramanian, Investigation into photocatalytic decolorisation of CI Reactive Black 5 using titanium dioxide nanopowder, Color, Technol. 128 (2011) 44–50, https://doi.org/10.1111/j.1478-4408.2011.00326.x.

[6] B. de Campos Ventura-Camargo, M. Aparecida Marin-Morales, Azo dyes: characterization and toxicity – a review, Text. Light Ind. Sci. Technol. 2 (2013) 85–103.

[7] K. Shang, X. Wang, J. Li, H. Wang, N. Lu, N. Jiang, Y. Wu, Synergetic degradation of Acid Orange 7 (AO7) dye by DBD plasma and persulfate, Chem. Eng. J. 311 (2017) 378–384, https://doi.org/10.1016/j.cej.2016.11.103.

[8] K. Shang, J. Li, R. Morent, Hybrid electric discharge plasma technologies for water decontamination: a short review, Plasma Sci. Technol. 21 (2019), 043001, https://doi.org/10.1088/2058-6272/aafbc6.

[9] M.S. Kostich, J.M. Lazorchak, Risks to aquatic organisms posed by human pharmaceutical use, Sci. Total Environ. 389 (2008) 329–339, https://doi.org/10.1016/j.scitotenv.2007.09.008.

[10] A.M.P.T. Pareira, L.J.G. Silva, C.M. Lino, L.M. Meisel, A. Pena, Assessing environmental risk of pharmaceuticals in Portugal: an approach for the selection of the Portuguese monitoring stations in line with Directive 2013/39/EU, Chemosphere 144 (2016) 2507–2515, https://doi.org/10.1016/j.chemosphere.2015.10.100.

[11] N.H. Tran, M. Reinhard, K. Yew-Hiing Gin, Occurrence and fate of emerging contaminants in municipal wastewater treatment plants from different geographical regions: a review, Water Res. 133 (2018) 182–207, https://doi.org/10.1016/j.watres.2017.12.029.

[12] R. Meffe, I. de Bustamante, Emerging organic contaminants in surface water and groundwater: a first overview of the situation in Italy, Sci. Total Environ. 481 (2014) 280–295, https://doi.org/10.1016/j.scitotenv.2014.02.053.

[13] J.J. Jimenez, M.I. Sanchez, R. Pardo, B.E. Munoz, Degradation of indomethacin in river water under stress and non-stress laboratory conditions: degradation products, long-term evolution and adsorption to sediment, J. Environ. Sci. 51 (2017) 13–20, https://doi.org/10.1016/j.jes.2016.08.021.

[14] G. Dai, J. Huang, W. Chen, B. Wang, G. Yu, S. Deng, Major pharmaceuticals and personal care products (PPCPs) in wastewater treatment plant and receiving water in Beijing, China, and associated ecological risks, Bull. Environ. Contam. Toxicol. 92 (2014) 655–661, https://doi.org/10.1007/s00128-014-1247-0.

[15] R. Rosal, A. Rodriguez, J.A. Perdigon-Melon, A. Petre, E. Garcia-Calvo, M. J. Gomez, A. Agüera, A.R. Fernandez-Alba, Occurrence of emerging pollutants in urban wastewater and their removal through biological treatment followed by ozonation, Water Res. 44 (2010) 578–588, https://doi.org/10.1016/j.watres.2009.07.004.

Appendix 3

Paper III

Onga, L.; Kattel-Salusoo, E.; Trapido, M.; Preis, S. (2022). Oxidation of Aqueous Dexamethasone Solution by Gas-Phase Pulsed Corona Discharge. Water, 14 (3), #467.

Article

Oxidation of Aqueous Dexamethasone Solution by Gas-Phase Pulsed Corona Discharge

Liina Onga, Eneliis Kattel-Salusoo, Marina Trapido and Sergei Preis *

Department of Materials and Environmental Technology, Tallinn University of Technology, Ehitajate tee 5, 19086 Tallinn, Estonia; liina.onga@taltech.ee (L.O.); eneliis.kattel@taltech.ee (E.K.-S.); marina.trapido@taltech.ee (M.T.)
* Correspondence: sergei.preis@taltech.ee

Abstract: The most widely used anti-inflammatory corticosteroid dexamethasone (DXM), frequently detected in waterbodies due to its massive consumption and incomplete removal in wastewater treatment processes, was experimentally studied for oxidation with gas-phase pulsed corona discharge (PCD) varied in pulse repetition frequency, pH, DXM initial concentration and additions of surfactant sodium dodecyl sulphate (SDS) and *tert*-butyl alcohol (TBA). The experimental study also included ozonation as compared to PCD in energy efficiency. The advantageous energy efficiency of PCD was observed in wide spans of pH and DXM initial concentrations surpassing ozonation by about 2.4 times. Identified transformation by- and end-products (fluoride and acetate), as well as the impact of radical scavengers, point to the prevalent radical oxidation of DXM. Somewhat increased toxicity observed on the course of PCD-treatment of high DXM concentrations presents a subject for further studies.

Keywords: dexamethasone; ozone; plasma; wastewater treatment; hydroxyl radicals

1. Introduction

The increasing aquatic occurrence of emerging contaminants, such as personal care products and pharmaceuticals, poses a threat to human health as well as the environment and animals [1]. Pharmaceuticals enter the environment from manufacturing, disposal of unused medicine, farming and excretion of patients [2,3]. Reports show that pharmaceuticals enter the environment mainly with wastewater effluents, since their conventional treatment technologies are often insufficient [4].

Steroidal anti-inflammatory drugs belong to the most frequently detected pharmaceuticals at the wastewater treatment plants and in waterbodies worldwide. Dexamethasone (DXM) (Figure 1) is one of the most widely used corticosteroids included in the list of essential medications by the World Health Organization. This substance has been extensively studied lately for its therapeutic benefit in COVID-19 treatment [5], predicting its growing use and disposal. Salas-Leiton et al. [6] found corticosteroids have a major effect on the immunocompetence and growth of fish making it susceptible to pathogens at a reduced growth rate as a result of long-lasting treatment with DXM. The immunosuppressive effect of DXM to fish was also reported by Ribas et al. [7]. Dexamethasone has been repeatedly reported in river waters at concentrations ranging from 0.02 to 6.0 ng L^{-1} [8–10] and in effluents of wastewater treatment plants at concentrations up to 155 ng L^{-1} [11,12]. One can conclude, therefore, that conventional biological wastewater treatment is insufficient in the removal of DXM to prevent accumulation in the environment.

Removal of refractory pharmaceuticals is of concern worldwide. Advanced oxidation processes (AOPs) have proven to efficiently remove recalcitrant compounds by oxidation with highly reactive OH-radicals [13,14], ozone [15,16] or SO_4^{2-} radicals [17]. The problem with AOPs, however, is in their high capital or operational costs, which obstruct their

marketing. Recently, the application of electric discharges has been gaining attention in the treatment of polluted aqueous media [18–20]. Keeping in mind the energy yield in pollutant removal as the contest criterion, the gas-phase pulsed corona discharge (PCD) has proven its advanced character, surpassing the closest competitor, conventional ozonation, a few times over in respect of various pollutants, including pharmaceuticals [21–23].
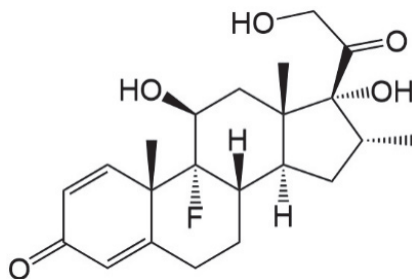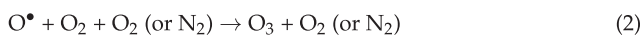

Figure 1. Molecular structure of dexamethasone.

In gas-phase PCD, the treated aqueous media are sprayed to the plasma zone, where long- (O_3) and short-living ($\bullet OH$, $\bullet O$) oxidative species are formed (Equations (1)–(4)) and utilized [24].

$$O_2 + e^- \rightarrow 2O^\bullet + e^- \tag{1}$$

$$O^\bullet + O_2 + O_2 \text{ (or } N_2) \rightarrow O_3 + O_2 \text{ (or } N_2) \tag{2}$$

$$H_2O + e^- \rightarrow HO^\bullet + H^\bullet + e^- \tag{3}$$

$$HO^\bullet + HO^\bullet \rightarrow H_2O_2 \tag{4}$$

Degradation of DXM was studied earlier using AOPs including UV-C/H_2O_2, UV-C/$S_2O_8^{2-}$ [25] and UV/iodide [26] combinations, photocatalysis [27,28], sono-nanocatalysis [29], gamma irradiation [30] and electrocoagulation [31]. The authors failed to find earlier reports related to DXM degradation by electric discharge treatment, although attempts to apply ozonation were undertaken [32,33]. Unfortunately, none of the articles on ozone application referred to contained sufficient data for the assessment of its energy efficiency.

An experimental study was undertaken into PCD performance in aqueous DXM oxidation and the effects of treatment parameters—pH, pulse repetition frequency, addition of the sodium dodecyl sulphate (SDS) surfactant and *tert*-butyl alcohol (TBA) as surface and in-bulk OH-radical scavengers, respectively. The effect of the initial DXM concentration was also studied, varying from 10 to 40 mg L^{-1}. The concentration range chosen for this study exceeds the one reported for polluted natural and wastewaters for the reliability of visible results. The comparative study of DXM ozonation was conducted by identifying transformation products in both ozonation and PCD treatment, and measuring the acute toxicity of treated DXM solutions.

2. Materials and Methods

2.1. Chemicals

Dexamethasone ($C_{22}H_{29}FO_5$, ≥98%, molecular weight 392.5 g mol^{-1}, Figure 1) was obtained from Alfa Aesar (Heysham, UK). Sodium carbonate (Na_2CO_3, 99%), sodium hydrogen carbonate ($NaHCO_3$, 99%), sodium sulphite (≥98% Na_2SO_3), sulphuric acid (H_2SO_4, 95–98%), sodium hydroxide (NaOH, ≥98%) and sodium chloride (NaCl, ≥99%) were purchased from Sigma-Aldrich (St. Louis, MO, USA). Acetonitrile (CH_3CN, LiChrosolv®), formic acid (CH_2O_2, 99%) and *tert*-butyl alcohol ((CH_3)$_3$COH, TBA, ≥99%) were obtained from Merck KGaA (Darmstadt, Germany). Sodium dodecyl sulphate ($NaC_{12}H_{25}SO_4$, SDS) was purchased from Lach-Ner (Neratovice, Czech Republic). All the chemicals were of analytical grade used without further purification. All stock solutions were prepared in

ultrapure water (Millipore Simplicity®UV System, Merck, Kenilworth, NJ, USA) or in bi-distilled water (>18.2 MΩ cm).

2.2. Experimental Equipment and Procedure

The PCD experimental device (Flowrox Oy, Lappeenranta, Finland) consists of a reactor with a 40-L storage tank, pulse generator and water circulation pump (Figure 2). The multiple string electrodes of 0.55 mm in diameter and 20 m total length are positioned horizontally between two vertical parallel plates. The distance between wire electrodes and the grounded plates is 18 mm. The horizontal cross-section of the plasma zone is 36 mm in width and 500 mm in length. The 5-L DXM solution samples were circulated in the PCD reactor with a flow rate of 0.8 m^3 h^{-1} using a circulation pump (Iwaki Suomi Oy, Kerava, Finland) to feed the treated solution from the storage tank to the top of the reactor. Treated solutions were dispersed through the perforated plate having 51 perforations of 1 mm diameter in a line coplanar with the high voltage electrodes. A pulse generator provides high voltage pulses to the reactor at frequencies of 50 to 880 pulses per second (pps) corresponding to an output power of 9 to 123.2 W with the current and voltage waveforms presented earlier [22]. The total treatment time varied between 60 and 120 min with sampling at fixed time intervals.
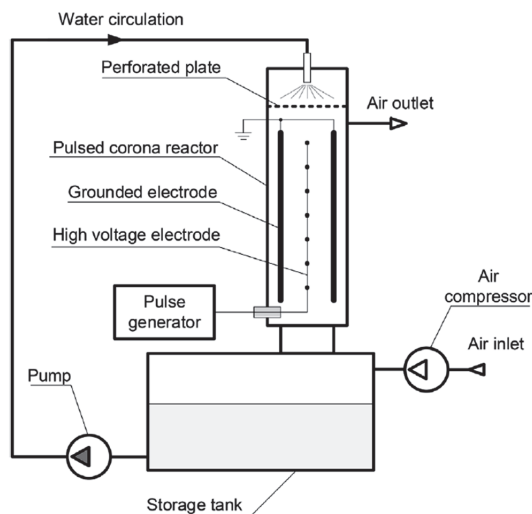

Figure 2. Schematic outline of pulsed corona discharge experimental device.

The energy efficiency of oxidation or energy yield E, g kW^{-1}h^{-1}, was calculated using Equation (5):

$$E = \frac{\Delta C \cdot V}{W} \qquad (5)$$

where ΔC is the decrease in DXM concentration, mg L^{-1}, V is the volume of treated solution L and W is the energy consumption as a product of power delivered to the reactor and the time of treatment, kWh. The energy efficiency was calculated for 80% DXM degradation.

Ozonation experiments were conducted in a 600-mL batch glass reactor (Figure 3). Ozonized air produced from dry air using an A2ZS-10GLAB O3 generator (A2Z Ozone Inc., Louisville, KY, USA) containing 3.0 mg L^{-1} of ozone was fed to the reactor at a flow rate of 0.4 L min^{-1}. The gaseous ozone concentration was monitored using an O$_3$ analyzer, BMT 965 (BMT Messtechnik GMBH, Monroe, WA, USA). The ozonation experiments were conducted for 60 min with sampling at fixed time intervals. Residual ozone in samples was quenched with sodium sulphite added to stop the reaction.
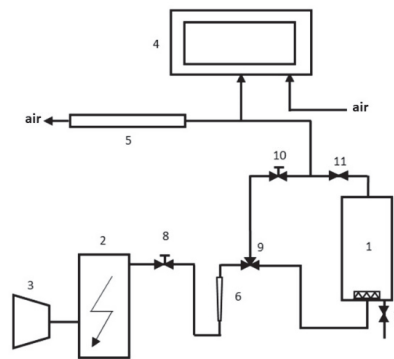
Figure 3. Ozonation gas distribution outline: 1—reactor; 2—O_3 generator; 3—compressor; 4—O_3 analyzer; 5—residual O_3 thermo-catalytic destructor; 6—rotameter; 7—sampling port; 11—non-return valve; 8, 10—gate valves with manual actuators; 9—3-way valve.

The energy efficiency for DXM degradation in ozonation experiments was calculated using Equation (6):

$$E = \frac{\Delta C \cdot V}{P \cdot t} \tag{6}$$

where ΔC is the decrease in DXM concentration, mg L^{-1}, V is the volume of treated solution, L, t is the treatment time, h, and P is the power consumed by ozone synthesis. The power was calculated from gaseous O_3 initial concentration, mg O_3 L^{-1}, the flow rate of ozone-containing air, L min^{-1}, and the energy consumed by O_3 synthesis in air comprising 30 kWh kg $O_3{}^{-1}$.

2.3. Methods of Analysis

The concentration of DXM was quantified using high performance liquid chromatography combined with a diode array detector (HPLC-PDA, Shimadzu, Japan) equipped with a Phenomenex Gemini column (150 × 2.0 mm, 1.7 mm) filled with stationary phase NX-C18 (110 Å, 5 μm). The analysis was performed using an isocratic method with a mobile phase mixture of 40% acetonitrile containing 0.3% formic acid and 60% of 0.3% formic acid aqueous solution. The eluent flow rate was 0.2 mL min^{-1}. A 75 μL quantity of samples was injected and analyzed at λ = 241 nm. The pH was measured using a S220 digital pH-meter (Mettler Toledo, Zurich, Switzerland). Total organic carbon (TOC) was measured using Multi N/C 3100 analyser (Analytic Jena, Jena, Germany).

2.4. Identification of DXM Transformation Products

Identification of DXM transformation products was performed by analyzing samples from selected trials by high performance liquid chromatography combined with a mass spectrometer (HPLC-MS, Shimadzu LC-MS, Okayama, Japan). Mass spectra were acquired in full-scan mode in the range of 50–500 *m/z*. The instrument was operated in positive ESI mode and the results obtained were handled using Shimadzu Lab Solutions software. Ion chromatography with chemical suppression of the eluent conductivity was used to measure concentrations of formed anions (761 Compact IC, Metrohm Ltd., Herisau, Switzerland).

2.5. Acute Toxicity Test

The acute toxicity was determined using the Microtoc® method (Model 500 Analyzer SDI) according to ISO 11348-3:2007 (ISO, 2007). The reconstitution solution was used to activate freeze-dried *Vibrio fischeri*. Concentrated salt solution (2% NaCl) was used to achieve 2% salinity for maintaining the osmotic pressure of the test bacteria suspension [34], having the salt solution used as a blank sample. The solutions containing 40 mg L^{-1} of DXM and those treated with an energy dose of 3.6 kWh m^{-3} delivered in ozonation and

PCD oxidation were analyzed for toxicity. Each toxicity test was performed in 10 dilutions and the luminescence was measured after 15 min of exposure. The bacterial luminescence inhibition (INH%) was calculated using Equations (7) and (8):

$$INH\% = \frac{IT_{15}}{KF \times IT_0} \times 100 \qquad (7)$$

$$KF = \frac{IC_{15}}{IC_0} \qquad (8)$$

where KF is a correction factor, IC_{15}—luminescence intensity of the blank sample after 15 min contact time, IC_0—initial luminescence intensity of the blank sample, IT_{15}—luminescence intensity of the test sample after 15 min contact time, IT_0—initial luminescence intensity of the test sample.

3. Results and Discussion

3.1. Oxidation Efficiency

The effect shown by the pulse repetition frequency on the efficiency of target compound oxidation exhibits the role of ozone [35]. Figure 4 shows DXM oxidation at 50, 200 and 880 pps with visible but minor differences in oxidation energy efficiency between 50 and 200 pps; the difference in efficiencies at these frequencies did not exceed 5% at 8.9 and 8.5 g kW^{-1}h^{-1}, respectively. With the pulse repetition frequency increased to 880 pps, however, the energy efficiency of DXM oxidation decreased noticeably comprising 6.0 g kW^{-1}h^{-1}, which is about 33% lower than at 50 pps. One should keep in mind that the rate of energy delivery is proportional to the pulse repetition frequency making the treatment longer at lower frequencies. This indicates a moderate contribution of ozone to the degradation, with a lower pulse repetition frequency giving ozone more time to react between pulses. The minor difference in efficiency between 50 and 200 pps may be explained by equal consumption of ozone synthesized at these frequencies by the substrate at the time of treatment.
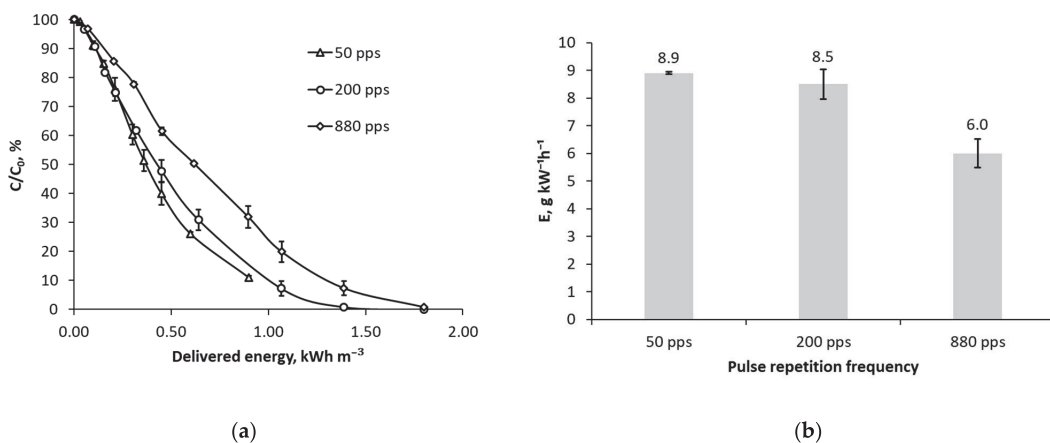

(a)   (b)

Figure 4. (**a**) Dexamethasone residual relative concentration dependent on delivered pulsed energy and (**b**) oxidation energy efficiencies at pulse repetition frequencies of 50, 200 and 880 pps: C_0 = 10 mg L^{-1}, initial pH 6.8, total treatment time was 30.0, 16.9 and 4.4 min for 50, 200 and 880 pps, respectively.

3.2. Effect of Initial Concentration

The initial concentration of the target pollutant determines the energy efficiency of oxidation as expected from the second-order reactions observed in PCD treatment of aqueous media [35]. The impact of variable DXM concentration was studied at initial

concentrations of 10, 20 and 40 mg L^{-1}. At the constant pulsed power released in the PCD reactor, the growing initial concentration exhibits a growing trend in oxidation efficiency (Figure 5), requiring, however, a higher energy dose and longer treatment time. Similarly, an increased DXM concentration resulted in better performance of, e.g., photocatalytic oxidation [25].
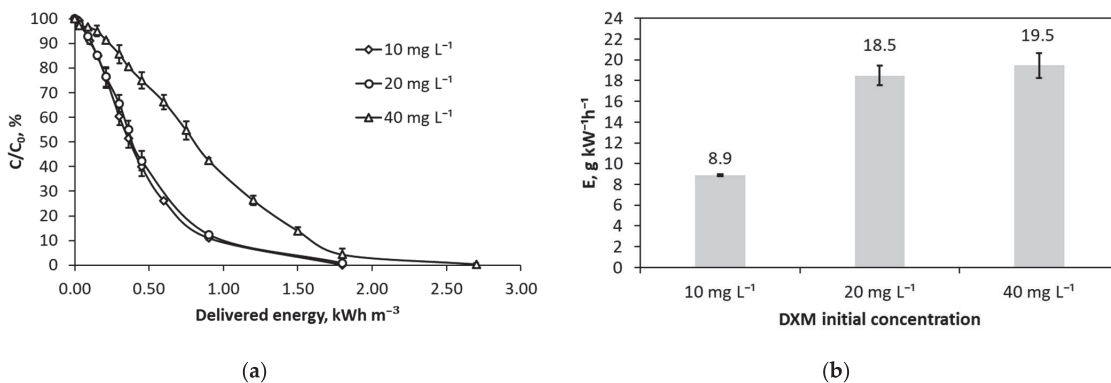

(a)　　　　　　　　　　　　　　　　　　　　　(b)

Figure 5. (**a**) Dexamethasone residual relative concentration dependent on delivered pulsed energy and (**b**) oxidation energy efficiencies (**b**) at DXM initial concentrations of 10, 20 and 40 mg L^{-1}: pulse repetition frequency 50 pps, initial pH 6.8, total treatment time 60 (10 and 20 mg L^{-1}) and 120 (40 mg L^{-1}) min for.

3.3. Effect of pH

Experiments with an initial pH of 3.0, 6.8 and 10.8 were conducted to evaluate the pH impact on DXM oxidation. During the experiments, the pH of acidic media remained practically constant, whereas in neutral and alkaline media the pH decreased from 6.8 and 10.8 to 4.1 and 10.0, respectively. Figure 6 reveals the oxidation of DXM being accelerated in acidic and alkaline media 2.1 and 1.6 times, respectively, as compared to the neutral medium. The decrease in energy efficiency with increasing pH may be attributed to the ●OH oxidation potential decreasing from 2.8 eV in an acidic medium to 1.9 eV at neutral pH [36]. A similar decrease in oxidation efficiency was observed with oxalate [37]. The energy efficiency increase with pH growing from neutral to alkaline media may be attributed to more quickly decomposed ozone molecules producing hydroxyl radicals in the solution. The dissociation of DXM alcohol moieties in alkaline solutions might also, to some extent, accelerate oxidation.

3.4. Effect of Radical-Scavenging Additives

Tert-butyl alcohol (TBA) as a common ●OH radical scavenger was added to assess the role of in-depth OH-radicals. Sodium dodecyl sulphate (SDS) surfactant is known for its surface radical-scavenging properties, showing, however, certain variations in scavenging effects dependent on the target compound molecular structure. Preliminary consideration of the DXM molecule allows the assumption of complex SDS impact: (a) the part of the molecule rich in polar hydroxyl groups provides good affinity with hydrolyzed sulphate moieties of SDS, thus sinking DXM under the gas–liquid interface reducing the rate of oxidation at the gas–liquid interface, whereas (b) the fluoride moiety, being easily displaced from the molecule with the ●OH radical (see the section entitled Identification of Oxidation End-Products), provides a convenient attachment site for the SDS-radical delivering the DXM molecule to the surface [22]. Figure 7 reveals that the addition of 50 to 100 mg L^{-1} TBA showed oxidation efficiency decreased 1.8–2.1 times, while the addition of the same amount of SDS reduced the efficiency 2.3–2.7 times, confirming the predominantly surface character of oxidation. The ●OH radical scavenging action of SDS is explained

by the dominant bonding of dissociated sulphate groups of SDS with DXM hydrophilic hydroxyls (mechanism (a)) overpowering DXM-radical lifting to the surface with SDS-radical (mechanism (b)). The scavenging effect of TBA is explained by the role of in-depth •OH radicals in DXM oxidation. The small difference between SDS and TBA effects points to opposing tendencies of mechanisms (a) and (b) in the DXM interaction with SDS: in the absence of mechanism (b) of SDS interaction with the target pollutant, the former shows remarkably stronger radical-scavenging properties than TBA [35].
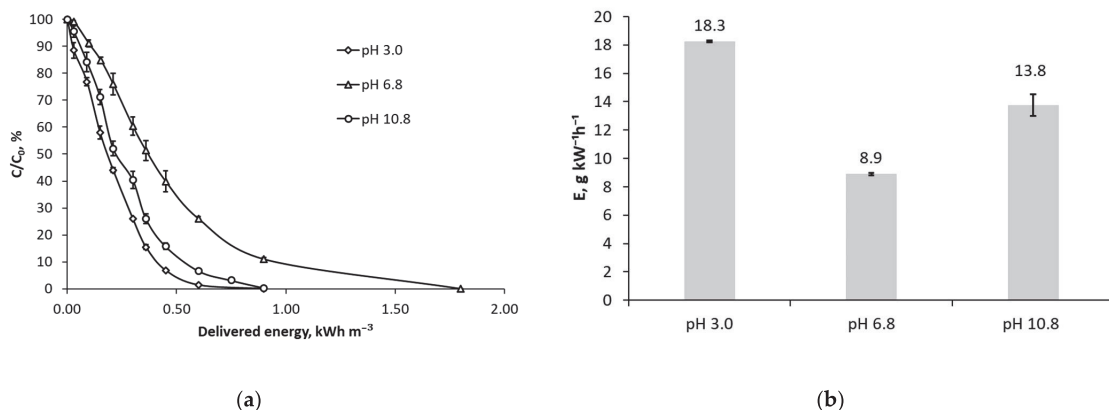

(a)

(b)

Figure 6. (**a**) Dexamethasone residual relative concentration dependent on delivered pulsed energy and (**b**) oxidation energy efficiencies at initial pH 3.0, 6.8 and 10.8: $C_0 = 10$ mg L^{-1}, pulse repetition frequency 50 pps, total treatment time 30 (pH 3.0 and 10.8) and 60 (pH 6.8) min.
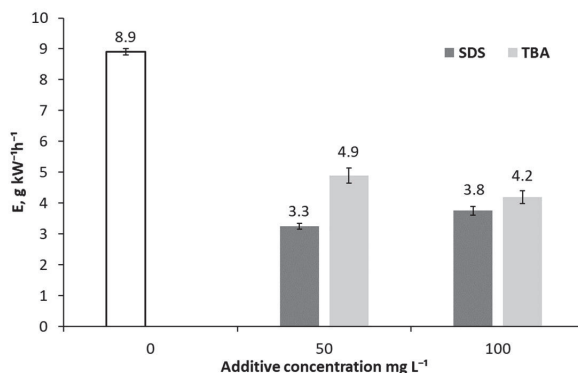

Figure 7. Oxidation energy efficiencies of DXM dependent on SDS and TBA concentrations: radical scavenger concentrations 50 and 100 mg L^{-1}; $C_0 = 10$ mg L^{-1}, pulse repetition frequency 50 pps, initial pH 6.8, total treatment time 60 (no additives) and 120 min (SDS or TBA).

3.5. Identification of Oxidation End-Products

In order to follow the oxidation product formation with higher reliability, DXM was degraded in PCD treatment and ozonation at a higher starting concentration of 40 mg L^{-1}. Both oxidation processes exhibited a similarity in pH, decreasing from 6.8 to 3.6 and 3.2 as a result of treatment with PCD and ozonation, respectively, associated with nitrate formation in the treated solutions: NO_3^- formed in amounts of approximately 36 mg L^{-1} at 3.6 kWh m^{-3} energy doses in both processes (Figures 8 and 9). Such a yield of nitrates comprising about 10 g kW^{-1}h^{-1} is consistent with that observed earlier in PCD experiments [38], although observation of substantial synthesis of nitrates in the ozone generator is characteristic for insufficient air drying prior to its delivery to the ozonation cell.
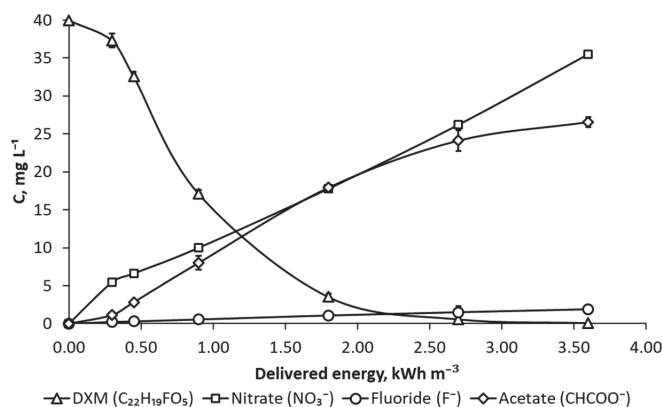
Figure 8. Dexamethasone degradation end-product accumulation in PCD oxidation: $C_0 = 40$ mg L^{-1}, initial pH 6.8, pulse repetition frequency 50 pps, total treatment time 120 min.
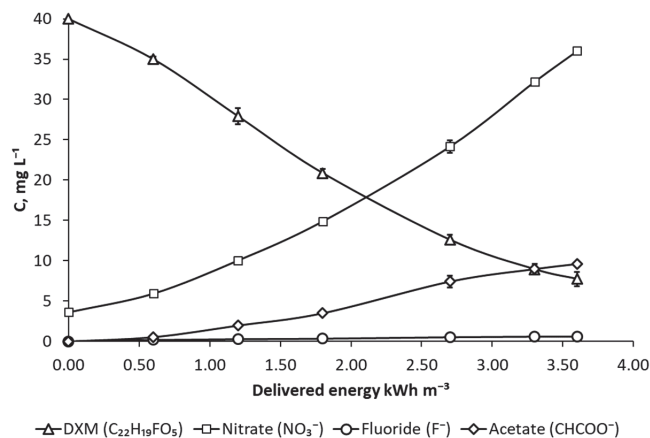

Figure 9. Dexamethasone degradation end-product accumulation in ozonation: $C_0 = 40$ mg L^{-1}, initial pH 6.8, inlet gaseous ozone concentration 3.0 mg L^{-1}, gas flow rate 0.4 L min^{-1}, total treatment time 60 min.

The treatment with PCD showed higher energy efficiency in DXM degradation, reaching 99% at an energy dose of 2.9 kWh m^{-3}. The reaction yield in PCD at 80% of DXM removal taken as a standard for the efficiency calculations in this work equals 22.9 g kW^{-1}h^{-1}. At the end of the ozonation experiment, applying the same energy dose of 3.6 kWh m^{-3}, the treated solution still contained 7.7 mg L^{-1}, i.e., 19.2% of residual DXM. The oxidation energy efficiency at 80% of DXM degradation thus comprised, in the ozonation experiment, about 9.7g kW^{-1}h^{-1}, which is 2.4 times smaller than the PCD efficiency. The obtained difference between PCD and ozonation is consistent with other works of the authors [39,40].

Ion chromatography analysis of the samples treated with PCD and ozone revealed fluoride and acetate being the main identified end-products of DXM oxidation (insets in Figures 8 and 9). It is worth noting that the formation of fluoride in PCD is in stoichiometric ratio with DXM removal: 40 mg L^{-1} or 0.1 mM of DXM provides about 1.9 mg L^{-1} of fluoride, which approximately equals 0.1 mM content. However, acetate was formed in a quantity of 26.6 mg L^{-1} or 0.45 mM which is about 40% of the initial carbon content. Being refractory towards oxidation, acetate accumulated along with DXM removal. In PCD experiments, traces of oxalate and formate were also detected, although no accumulation of these products was observed (Figure 8).

Both fluoride and acetate anions were also quantified by means of ion chromatography in ozonized DXM solution samples (inset in Figure 9), although in amounts about three times smaller than in PCD-treated samples at the same energy delivery level. No stoichiometric ratio was observed between removed DXM and formed fluoride: only 0.03 mM of fluoride formed out of 0.08 mM of removed DXM. A smaller yield of acetate was observed: 0.8 mM of degraded DXM provided about 0.16 mM of acetate (about 15% of initial carbon content). Smaller amounts of the identified end-products are consistent with smaller DXM removal and the smaller oxidation potential of ozone. Formate was present in ozonated samples in trace amounts; no oxalate was observed. Since measurement of TOC showed no decrease in comparison with the original DXM solution remaining at 26.1 mg C L^{-1} in all samples treated with either oxidation method, smaller amounts of identified oxidation end-products in ozonated samples indicate a smaller degree of DXM destruction.

3.6. Identification of Oxidation By-Products

The proposed fragments of DXM obtained from LC-MS analysis were 393 and 373, the latter being associated with breaking C-F bonds and the release of HF during analysis [27]. Thus, several proposed transformation products were detected in two fragments with an m/z difference of 20.

The six most common DXM transformation products numbered as TPs are shown in Figure 10 for ozonation and PCD oxidation reactions. No qualitative difference in product composition was observed between the two treatment processes. The most frequent products were TP2, TP3 and TP6 with m/z values of 409, 407 and 413, respectively. TP1 with m/z 391 could be associated with alcohol moiety oxidation to the aldehyde moiety. TP2 can be associated with OH-radical attack with addition of OH group. Further OH-radical attack results in TP3 in the oxidation of the alcoholic group to the aldehyde one, followed by carboxylic derivative formation and the generation of TP5. Double initial OH-radical attack to DXM could explain TP4 formation (Figure 10a). The products TP1-TP5 have been previously reported in photocatalysis studies [27] and TP4 in gamma irradiation studies [29]. Cycloaddition (Criegee mechanism) with further hydroxylation and loss of HCOOH [41] is suggested to lead to TP6 as a product of ozonation (Figure 10b). These results further suggest that OH-radicals have the main role in the oxidation of DXM.

3.7. Acute Toxicity of By-Products

Dexamethasone appears having low acute toxicity for living organisms [42,43], although the products of its photolysis exhibit slightly higher toxicity [44]. The toxicity assessment undertaken in this study established the formation of products somewhat more toxic than the parent compound as a result of PCD treatment.

To assess the formation of toxic intermediates, the *Vibrio fischeri* bioluminescence inhibition assay was used as an acute toxicity test of DXM aqueous solutions treated with PCD and ozone at an energy dose of 3.6 kWh m^{-3}. The effective concentration for 30% bacterial bioluminescence inhibition (EC$_{30}$) of the solution containing 40 mg L^{-1} of DXM was 37.5%. Treatment with ozone did not noticeably affect the toxicity of the solution, showing negligible EC$_{30}$ growth to 39.3%, i.e., a small toxicity reduction. The treatment with PCD, however, showed increased inhibition of *Vibrio fischeri* bioluminescence resulting in an EC$_{30}$ of 23.3%, i.e., the toxicity somewhat increased as a result of treatment. This result showed a stable character: the toxicity test showed no difference when carried out immediately after treatment and 24 h later. This result may show the formation of DXM by-products with a higher toxicity in the course of its progressive destruction in PCD treatment. The stable character of the treated samples' toxicity excludes the impact of active compounds temporarily suppressing bacterial activity, e.g., peroxides. According to the test requirements, the pH of the analyzed samples was adjusted to the neutral range, thus excluding its interference with the toxicity. The smaller DXM-removal effect of ozone may be the reason for the lesser toxicity of the treated samples.
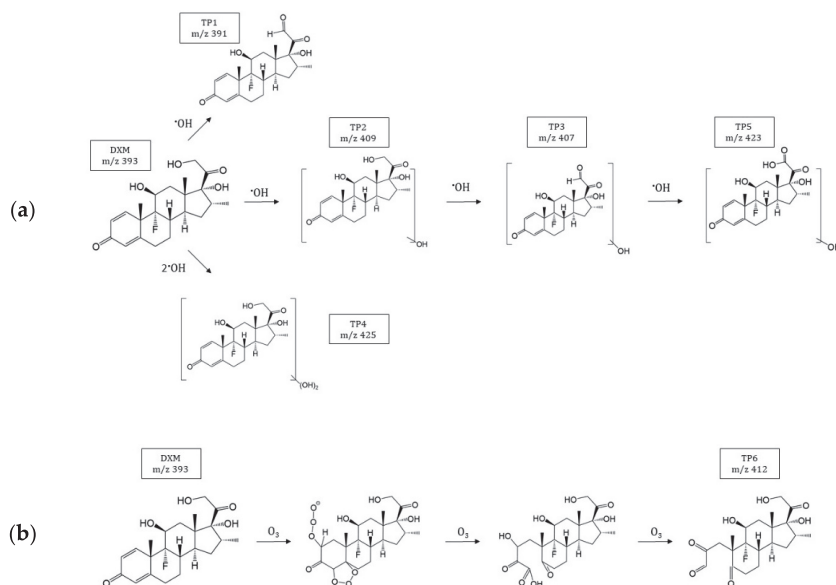
Figure 10. Proposed degradation pathways and transformation products of DXM in oxidation with (**a**) hydroxyl radicals and (**b**) ozone.

4. Conclusions

The authors failed to find studies reported earlier on DXM oxidation using pulsed corona discharge. The study showed the promising character of PCD as a method of oxidation of aqueous corticosteroid with reliable performance in a variety of initial concentrations and pH values. Comparative ozonation demonstrated 2.4 times lower efficiency than PCD oxidation under analogous environmental conditions. The addition of TBA and SDS resulted in decreased oxidation energy efficiency, indicating the major role of •OH radicals in the oxidation process. Suggested transformation by-products confirm the prevalence of •OH radicals in oxidation. The identification of oxidation end-products revealed fluoride and acetate as the products of DXM oxidation accumulating in the course of treatment; fluoride was produced in stoichiometric amounts in DXM PCD oxidation, i.e., was fully mineralized. An ecotoxicity *Vibrio fischeri* test of PCD-treated DXM solutions increased, indicating toxic transformation products, which were observed at a rather high DXM starting concentration of 40 mg L^{-1}. The oxidation of toxic by-products in further toxicity abatement presents a subject for supplementary studies.

Author Contributions: Conceptualization, L.O., E.K.-S., M.T. and S.P.; methodology, L.O. and E.K.-S.; validation, L.O.; formal analysis, L.O.; investigation, L.O.; resources, S.P.; data curation, L.O.; writing—original draft preparation, L.O.; writing—review and editing, S.P., E.K.-S. and M.T.; visualization, L.O.; supervision, S.P.; project administration, S.P.; funding acquisition, S.P. All authors have read and agreed to the published version of the manuscript.

Data Availability Statement: Not applicable.

References

1. Kasonga, T.K.; Coetzee, M.A.A.; Kamika, I.; Ngole-Jeme, V.M.; Momba, M.N.B. Endocrine-disruptive chemicals as contaminants of emerging concern in wastewater and surface water: A review. *J. Environ. Manag.* **2011**, *277*, 111485. [CrossRef]
2. Kostich, M.S.; Lazorchak, J.M. Risks to aquatic organisms posed by human pharmaceutical use. *Sci. Total Environ.* **2008**, *389*, 329–339. [CrossRef] [PubMed]
3. Kümmerer, K. Antibiotics in the aquatic environment—A review—Part I. *Chemosphere* **2009**, *75*, 417–434. [CrossRef]
4. Tran, N.H.; Reinhard, M.; Gin, K.Y.H. Occurrence and fate of emerging contaminants in municipal wastewater treatment plants from different geographical regions-a review. *Water Res.* **2018**, *133*, 182–207. [CrossRef] [PubMed]
5. The RECOVERY Collaborative Group, Dexamethasone in Hospitalized Patients with COVID-19. *N. Engl. J. Med.* **2021**, *384*, 693–704. [CrossRef] [PubMed]
6. Salas-Leiton, E.; Coste, O.; Arsensio, E.; Infante, C.; Canavate, J.P.; Manchado, M. Dexamethasone modulates expression of genes involved in the innate immune system, growth and stress and increases susceptibility to bacterial disease in Senegalese sole (*Solea senegalensis* Kaup, 1858). *Fish Shellfish. Immunol.* **2021**, *32*, 769–778. [CrossRef]
7. Ribas, J.L.C.; Zampronio, A.R.; de Assis, H.C.S. Effects of trophic exposure to diclofenac and dexamethasone on hematological parameters and immune response in freshwater fish. *Environ. Toxicol. Chem.* **2016**, *35*, 975–982. [CrossRef]
8. Chang, H.; Hu, J.; Shao, B. Occurrence of Natural and Synthetic Glucocorticoids in Sewage Treatment Plants and Receiving River Waters. *Environ. Sci. Technol.* **2007**, *41*, 3462–3468. [CrossRef]
9. Macikova, P.; Groh, K.J.; Ammann, A.A.; Schirmer, K.; Suter, M.J.-F. Endocrine Disrupting Compounds Affecting Corticosteroid Signaling Pathways in Czech and Swiss Waters: Potential Impact on Fish. *Environ. Sci. Technol.* **2014**, *48*, 12902–12911. [CrossRef]
10. Gong, J.; Lin, C.; Xiong, X.; Chen, D.; Chen, Y.; Zhou, Y.; Wu, C.; Du, Y. Occurrence, distribution, and potential risks of environmental corticosteroids in surface waters from the Pearl River Delta, South China. *Environ. Pollut.* **2019**, *251*, 102–109. [CrossRef]
11. Jia, A.; Wu, S.; Daniels, K.D.; Snyder, S.A. Balancing the Budget: Accounting for Glucocorticoid Bioactivity and Fate during Water Treatment. *Environ. Sci. Technol.* **2016**, *50*, 2870–2880. [CrossRef]
12. Nakayama, K.; Sato, K.; Shibano, T.; Isobe, T.; Suzuki, G.; Kitamura, S.-I. Occurrence of glucocorticoids discharged from a sewage treatment plant in Japan and the effects of clobetasol propionate exposure on the immune responses of common carp (Cyprinus carpio) to bacterial infection. *Environ. Toxicol. Chem.* **2015**, *35*, 946–952. [CrossRef]
13. Klauson, D.; Romero Sarcos, N.; Krichevskaya, M.; Kattel, E.; Dulova, N.; Dedova, T.; Trapido, M. Advanced oxidation processes for sulfonamide antibiotic sulfamethizole degradation: Process applicability study at ppm level and scale-down to ppb level. *J. Environ. Chem. Eng.* **2019**, *7*, 103287. [CrossRef]
14. Oller, I.; Malato, S. Photo-Fenton applied to the removal of pharmaceutical and other pollutants of emerging concern. *Curr. Opin. Green Sustain. Chem.* **2021**, *29*, 100458. [CrossRef]
15. Olak-Kucharczyk, M.; Foszpańczyk, M.; Żyłła, R.; Ledakowicz, S. Photodegradation and ozonation of ibuprofen derivatives in the water environment: Kinetics approach and assessment of mineralization and biodegradability. *Chemosphere* **2022**, *291*, 132742. [CrossRef] [PubMed]
16. Patel, S.; Majumder, S.K.; Ghosh, P. Ozonation of diclofenac in a laboratory scale bubble column: Intermediates, mechanism, and mass transfer study. *J. Water Process. Eng.* **2021**, *44*, 102325. [CrossRef]
17. Sun, S.; Ren, J.; Liu, J.; Rong, L.; Wang, H.; Xiao, Y.; Sun, F.; Mei, R.; Chen, C.; Su, X. Pyrite-activated persulfate oxidation and biological denitrification for effluent of biological landfill leachate treatment system. *J. Environ. Manage* **2022**, *304*, 114290. [CrossRef]
18. Malik, M.A.; Ghaffar, A.; Malik, S.A. Water purification by electrical discharges. *Plasma Sources Sci. Technol.* **2001**, *10*, 82–91. [CrossRef]
19. Bogaerts, A.; Neyts, E.; Gijbels, R.; van der Mullen, J. Gas discharge plasmas and their applications. *Spectrochim. Acta Part B* **2002**, *57*, 609–658. [CrossRef]
20. Magureanu, M.; Bradu, C.; Parvulescu, V.I. Plasma processes for the treatment of water contaminated with harmful organic compounds. *J. Phys. D Appl. Phys.* **2018**, *51*, 313003. [CrossRef]
21. Panorel, I.; Preis, S.; Kornev, I.; Hatakka, H.; Louhi-Kultanen, M. Oxidation of aqueous pharmaceuticals by pulsed corona discharge. *Environ. Technol.* **2013**, *34*, 923–930. [CrossRef] [PubMed]
22. Onga, L.; Boroznjak, R.; Kornev, I.; Preis, S. Oxidation of aqueous organic molecules in gas-phase pulsed corona discharge affected by sodium dodecyl sulphate: Explanation of variability. *J. Electrostat.* **2021**, *111*, 103581. [CrossRef]
23. Derevshchikov, V.; Dulova, N.; Preis, S. Oxidation of ubiquitous aqueous pharmaceuticals with pulsed corona discharge. *J. Electrost.* **2021**, *110*, 103567. [CrossRef]
24. Ono, R.; Oda, T. Dynamics of ozone and OH radicals generated by pulsed corona discharge in humid-air flow reactor measured by laser spectroscopy. *J. Appl. Phys.* **2003**, *93*, 5876. [CrossRef]
25. Markic, M.; Cvetnic, M.; Ukic, S.; Kusic, H.; Bolanca, T.; Bozic, A.L. Influence of process parameters on the effectiveness of photooxidative treatment of pharmaceuticals. *J. Environ. Sci. Heal. A* **2018**, *53*, 338–351. [CrossRef] [PubMed]
26. Rasolevandi, T.; Naseri, S.; Azarpira, H.; Mahvi, A.H. Photo-degradation of dexamethasone phosphate using UV/Iodide process: Kinetics, intermediates, and transformation pathways. *J. Mol. Liq.* **2019**, *295*, 111703. [CrossRef]

27.　Calza, P.; Pelizzetti, E.; Brussino, M.; Baiocchi, C. Ion Trap Tandem Mass Spectrometry Study of Dexamethasone Transformation Products on Light Activated TiO$_2$ Surface. *J. Am. Soc. Mass Spectrom.* **2001**, *12*, 1286–1295. [CrossRef]

28.　Ghenaatgar, A.; Tehrani, R.M.A.; Khadir, A. Photocatalytic degradation and mineralization of dexamethasone using WO$_3$ and ZrO$_2$ nanoparticles: Optimization of operational parameters and kinetic studies. *J. Water Process. Eng.* **2019**, *32*, 100969. [CrossRef]

29.　Rahmani, H.; Rahmani, K.; Rahmani, A.; Zare, M.-R. Removal of dexamethasone from aqueous solutions using sono-nanocatalysis process. *Res. J. Environ. Sci.* **2015**, *9*, 320–331. [CrossRef]

30.　Guo, Z.; Guo, A.; Guo, Q.; Rui, M.; Zhao, Y.; Zhang, H.; Zhu, S. Decomposition of dexamethasone by gamma irradiation: Kinetics, degradation mechanisms and impact on algae growth. *Chem. Eng. J.* **2017**, *307*, 722–728. [CrossRef]

31.　Arsand, D.R.; Kümmerer, K.; Martins, A.F. Removal of dexamethasone from aqueous solution and hospital wastewater by electrocoagulation. *Sci. Total Environ.* **2013**, *443*, 351–357. [CrossRef] [PubMed]

32.　Asgari, G.; Salari, M.; Faraji, H. Performance of heterogeneous catalytic ozonation process using Al2O3 nanoparticles in dexamethasone removal from aqueous solutions. *Desalin. Water Treat.* **2020**, *189*, 296–304. [CrossRef]

33.　Quaresma, A.V.; Rubio, K.T.S.; Taylor, J.G.; Sousa, B.A.; Silva, S.Q.; Werle, A.A.; Alfonso, R.J.C.F. Removal of dexamethasone by oxidative processes: Structural characterization of degradation products and estimation of the toxicity. *J. Environ. Chem. Eng.* **2021**, *9*, 106884. [CrossRef]

34.　Kahru, A.; Kurvet, M.; Külm, I. Toxicity of phenolic wastewater to luminescent bacteria photobacterium phosphoreum and activated sludges. *Water Sci. Technol.* **1996**, *33*, 139–146. [CrossRef]

35.　Preis, S.; Panorel, I.C.; Kornev, I.; Hatakka, H.; Kallas, J. Pulsed corona discharge: The role of ozone and hydroxyl radical in aqueous pollutants oxidation. *Wat. Sci. Technol.* **2013**, *68*, 1536–1542. [CrossRef]

36.　Wardman, P. Reduction potentials of one electron couples involving free radicals in aqueous solution. *J. Phys. Chem. Ref. Data* **1989**, *18*, 1637–1755. [CrossRef]

37.　Tikker, P.; Kornev, I.; Preis, S. Oxidation energy efficiency in water treatment with gas-phase pulsed corona discharge as a function of spray density. *J. Electrost.* **2020**, *106*, 103466. [CrossRef]

38.　Preis, S.; Panorel, I.C.; Llauger Coll, S.; Kornev, I. Formation of nitrates in aqueous solutions treated with pulsed corona discharge: The impact of organic pollutants. *Ozone Sci. Eng.* **2014**, *36*, 94–99. [CrossRef]

39.　Kask, M.; Krichevskaya, M.; Preis, S.; Bolobajev, J. Oxidation of aqueous N-nitrosodiethylamine: Experimental comparison of pulsed corona discharge with H$_2$O$_2$-assisted ozonation. *J. Environ. Chem. Eng.* **2021**, *9*, 105102. [CrossRef]

40.　Tikker, P.; Dulova, N.; Kornev, I.; Preis, S. Effects of persulfate and hydrogen peroxide on oxidation of oxalate by pulsed corona discharge. *Chem. Eng. J.* **2021**, *411*, 128586. [CrossRef]

41.　He, X.; Huang, H.; Tang, Y.; Guo, L. Kinetics and mechanistic study on degradation of prednisone acetate by ozone. *J. Environ. Sci. Health A* **2019**, *55*, 292–304. [CrossRef]

42.　Zhong, L.; Liang, Y.-Q.; Lu, M.; Pan, C.-G.; Dong, Z.; Zhao, H.; Li, C.; Lin, Z.; Yao, L. Effects of dexamethasone on the morphology, gene expression and hepatic histology in adult female mosquitofish (*Gambusia affinis*). *Chemosphere* **2021**, *274*, 129797. [CrossRef] [PubMed]

43.　Zhang, D.; Liu, K.; Hu, W.; Lu, X.; Li, L.; Zhang, Q.; Huang, H.; Wang, H. Prenatal dexamethasone exposure caused fetal rats liver dysplasia by inhibiting autophagy-mediated cell proliferation. *Toxicology* **2021**, *449*, 152664. [CrossRef] [PubMed]

44.　DellaGreca, M.; Fiorentino, A.; Isidori, M.; Lavorgna, M.; Previtera, L.; Rubino, M.; Temussi, F. Toxicity of prednisolone, dexamethasone and their photochemical derivatives on aquatic organisms. *Chemosphere* **2004**, *54*, 629–637. [CrossRef] [PubMed]

Curriculum vitae

Personal data

Name:	Liina Onga (née Kuntus)
Date of birth:	29.12.1993
Place of birth:	Võru, Estonia
Citizenship:	Estonian

Contact data

E-mail:	liina.onga@taltech.ee

Education

2018–2022	Tallinn University of Technology, Department of Materials and Environmental Technology, Doctoral Studies
2016–2018	Tallinn University of Technology, MSc in Engineering (*cum laude*)
2013–2016	Tallinn University of Technology, BSc in Engineering
2010–2013	Tallinn Art Gymnasium (high school, gold medal)

Language competence

Estonian	native speaker
English	fluent
Russian	beginner

Professional employment

2017–2022	Tallinn University of Technology, School of Engineering, Department of Materials and Environmental Technology, Junior Researcher

Defended dissertations

Master's Degree, 2018, Degradation of ceftriaxone in water by heterogeneously activated persulfate, Tallinn University of Technology School of Engineering, Department of Materials and Environmental Technology. Supervisors Eneliis Kattel, Niina Dulova.

Main areas of scientific work

1. Biosciences and Environment; 1.8. Research relating to the State of the Environment and to Environmental Protection; CERCS CLASSIFICATION: T270 Environmental technology, pollution control

1. Biosciences and Environment; 1.9. Research into Substances Hazardous to the Environment; CERCS CLASSIFICATION: P305 Environmental chemistry

4. Natural Sciences and Engineering; 4.11. Chemistry and Chemical Technology; CERCS CLASSIFICATION: T350 Chemical technology and engineering

Involvement in research projects

PRG776 Innovative energy-efficient abatement of aqueous and airborne hazardous pollutants combining pulsed corona discharge plasma with catalysis/photocatalysis

LEEAE20017 Expertise of leakage current on water pipes and water parameters of the KUMU Art Museum building

IUT1-7 Chemical engineering approach to removal of priority pollutants and emerging micropollutants from water/wastewater and soil: implementation and optimization of advanced oxidation technologies

Awards

| 2019 | FMDTK scholarship for the participation in the 3rd European Summer School of Environmental Applications on Advanced Oxidation Processes, 3–7 June 2019, Alcoy, Spain |

2019   FMDTK scholarship for the participation in the 3rd European Summer School of Environmental Applications on Advanced Oxidation Processes, 3–7 June 2019, Alcoy, Spain

2019   Dora Plus programme (activity 1) scholarship for the participation in the 6th European Conference on Environmental Applications of Advanced Oxidation Processes (EAAOP-6), 26–30 June, 2019, Portoroz-Portorose, Slovenia

Attendance at conferences and training schools

2021   Attendance with a poster presentation at Graduate School of Functional Materials and Technologies (GSFMT) scientific conference, June 14–15, 2021, Tartu, Estonia

2020   Attendance with a poster presentation at Graduate School of Functional Materials and Technologies (GSFMT) scientific conference, February 4–5, 2020, Tallinn, Estonia

2019   Attendance with a poster presentation at "6th European Conference on Environmental Applications of Advanced Oxidation Processes (EAAOP-6)"; June 26–30, 2019, Portorož-Portorose, Slovenia (Dora Plus scholarship)

2019   Attendance with a poster presentation at "3rd European Summer School on Environmental Applications of Advanced Oxidation Processes", June 3–7, 2019, Alcoy, Spain (GSFMT financial support)

2019   Attendance with a poster presentation at XXXIV Estonian Chemistry Days, April 18, 2019, Tallinn, Estonia

2019   Attendance with a poster presentation at Graduate School of Functional Materials and Technologies (GSFMT) scientific conference, February 4–5, 2019, Tartu, Estonia

Supervised dissertations

Alo Landberg, Master's Degree, 2021, (sup) Eneliis Kattel-Salusoo; Liina Onga, Degradation of micropollutant in water by hydroxyl radical-based processes, Tallinn University of Technology School of Engineering, Department of Materials and Environmental Technology

Birgit Ashour, Master's Degree, 2021, (sup) Eneliis Kattel-Salusoo; Liina Onga, Degradation of corticosteroid in water by pulsed corona discharge combined with persulfates, Tallinn University of Technology School of Engineering, Department of Materials and Environmental Technology

Chika Constance Ogumka, Master's Degree, 2020, (sup) Sergei Preis; Liina Onga, Oxidation of Acid Orange 7 and Indigotetrasulfonate Textile dyes with Pulsed Corona Doscharge: Impact of Treatment Conditions, Tallinn University of Technology School of Engineering, Department of Materials and Environmental Technology

Publications

Onga, L.; Kattel-Salusoo, E.; Trapido, M.; Preis, S. (2022). Oxidation of Aqueous Dexamethasone Solution by Gas-Phase Pulsed Corona Discharge. Water, 14 (3), #467. DOI: 10.3390/w14030467.

Onga, L.; Boroznjak, R.; Kornev, I.; Preis, S. (2021). Oxidation of aqueous organic molecules in gas-phase pulsed corona discharge affected by sodium dodecyl sulphate: Explanation of variability. Journal of Electrostatics, 111, #103581. DOI: 10.1016/j.elstat.2021.103581.

Onga, L.; Kornev, I.; Preis, S. (2020). Oxidation of reactive azo-dyes with pulsed corona discharge: surface reaction enhancement. Journal of Electrostatics, 103, 103420. DOI: 10.1016/j.elstat.2020.103420.

Balpreet Kaur; **Kuntus, L**.; Tikker, P.; Kattel, E.; Trapido, M.; Dulova, N. (2019). Photo-induced oxidation of ceftriaxone by persulfate in the presence of iron oxides. The Science of The Total Environment, 676, 165–175. DOI: 10.1016/j.scitotenv.2019.04.277.

Elulookirjeldus

Isikuandmed

Nimi: Liina Onga (endine Kuntus)
Sünniaeg: 29.12.1993
Sünnikoht: Võru, Eesti
Kodakondsus: Eesti

Kontaktandmed

E-post: liina.onga@taltech.ee

Hariduskäik

2018–2022	Tallinna Tehnikaülikool, Materjali- ja keskkonnatehnoloogia instituut, doktorantuur
2016–2018	Tallinna Tehnikaülikool, tehnikateaduse magister (*cum laude*)
2013–2016	Tallinna Tehnikaülikool, tehnikateaduse bakalaureus
2010–2013	Tallinna Kunstigümnaasium (keskharidus, kuldmedal)

Keelteoskus

Eesti	emakeel
Inglise	kõrgtase
Vene	algtase

Teenistuskäik

2018–2022	Tallinna Tehnikaülikool, Inseneriteaduskond, Materjali- ja keskkonnatehnoloogia instituut, doktorant-nooremteadur

Kaitstud lõputööd

Tehnikateaduse magistrikraad: Tseftriaksooni lagundamine vees heterogeenselt aktiveeritud persulfaadiga, Tallinna Tehnikaülikool, Inseneriteaduskond, Materjali- ja keskkonnatehnoloogia instituut, 2018, juhendajad Eneliis Kattel, Niina Dulova

Uurimustöö põhisuunad

1. Bio- ja keskkonnateadused; 1.8. Keskkonnaseisundit ja keskkonnakaitset hõlmavad uuringud; CERCS KLASSIFIKAATOR: T270 Keskkonnatehnoloogia, reostuskontroll

1. Bio- ja keskkonnateadused; 1.9. Keskkonnaohtlikke aineid käsitlevad uuringud; CERCS KLASSIFIKAATOR: P305 Keskkonnakeemia

4. Loodusteadused ja tehnika; 4.11. Keemia ja keemiatehnika; CERCS KLASSIFIKAATOR: T350 Keemiatehnoloogia ja –masinaehitus

Osalemine uurimisprojektides

PRG776 Ohtlike vee ja õhu saasteainete lagundamine innovatiivse energiatõhusa kombineeritud impulss-koroona elektrilahenduse ja katalüüsi/fotokatalüüsiga

LEEAE20017 KUMU kunstimuuseumi hoone veetorustiku uitvoolude ja veeparameetrite ekspertiis

IUT1-7 Keemiatehnikapõhine lähenemisviis prioriteetsete saasteainete ja uute esilekerkivate mikrosaasteainete kõrvaldamisele veest/reoveest ja pinnasest: täiustatud oksüdatsioonitehnoloogiate kasutamine ja optimeerimine

Tunnustused

2019	FMDTK stipendium osalemiseks suvekoolis 3rd European Summer School of Environmental Applications on Advanced Oxidation Processes, 3.–7. Juuni 2019, Alcoi, Hispaania
2019	Dora Pluss (tegevus 1) stipendium osalemiseks konverentsil 6th European Conference on Environmental Applications of Advanced Oxidation Processes (EAAOP-6), 26.–30. juuni, 2019, Portoroz-Portorose, Sloveenia

Konverentsidel ja treeningkoolides osalemine

2021	Posterettekandega esinemine Funktsionaalsete materjalide ja tehnoloogiate doktorikooli (FMTDK) teaduskonverentsil, 14.–15.06.2021, Tartu, Eesti
2020	Posterettekandega esinemine Funktsionaalsete materjalide ja tehnoloogiate doktorikooli (FMTDK) teaduskonverentsil, 4.–5.02.2020, Tallinn, Eesti
2019	Posterettekandega esinemine konverentsil "6th European Conference on Environmental Applications of Advanced Oxidation Processes (EAAOP-6)", 26.–30.06.2019, Portorož-Portorose, Sloveenia (Dora Pluss stipendium)
2019	Posterettekandega esinemine suvekoolis "3rd European Summer School on Environmental Applications of Advanced Oxidation Processes", 3.–7.06.2019, Alcoi, Hispaania (FMTDK poolne finantseerimine)
2019	Posterettekandega esinemine XXXIV Eesti Keemiapäevad 100. aastapäeva teaduskonverentsil, 18.04.2019, Tallinn, Eesti
2019	Posterettekandega esinemine Funktsionaalsete materjalide ja tehnoloogiate doktorikooli (FMTDK) teaduskonverentsil, 4.–5.02.2019, Tartu, Eesti

Juhendatud magistritööd

Alo Landberg, magistrikraad, 2021, (juh) Eneliis Kattel-Salusoo; Liina Onga, Mikrosaasteaine lagundamine vees hüdroksüülradikaali-põhiste protsessidega, Tallinna Tehnikaülikool, Inseneriteaduskond, Materjali- ja keskkonnatehnoloogia instituut

Birgit Ashour, magistrikraad, 2021, (juh) Eneliis Kattel-Salusoo; Liina Onga, Kortikosteroidi lagundamine vees koroona impulss-elektrilahenduse kombinatsioonil persulfaatidega, Tallinna Tehnikaülikool, Inseneriteaduskond, Materjali- ja keskkonnatehnoloogia instituut

Chika Constance Ogumka, magistrikraad, 2020, (juh) Sergei Preis; Liina Onga, Oxidation of Acid Orange 7 and Indigotetrasulfonate Textile dyes with Pulsed Corona Doscharge: Impact of Treatment Conditions (Tekstiilvärvide happeoranž 7 ning indigotetrasulfonaadi oksüdeerimine impulss-koroona elektrilahendusega: töötlemise tingimuste mõju), Tallinna Tehnikaülikool, Inseneriteaduskond, Materjali- ja keskkonnatehnoloogia instituut

Publikatsioonid

Onga, L.; Kattel-Salusoo, E.; Trapido, M.; Preis, S. (2022). Oxidation of Aqueous Dexamethasone Solution by Gas-Phase Pulsed Corona Discharge. Water, 14 (3), #467. DOI: 10.3390/w14030467.

Onga, L.; Boroznjak, R.; Kornev, I.; Preis, S. (2021). Oxidation of aqueous organic molecules in gas-phase pulsed corona discharge affected by sodium dodecyl sulphate: Explanation of variability. Journal of Electrostatics, 111, #103581. DOI: 10.1016/j.elstat.2021.103581.

Onga, L.; Kornev, I.; Preis, S. (2020). Oxidation of reactive azo-dyes with pulsed corona discharge: surface reaction enhancement. Journal of Electrostatics, 103, 103420. DOI: 10.1016/j.elstat.2020.103420.

Balpreet Kaur; **Kuntus, L**.; Tikker, P.; Kattel, E.; Trapido, M.; Dulova, N. (2019). Photo-induced oxidation of ceftriaxone by persulfate in the presence of iron oxides. The Science of The Total Environment, 676, 165–175. DOI: 10.1016/j.scitotenv.2019.04.277.